R.J.W. Bloem

Dynamic behaviour of slab track on pile foundation

Analysis method based on dynamic behaviour of a high-speed slab track and settlements in the substructure

TUDelft

Dynamic behaviour of slab track on pile foundation

Analysis method based on dynamic behaviour of a high-speed slab track and settlements in the substructure

By

R.J.W. Bloem

in partial fulfilment of the requirements for the degree of

Master of Science
in Applied Physics

at the Delft University of Technology,
to be defended publicly on Wednesday March 31, 2021 at 15:00.

Chair:	Dr. ir. V.L. Markine	
Thesis committee:	Prof. dr. ir R.P.B.J. Dollevoet	TU Delft
	Dr. F. Pisanò	TU Delft
	Ir. A.A. Hertogs	Infraspeed Maintenance BV

This thesis is confidential and cannot be made public until December 31, 2021.

An electronic version of this thesis is available at http://repository.tudelft.nl/.

TUDelft

Abstract

The High speed line, HSL, in the Netherlands is constructed as a slab track, where the rails are connected to a concrete slab, the Rheda slab. Slab track is a proven technology for high speed lines and one advantage of slab track is that it has lower maintenance costs. A disadvantage of the slab track structure is that it has a limited adjustability if the railway track is displaced from its original position. Therefore, the Rheda slab is constructed on top of another concrete slab, the settlement free plate (SFP), which has a pile foundation. The SFP has to prevent that the railway track will get large settlements.
However, during regular maintenance inspections it was revealed that at the location of Schuilingervliet large settlements of the HSL occurred. At some places at Schuilingervliet the limited adjustability of the slab track to correct the level of the rail is almost reached. Closer inspections at Schuilingervliet showed that the pile foundation shows settlements. These settlements have resulted in multiple problems for the structure of the railway track.

In this master thesis the behaviour of a high speed railway track constructed on top of a pile foundation with settlements under a dynamic load has been analysed. Therefore, a model was developed in the software program DARTS, dynamic analysis of rail track structures. In DARTS the railway track was modelled by stiff and elastic layers, which were loaded by a moving train load. The train was modelled as a mass spring system. A limitation of DARTS was that permanent displacements, such as settlements, could not be modelled.

The results of DARTS were analysed and validated with field measurements of the HSL. After the validation of the model multiple simulations were performed to analyse the structure for different uncertainties and possible solutions. The uncertainties that have been studied include multiple velocities for the different trains that use the HSL, different pile stiffness to model the different length in pile foundation per SFP and to model the settlement of the pile foundation. Also, a pile foundation with larger piles was simulated and the vertical rail geometry, which is used in DARTS to determine the dynamic train loading, was altered. These simulations showed that the model in DARTS is sensitive for changes of the pile stiffness. The results also show that it is difficult to model permanent displacements in DARTS.

Three possible solutions have been modelled. The first solution studied a connection between two consecutive SFP. In the second solution a Rheda slab is placed over the joint between two SFP and in the last solution the pile stiffness was increased for piles next to the joint.
All three solutions showed a decrease in elastic displacements and have a possibility to reduce the problem. The first solution has the possibility to reduce the difference in settlement between two consecutive SFP. The third solution with higher pile stiffness can be obtained by pile toe injections. If these pile toe injections are successful, there might be a possibility that these pile toe injections could stop the settlement of the pile foundation.

From this research it can be concluded that the model of the HSL in DARTS is sensitive for changes in the pile stiffness. An increase in pile stiffness results in a decrease in displacements. Also can be concluded that due to the limitations in DARTS it is difficult to model the effects of a permanent displacement. Furthermore, the simulations in DARTS and field measurements of the HSL show that slab track is sensitive for settlements. Therefore, it is important that during the design of the pile foundation for slab track the settlements and the effect that settlements have on the slab track structure are analysed.

This research has the following recommendations for further research. To improve the model validation more field measurements of the displacement of the HSL are advised. Secondly, the soil characteristics around Schuilingervliet should be investigated. This investigation can help to improve the DARTS model by using a better estimate for the pile stiffness and could be useful to determine the cause of the settlements. Lastly, further research is advised on the influence of the gap between the Rheda slab and SFP, because it is not possible in DARTS to model permanent displacements.

Preface

This master thesis is written to complete my study of Structural Engineering and the track Road and Railroad Engineering at the TU Delft. In this master thesis I discuss the problem of the HSL-South due to settlements of the pile foundation. During this thesis I had the opportunity to do an internship period at Infraspeed Maintenance B.V., the asset manager and contractor of the HSL-South.

In this preface I would like to thank Aad Hertogs for giving me this interesting but also complex problem and for inviting me to join the Denktank meetings, in which a team of Infraspeed and ProRail discussed the problem and solutions for the settlement problem of the HSL. These meetings were really interesting and helpful to understand the problem and also learn about the complexity of the HSL. I would also like to thank all members of the Denktank meetings for answering my question and sharing their information and knowledge of the HSL with me.

I also would like to thank Valeri Markine for his supervision and for helping me with all my questions and problems that I had during this thesis. I also like to thank the rest of the committee Federico Pisanò and professor Rolf Dollevoet for their feedback during the meetings. Finally I would like to thank my family and friends for their support during my study and thesis.

Reltje Jan Bloem
Delft, March 2021

Content

1 Introduction

The HSL-South is a high-speed railway line in the Netherlands running from Schiphol Airport to the Belgium border. This high-speed line connects Amsterdam and Rotterdam with the European high-speed railway network. Thalys and Eurostar use the HSL-South in their high-speed train service from Amsterdam to Brussels, Paris and London. Also, the NS, Dutch Railways, uses the line for domestic services. The HSL-South is the only railway line designed for 300 km/h in the Netherlands. Besides the higher maximum speed the HSL-South is different from any other railway line in the Netherlands. The biggest difference is that the high-speed line is constructed for the largest part as a slab track. All other tracks in The Netherlands are built as a ballast track.

1.1 Problem description

The superstructure of the HSL-South is built as a Rheda2000 slab track, where the sleepers are embedded in the in-situ casted concrete slab. The advantages of a slab track over a ballast track are that slab track is to a large extent maintenance free and that slab track has an increased service life. One large disadvantage of slab track is that the track after construction cannot easily be corrected for large displacements of the structure. One of the requirements of the Rheda2000 slab track is a settlement free foundation. Therefore, the Rheda2000 concrete slabs are constructed on top of settlement free plate, SFP. This SFP, is a concrete slab which is built on top of a pile foundation. As a result a large part of the HSL-South is constructed on top of a pile foundation.

Despite the pile foundation some parts of the HSL-South have shown settlement. Small settlements can be compensated by adjusting the vertical level of the rail. However, larger displacements are a problem for slab track because the maximum level for rail adjustment is limited. Meanwhile, measurements have shown that at some locations the HSL-South still undergoes settlements and that the maximum level for rail adjustment is almost reached. To stop these settlements and to reduce the problems due to the settlements actions are being performed.

1.2 Research questions

To get a better insight into the actions that can be taken, this thesis will investigate the dynamic interaction between train, slab track and the substructure taking settlements into account. This results in the following research question:

How to develop a design methodology for a high-speed slab track under dynamic loading accounting for initial settlements of the substructure?

This question will be split into the following sub-questions to formulate an answer:
- *What are the actual train loads of trains which are using the HSL?*
  First the train loads will be determined. These loads are required for further assessment of the problem. Therefore type of train, axle loads and speed will be investigated.
- *What are the internal forces in the slab track?*
  In this phase the internal forces in the slab track are analysed. The dynamic train load is resisted by the slab track before it is further distributed to the substructure.
- *How are the train loads distributed between the slab track and the substructure?*
  The train loads are distributed from the slab track to the substructure. In this stage is determined how much of the dynamic forces of the train load are still there.
- *What is the influence of an initial settlement on the behaviour of the construction?*
  In this stage the influence of an initial settlement on the construction will be determined.
- *What is the effect of uncertainties on the design of slab track?*
  Not all parameters are known and therefore there are some uncertainties. In this phase the effect of the uncertainties in the design should be taken into account.
- *What are the reasons of settlement and what solutions are there to mitigate these settlements?*
  In the last stage there will be a closer look into the reasons of settlements of the substructure and to possible solutions to mitigate these settlements.

1.3 Approach

For a good analysis of the problem an overview of the situation is given in Chapter 2. The track structure is discussed, where the slab track superstructure of the HSL is analysed. Also, the settlement free plate that the HSL uses as substructure is discussed. In this chapter also the trains that use the HSL and their axle loads are analysed.

In Chapter 3 a case study is performed at the location of Schuilingervliet where large settlements occur. The pile foundation of the HSL is analysed in more detail for this location as well as the soil. The problems that occur due to the settlements of the HSL are also briefly discussed.

Chapter 4 discusses the numerical model that is used. The model is made in the software program DARTS. The track structure is modelled and models of the trains are made. These trains drive over the track structure to dynamically analyse the track structure of the HSL.

In Chapter 5 the results of the numerical simulations are analysed. Multiple simulations are performed to analyse different factors and uncertainties. Difference in track structure, trains, velocity of the trains are modelled to take these uncertainties into account.

In Chapter 6 three possible solutions are modelled to see what the effects are on the structure of the HSL and to see if these solutions can be helpful to solve the settlement problem of the HSL.

The results of the simulations are discussed in Chapter 7 and followed by the conclusion in Chapter 8. The last chapter of this report is Chapter 9 where the recommendations are presented.

2 Situation Description

In this chapter the structure of the HSL-South will be discussed from the rails down to the foundation. The construction is separated and constructed into two parts. The superstructure, the upper part that includes all elements from the rails down to the Rheda2000 slab, and the substructure, the Settlement Free Plate with pile foundation. Furthermore, the trains driving over the HSL-South will be investigated. The different types of trains driving over the track result in different loading of the structure. Also, Schuilingervliet one of the locations with large settlements will be discussed.

2.1 Superstructure

The HSL-South is constructed as a slab track. This slab track structure is chosen because it is a proven technology for high-speed operations. Furthermore, slab track has low maintenance cost due to the track alignment is fixed and therefore less correction of track alignment is required during its service life. Also, if the slab track has a proper foundation the track structure is settlement free due to the stiffer concrete slabs. Ballast tracks require more maintenance mostly due to ballast deteriorating over time and therefore correcting the track alignment. Furthermore, passing trains can suck up ballast, which can damage the train and the track.

The superstructure of the HSL-South was constructed by starting at the top and going downwards. Therefore, first the rails were aligned and later the concrete for the Rheda slab was casted. For the slab track the Rheda2000 system was used. The Rheda2000 system is a further development of the German Rheda system [1]. Figure 1 shows the cross section of the HSL-South.
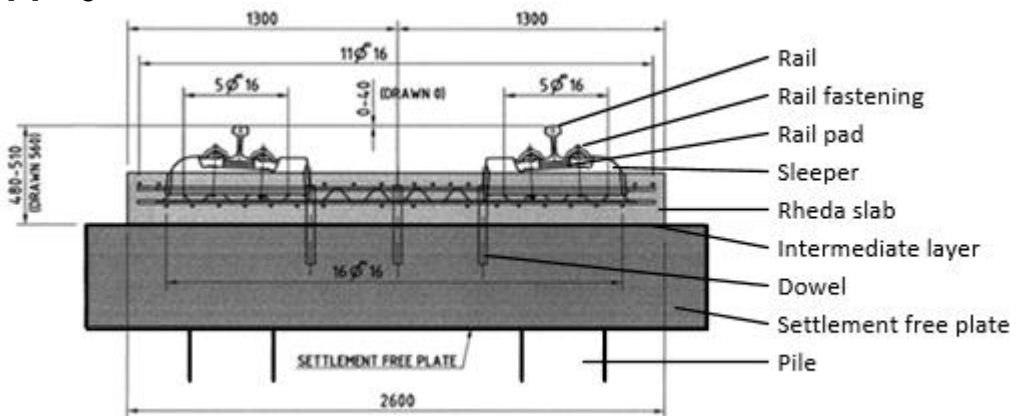

Figure 1: Cross section track structure HSL-South. [2]

For the rails on the HSL-South the UIC60E1 rail profile was used. The rails are connected to sleepers by casting them into the Rheda slab. For the connection between the rails and the Rheda slab the Vossloh 300 HSL fastening system was used [3]. Between the rails and the sleeper elastic pads were inserted to add some elasticity into the fasting system. The stiffness of the elastic rail pad is higher for loads with a short duration. In Table 1 the characteristics of the rails and fastening are given.

Rail	
Rail profile	UIC60E1
Area cross section [cm^2]	76.87
Mass per meter [kg/m]	60.34
Moment of inertia [cm^4]	3055
Section modulus head [cm^3]	335.5
Young's modules [N/mm^2]	210000
Fastening	
Mass fastening system [kg]	12
Support spacing [mm]	600-650
Static vertical stiffness [MN/m]	18.0-22.5
Dynamic vertical stiffness [MN/m]	18.0-60.0
Dynamic vertical damping [kNs/m]	8.0 (10%)

The centre to centre distance of the sleepers is between 600 – 650 mm [3]. Therefore, the rails are not continuously supported, but are discretely supported just like ballast track. For the sleepers prefabricated bi-block sleepers B355.1 NL made by Pfleiderer are used [3]. These sleepers are casted into the Rheda slab. The Rheda slab is in-situ casted during the construction of the HSL-South. The Rheda slab has a variating length depending on the centre tot centre distance of the sleepers and the amount of sleepers per slab. Every Rheda slab has 6, 8 or 10 sleepers which have distance between 600 - 650 mm. Between each Rheda slab there is a joint of 100 mm. The length of the Rheda slab is therefore between 3500 – 6400 mm [4]. To prevent a bond between the Rheda slab and the substructure a geotextile is placed in between. This geotextile adds also elasticity and damping to the construction [5]. The stiffness of the intermediate layer is higher for loads which are only applied shortly. The Rheda slab and SFP are connected by vertical dowels to prevent that the Rheda slab and SFP move horizontally to each other. The dowels can be seen in Figure 1. In Table 2 the characteristics of the Rheda slab and the intermediate layer can be found.

Table 2: Properties of Rheda2000 slab and geotextile in intermediate layer of HSL-South. [3][5]

Rheda2000 slab	
Concrete quality [-]	B35
Length [m]	3.5-6.4
Width [m]	2.6
Height [mm]	240
Bending stiffness [m^4]	0.003
Young's modulus [N/mm^2]	31000
Fictive Young's modulus [N/mm^2]	8570
Mass per meter[kg/m]	1560
Geotextile	
Thickness [mm]	4
Width [m]	2.6
Static vertical stiffness per meter [GN/m]	2.16
Dynamic vertical stiffness per meter [GN/m]	5.8
Dynamic vertical damping per meter [MNs/m]	0.06

2.2 Substructure

The substructure of the HSL-South consists of concrete plates that are constructed onto a pile foundation. As a results these plates should not undergo any settlement and are therefore called a settlement free plate, SFP. Every track is constructed on its own sets of SFP and the SFP of one track is longitudinal nor lateral connected with the SFP of the another track. A single SFP has a length of 30 meter, a width of 3 meter and a height of 500 mm. Every SFP is horizontally connected with the SFP before and after it. This is done to prevent horizontally displacement of the SFP lateral to the track. The SFP are vertically not connected to each other [6].

The pile foundation of a SFP consists of 2 rows of piles, one pile beneath each rail with a centre to centre distance of 1.5 meter [6]. The longitudinal centre to centre pile distance is depending on the local soil conditions. The size and length of the pile is depending on how deep the piles had to been driven into the ground. At the edge of the SFP the piles are placed closer together to reduce a difference in settlement between two SFP [6]. The properties of the SFP can be found in Table 3.

Table 3: Properties of SFP. [6]

Settlement free plate	
Concrete quality [-]	B35
Length [m]	30
Width [mm]	3000
Height [mm]	500

2.3 Type of trains

For the train services over the HSL-South different types of trains are used. At the moment there are three types of trains using the HSL. The types of trains can be divide into high speed trains that reach 300 km/h and conventional trains that drive 160 km/h. Eurostar and Thalys are both using high speed trains and the NS uses conventional trains for their domestic Intercity Direct service.

- Thalys uses the TGV build by Alstom that consists of two locomotives and the carriages in between have Jacob bogies. Figure 2 shows a picture of the Thalys.
- Eurostar uses the Valero e320, an EMU build by Siemens and can be seen in Figure 3.
- NS uses trains that consist of two Bombardier TRAXX locomotives and in between these two locomotives there are 7 or 9 passenger carriages. Figure 4 shows an Intercity Direct.

Figure 2: Thalys [7]

Figure 3: Eurostar [8]

Figure 4: Intercity Direct [9]

Table 4: Train characteristics.

Type of train	Length [m]	Number of carriages [-]	Number of axles [-]
Thalys	200	10	26
Eurostar	399	16	64
Intercity Direct	222	7	36
	275	9	44

2.4 Axle loads

The different types of trains have each their specific axle loads. The TRAXX locomotives have higher axle loads than the coaches in between. But also the Thalys and Eurostar have different axle loads. At the HSL the axle loads and speed of the trains are measured at two locations. These loads are measured by the wheel defect detection system to determine the wheel loads on the track. Figure 5 shows the axle loads of the Thalys, Figure 6 shows the axle loads of the Eurostar and Figure 7 shows the axles loads of the IC Direct. These axle loads have all been measured within the month July of 2019. The data consists the axle loads of 7075 trains. The axle load has been measured for 5182 Intercity Direct, 1566 Thalys and 327 Eurostar.

As can be seen from Figure 5 the most common axle load of the Thalys is around 16.4 ton. The axle loads of the locomotives and the Jacob bogies of the Thalys have roughly the same axle load which results in the common axle load of 16.4 ton. There is also a smaller peak in the graph around 13 ton These smaller peak is caused by the axle loads of the first bogie after the locomotive, which are lower than the other axle loads of the other bogies of the Thalys.
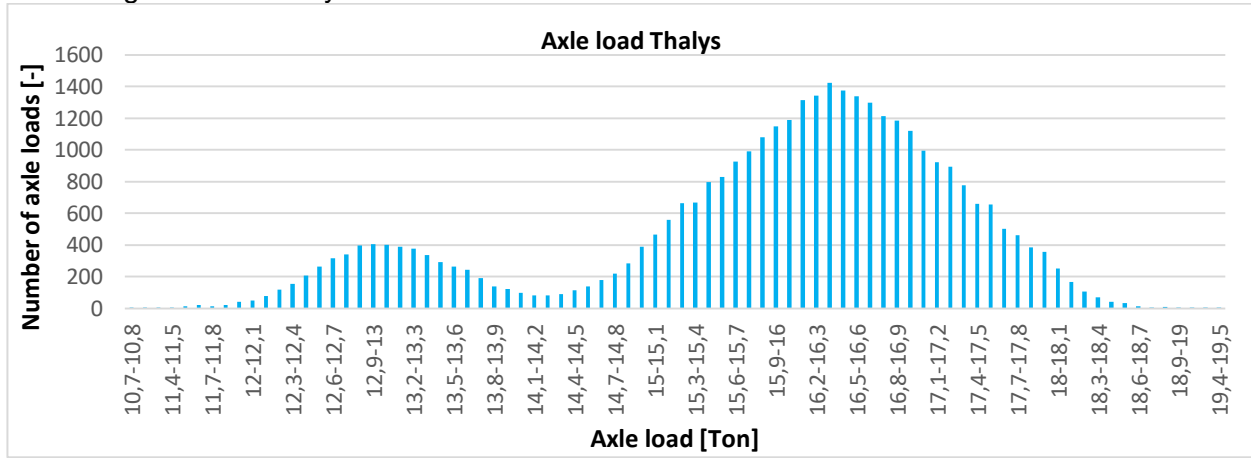

Figure 5: Axle loads of Thalys.

Figure 6 shows the axle loads of the Eurostar. The axle loads of the Eurostar have a greater variation and the magnitude of the axle load ranges between 13.8 and 16 ton. Because the Eurostar uses an EMU as train, the motors of the train are divided over the whole train resulting in lower axle loads. A few axles of the Eurostar have quite a significant lower axle load and have only an average axle load of 12.5 ton.
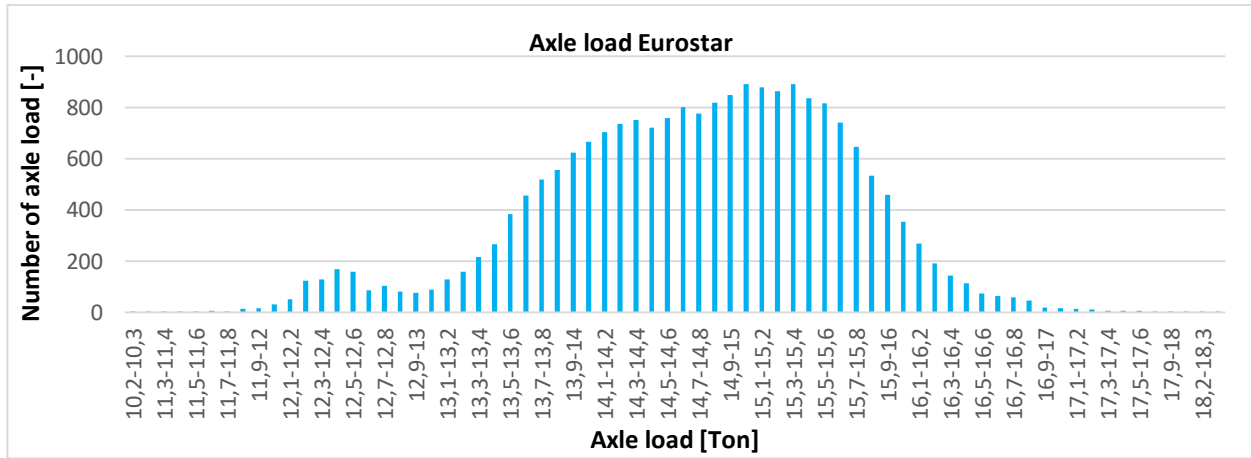

Figure 6: Axle loads of Eurostar.

As can been seen from Figure 7 the axle loads of the IC Direct. Clearly visible is the difference in axle loads of the TRAXX locomotive and the carriages. The locomotive has an average axle load of 21.5 ton. The carriages have much lower average axle load of only 11.4 ton. The axle loads of the Traxx locomotive are also much larger than the axle loads of the Eurostar and the Thalys which have an average axle load of 14.7 ton and 16.4 ton respectively.
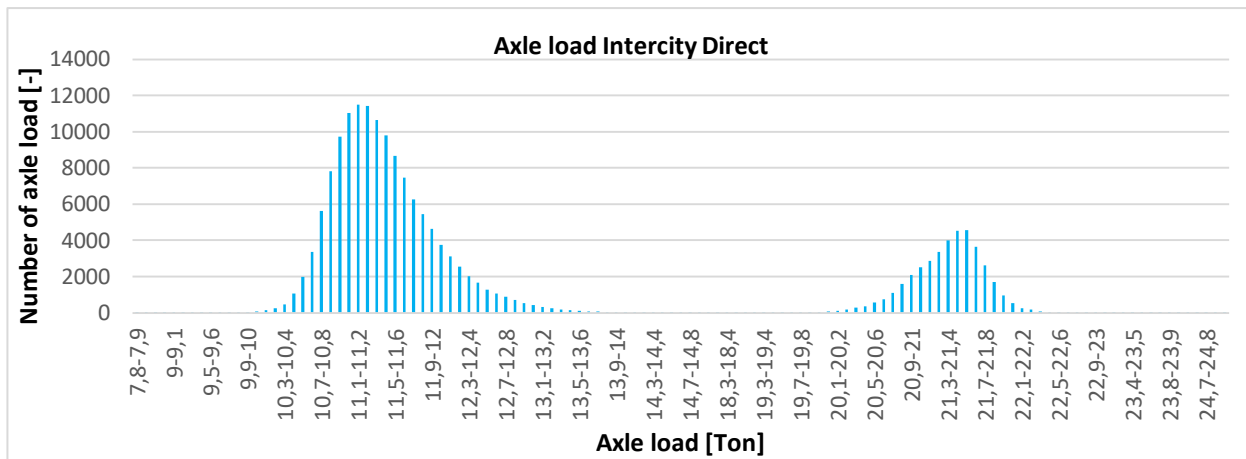
Figure 7: Axle loads of IC direct.

3 Case-study: Schuilingervliet

The substructure of the HSL-South is for a large part constructed as an SFP on a pile foundation. Also, at the location of Schuilingervliet this construction is used. The goal of this construction was to prevent settlements of the HSL-South. However, during measurements it was discovered that at the location of Schuilingervliet large settlements have occurred. Closer investigation learned that there is a difference in settlement between SFP over a length of 3 km. Between two SFP a settlement difference of 0.75 mm is allowed. However, during inspection a settlement difference of 25 mm was measured [10]. The cause of these settlements is unknown, but it is expected to be due to the dynamic loads of the trains driving over the HSL-South.

3.1 Vertical rail geometry

The settlement of the SFP has an influence on the rail geometry of the HSL-South. The vertical rail geometry is the vertical position of the rail along the track. Large deviations of this position can result in derailments. Therefore the rail geometry is measured every three months. In Figure 8 the vertical rail geometry around Schuilingervliet is shown. The data of the measurements is analysed to check if corrections to the rail alignment are required. These corrections to the rail alignment are necessary to maintain the track in operation for high-speed. The rail alignment is corrected by adjusting the level of the rail horizontally and vertically. These corrections are done by adding and removing rail pads in the fastening system. Normally rail pads are used to add elasticity in the rail system, but add the HSL rail pads are also used to realign the track. The fastening system has a limited vertical adjustability with -4 to +56 mm [11]. At some locations at Schuilingervliet the limit of the adjustability of the fastening system is almost reached. At one location the alignment is already corrected with 47 mm [11].
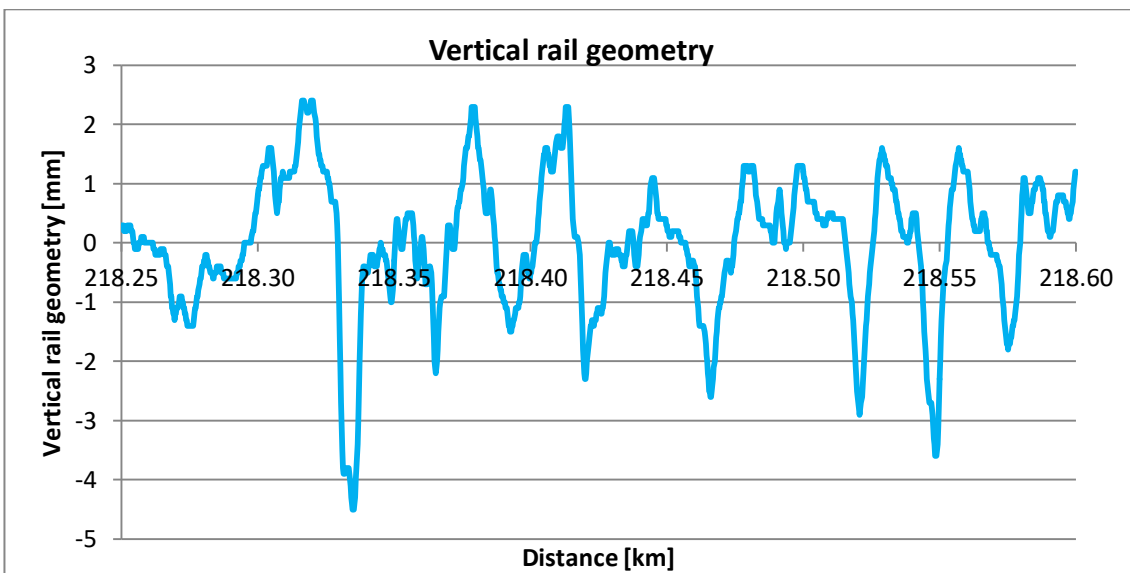

Figure 8: Vertical rail geometry of HSL-South at Schuilingervliet.

3.2 Settlement

To determine the magnitude of the settlement of the SFP measurements have been performed. Figure 9 shows the settlement of different SFP. The measurements in Figure 9 were performed along a part of the track at the location of Schuilingervliet with distance numbers 18.3 - 18.5 km. The rest of the settlement measurements for Schuilingervliet can be found in Appendix A. The settlement is measured at both ends and in the middle of the SFP and is not uniform over the length of the SFP. The middle of the SFP has a lower settlement than the ends of the SFP. The driving direction of the track has also no influence, both the east and west track have the same settlements. Between two adjacent SFP the settlement can be different. Due to this difference in the settlement of the SFP a gap is created between the SFP and the Rheda slab. The Rheda slab is connected to the rails and therefore the Rheda slab starts to hang above the SFP, see Figure 10. This gap between the Rheda slab and the SFP is closed every time a train passes and creates

an extra dynamic load on the pile foundation and the SFP. During measurements it was concluded that the gap varies between 0.89 mm and 1.33 mm [13].
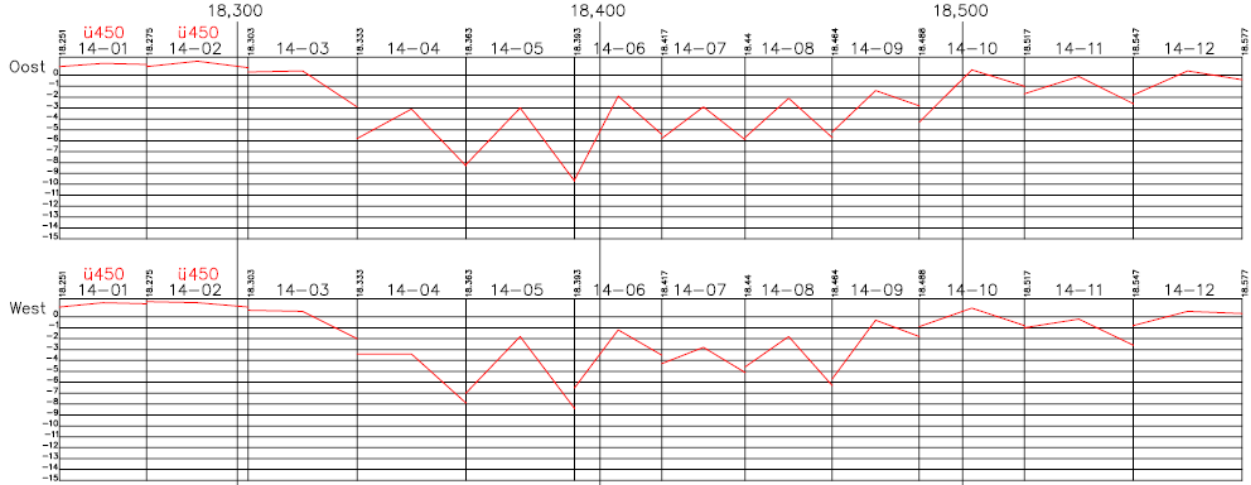

**Figure 9: Settlement of SFP at Schuilingervliet for east (Oost) and west (West) track in mm. [12]**
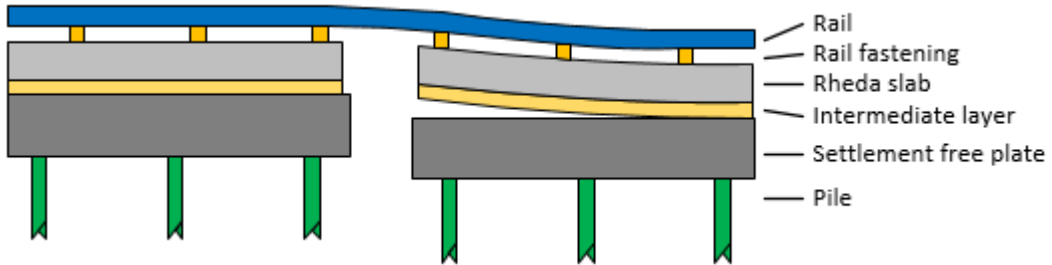
Figure 10: Schematic overview of gap between Rheda slab and SFP.

3.3 Pile foundation

The settlement of the SFP at the location of Schuilingervliet is caused by settlement of the pile foundation. At the location of Schuilingervliet the pile foundation is different than at other locations of the HSL-South. At most places piles with a cross section of 450x450 mm and a length of 30 meters are used. At Schuilingervliet the piles rest on a sand layer closer to the surface. Therefore, piles of 220x220 mm and a length between 7,75 and 10,75 meter are used [10]. The length of the piles varies over the length of track, because the depth of the sand layer regarding to the surface is not constant. Figure 11 shows the depth of the pile toes for each individual SFP for a part of the location of Schuilingervliet with a red line. And as can be seen the depths of the pile toes are not uniform. Figure 11 also shows the geotechnical profile and the green shows the results of different cone penetration test. The cone penetration tests are performed to determine the resistance of the soil. The geotechnical profile and pile depth for the rest of the location of Schuilingervliet can be found in Appendix A.
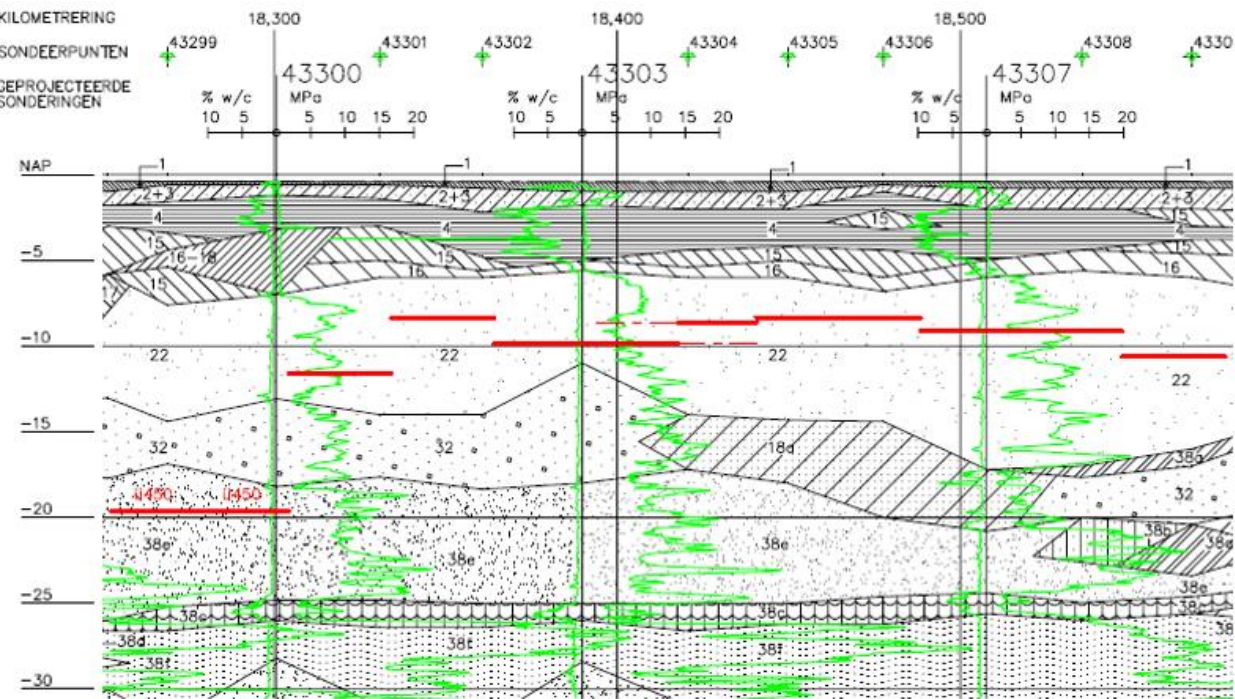
Figure 11: Red line shows pile toe depth for each SFP at location of Schuilingervliet in meter below NAP. [14]

The shorter piles are placed closer to each other, resulting in more piles per SFP. At Schuilingervliet 2 rows of 28 piles have been constructed. The SFP has a length of 29.9 meter and the centre-to-centre distance of the piles is: 0.375 – 0.75 x2 – 1.0 – 1.15 x21 – 1.0 – 0.75 x2 – 0.375 meter. The characteristics of the pile foundation near Schuilingervliet are given in Table 5. At locations were the bearing capacity of the cross sectional 220x220 mm piles was not strong enough, larger piles with a cross section of 250x250 mm have been used. These are mostly used near the edges of the SFP to reduce settlement difference between the SFP. At places where the higher located sand layer had not enough bearing capacity larger cross sectional 450x450 mm piles are used. These piles are driven into a deeper sand layer and have a length of 20 meter. At locations where larger piles were used the SFP has an length of 28 meter and the piles have a centre-to-centre distance of 0.7 – 3.3 – 4.0 x5 – 3.3 – 0.7 meter [6]. The characteristics of the longer piles are also shown in Table 5.

Table 5: Pile foundation at location of Schuilingervliet. [6]

Pile foundation Schuilingervliet		
Pile size [mm]	220	450
Number of piles per row [-]	28	8
Centre to centre edge of slab [mm]	750	700
Centre to centre middle of slab [mm]	1150	4000
Pile stiffness per pile [MN/m]	65	200

3.4 Train speed

During the investigations of the settlement also the train speed of the trains was measured by Dekra Rail [15, 16, 17, 18]. The train speed of the different trains at the location of Schuilingervliet is given in Table 6.

Table 6: Train speed at Schuilingervliet. [15][16][17][18]

	Minimum speed [km/h]	Average speed [km/h]	Median speed [km/h]	Maximum speed [km/h]
IC Direct	137.5	159.3	160.2	164.0
Thalys	149.5	237.1	255.6	299.1
Eurostar	152.6	252.5	272.1	307.2

3.5 Injections

To mitigate the problems due to the settlement of the SFP at Schuilingervliet a test was performed to increase the bearing resistance of the pile foundation. The test consist of pile toe injections with micro-cement to increase the bearing resistance [19]. At the level of the pile toe micro-cement is injected into the soil. The micro-cement forms spheres in the soil which increases the length and size of the piles. Also, the injections results in an increase of stiffness and strength of the soil around the pile toe [19]. Figure 12 shows a cross section of the plan of the pile toe injections. The pile toe injections are only performed at one side of the dilation of the SFP at the test location [20]. The pile toe injections results in an estimated increase of the bearing resistances of the pile foundation with a factor 2.2 to 3.3. Also, the pile stiffness can be increased with a factor of 2.3 from 65 kN/m to 154 kN/m [19]. This new pile stiffness is slightly overestimated due to using the stiffness of concrete for the elongated pile toe [19]. Although the first results of this method were promising and no settlements occurred for these joints. After two years of measuring one joint shows again problems with settlements.
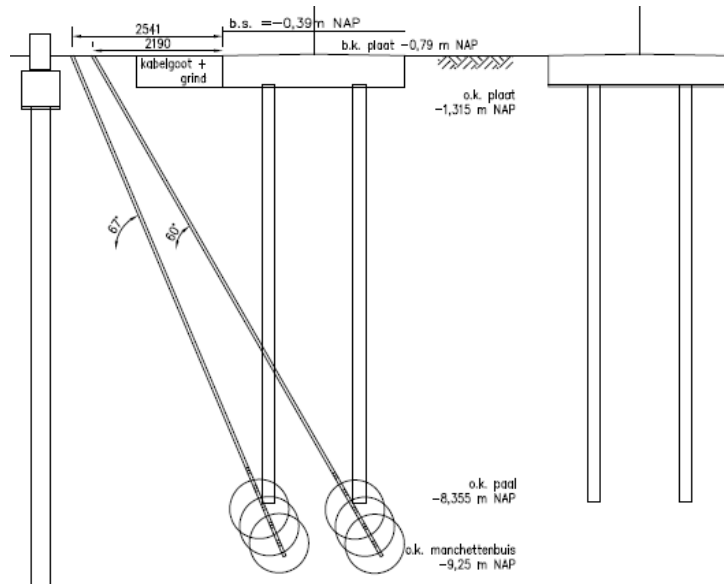

Figure 12: Cross section pile toe injections. [20]

4 Numerical Modelling

In this chapter the simulation software program DARTS will be discussed. DARTS stands for Dynamic Analysis of Rail Track Structures. This software program is used to simulate the dynamic behaviour of the HSL-South in order to get more insight in how to mitigate the problems caused by settlements of the track structure. The different input parameters of track structure and train models for DARTS will also be discussed. DARTS is developed at the TU Delft within a Fortran environment. The program runs on a Windows XP computer. The time to perform a simulation depends on the length of the model and the integration time. The simulations that have been performed in this research took between 7 and 45 minutes.

4.1 DARTS

For the dynamic analysis of the HSL-South slab track, the software program Dynamic Analysis of Rail Track Structures (DARTS) has been used. DARTS is written to analyse track structures on an elastic foundation loaded by moving vehicles [21]. To analyse the strength and stiffness of railway structures an one dimensional beam model is used. In DARTS it is possible to analyse classical track structures, which consist of a rail, sleeper and ballast or embedded track structures, which consist of rail which is continuously supported. To model these structures a two or three beam model is made in which the rigid beams are separated by an elastic layer [22]. In classic track structures between the rail and sleeper a rail pad is used as an elastic layer. In continuous supported rail structures between the rail and supported stiff slab an elastic material is placed. This results in a structure where stiff and elastic layers are alternated. In Figure 13 an example of the schematized track structure is given.

In DARTS the track structured can be loaded by different types of loads. Static point or distributed loads can be applied. Also, moving loads or dynamic loads can be used [22]. Furthermore, the structure in DARTS can be loaded by a moving train. A moving train is modelled as a series of masses, springs and dampers driving on the track [22]. The modelled train creates a dynamic load by driving over the track and following the vertical rail geometry. Between the rails and wheels of the train a so-called Hertzian spring is located. The distance between the wheel of the train and the rail changes and the Hertz spring applies a load at the track and the train [21]. And due to this the vertical rail geometry creates a dynamic load on the track.

In DARTS the results of the moving load are calculated by integrating the responses over time. The track model is divided into elements and the displacements due to the load are evaluated for each time step. The resulting stresses and forces of the moving load are determined by fine element method processes [22].
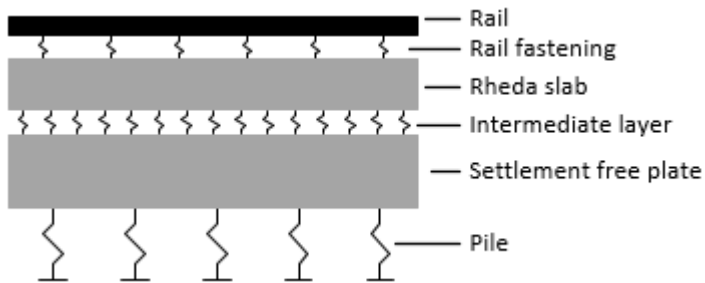
Figure 13: Schematic drawing of track structure.

4.2 DARTS track model

In DARTS the HSL-South is modelled as a three beam model where the beams are separated by an elastic layer. Therefore, the model consists in total of six layers. From top to bottom the six layers are: rail; fill (rail fastening); Rheda slab; intermediate layer; foundation (SFP); formation (pile foundation). An schematic overview of the model is given in Figure 14.

Some assumptions are made for the model in DARTS. Only half of the cross section of the structure is modelled in DARTS, this is done because of symmetry of the track structure and to reduce computation times. The element length is chosen to be 0.13 meter, because the distance between sleepers is 0.65 meter. Therefore, the fill layer in DARTS consists of five elements, one for the sleeper and rail fastening and four elements for the gap in between the sleepers. The model has a length of 10 SFP resulting in a total

length of 299 meter and 2300 elements. There is chosen for a length of 10 SFP, because the track model should have twice the length of the trains in DARTS. As a result of this decision the trains will be shorter than described in Chapter 2. However, the effect of this decrease in length of the trains is expected to have negligible effect on the results. By shorting the trains the number of load repetitions will be decreased, but this will not have an influence on the load that is applied. With this decrease in length the computation time will be reduced.

In DARTS two versions of the track model have been made. One model is made with the smaller 0.22x0.22 meter piles. This model has a length of 299 meter. The other model that is made has the larger 0.45x0.45 meter piles and is 286 meter long. For both models the element length of 0.13 meter is used. The other input parameters are based on the characteristics of the HSL-South given in Chapter 2 and can be found in Table 7. An example of the input file for DARTS can be found in Appendix B.
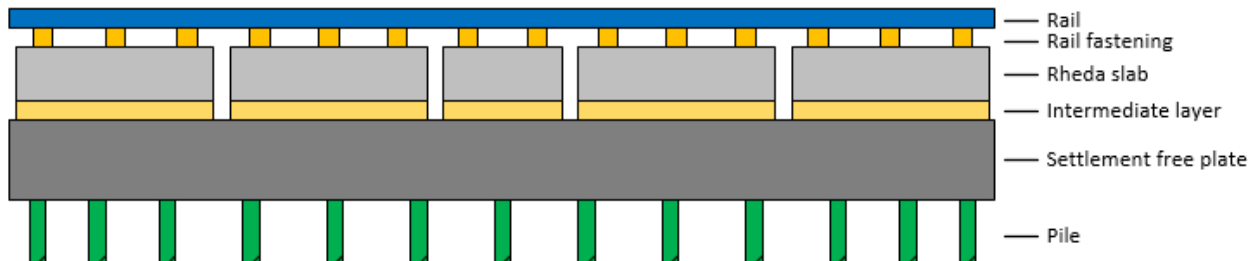

Figure 14: Schematic overview of SFP in DARTS. Not all piles and rail fastening are shown.

Table 7: Input parameter of rail and fill layer in DARTS.

Rail properties	
Rail profile	UIC60E1
Area cross section [cm^2]	76.87
Moment of inertia [cm^4]	3055
Rail radius [mm]	300
Fill properties	
Young's modulus [N/m^2]	4.62E+08
Damping [Ns/m^2]	6.15E+04

For the model version with smaller piles is chosen to have 5 Rheda slabs on each SFP. Four Rheda slabs have 10 rail supports per slab and are 49 elements long, resulting in a length of 6.37 meter for each slab The middle Rheda slab on the SFP is shorter with 6 rail supports and is 29 elements or 3.77 meter long. The Rheda slabs are 0.03 meter shorter than at the HSL and the gap between the Rheda slab is 0.03 meter longer. This small difference is due to the chosen element length of 0.13 meters.
The model version with larger piles is 0.6 meter longer and therefore the Rheda slabs are also longer. Also in the model with larger piles there are 5 slabs on each SFP. There are two slabs which have 10 rail supports and are 49 elements long, which is 6.37 meter. The other three slabs have 8 rail supports each and are 39 elements long or 5.07 meter long. Also in this version the Rheda slabs are 0.03 meters shorter and the gap between the Rheda slabs is 0.03 meters longer. Between the Rheda slab and the SFP the Geotextile is simulated by an intermediate layer. The input parameters for DARTS of the Rheda slab and the intermediate layer are given in Table 8 and result from the characteristics of the elements in Chapter 2.

Slab properties	
Width [m]	1.3
Height [m]	0.24
Young's modulus [N/m^2]	8.57E+09
Poisson's ratio [-]	0.16
Mass [kg/m^3]	2500
Intermediate layer properties	
Young's modulus [N/m^2]	2.23E+09
Damping [Ns/m^2]	2.31E+04
Width [m]	1.3

The SFP in the model with smaller piles is 229 elements long, which is 29.77 meter long and therefore 0.13 meter shorter. Between the different SFP there is a gap with the length of 1 element. The pile foundation is simulated with a length of 2 elements, 0,26 meter, instead of 0,22 meter. The centre-to-centre pile distance is in the model also different with: 0.39 – 0.65 x2 – 1.04 – 1.17 x21 – 1.04 – 0.65 x2 – 0.26 meter. At the end of the SFP the piles are placed closer together than in the middle of the slab where there is more space between them. The SFP of model with larger piles is 219 elements long or 28.47 meter. This is 0.6 meters longer than the SFP of the HSL-South. Therefore, also the pile distances will be larger. The piles have been simulated with three elements and are 0.39x0.39 meter, which is smaller than the 0.45x0.45 meter piles. The centre-to-centre pile distance of the model are: 0.585 – 3.25 – 4.16 x5 – 3.25 – 0.585 meter. All input parameters for both models of the SFP and the piles in DARTS are in Table 9. The pile damping is based on the vertical stiffness of the pile. Therefore, Equation 1.1 is used. For the damping value a percentage of 20% is used [23]. This value is based on assumptions made in the design process of the HSL-South. The mass of the track structure is based on the mass per meter multiplied with the pile distance.

$$c = 2\zeta\sqrt{km} \qquad (1.1)$$

In which:
- c = vertical pile damping
- ζ = damping value
- k = vertical pile stiffness
- m = mass of track structure

Table 9: Input parameters of foundation and formation layer.

Foundation properties	
Width [m]	1.5
Height [m]	0.5
Young's modulus [N/m^2]	2.00E+10
Poisson's ratio [-]	0.16
Mass [kg/m^3]	2500
Formation properties small piles	
Young's modulus [N/m^2]	9.62E+08
Damping [Ns/m^2]	2.67E+06
Width [m]	0.26
Formation properties large piles	
Young's modulus [N/m^2]	1.31E+09
Damping [Ns/m^2]	3.88E+06
Width [m]	0.39

4.3 DARTS train models

The track model of DARTS is load by a moving train model. The train model consists of series of masses, springs and dampers. Properties for the spring and dampers are based on assumptions made during the design of the HSL-South. These assumptions can be found in Appendix B [24]. For the masses of the bodies, bogies and wheels of the train models the assumptions have been adjusted to match the measured axle loads of Chapter 2. Therefore, the average axle load of every axle is determined, these axle loads can also be found in Appendix B. With this average axle load the body mass is adjusted in such way that it matches the average axle load.

Due to length of the model in DARTS of 299 meter the train models are also shorter. The model of the train is about half of the length of the track model to be able to drive freely over the track model. Therefore, the trains models have been reduced to a length of 125 meter. The trains have been shorted by reducing the number of carriages of the trains and by removing the second TRAXX locomotive of the Intercity Direct. It is expected that this reduction in the length of the trains will not have an influence on the results, because only the number of wheel loads has been reduced. Due to a lower number of wheel loads there will be less load cycles which results in a shorter computation time. The assumptions for the train models are shown in Table 10. The input files for the trains in DARTS can be found in Appendix B.

4.4 Model limitations

The model in DARTS is a simplification of the structure of the HSL and therefore the DARTS model will have some limitations. The largest simplification in the DARTS model is the formation layer which is used to simulate the pile foundation. The pile foundation consists of concrete piles that transfers the load along the shaft and through the pile toe to the soil layers. In the simulations in DARTS the concrete pile and the soil layers are modelled as one elastic layer with stiffness and damping characteristics. Due to this simplification it is not possible to simulate the different characteristics of the soil layers or the changing pile length. Only the stiffness and damping of the formation layer can be altered.

Another limitation of the model in DARTS is that the displacements are elastic. Therefore, the elements will return to their original position after a train passage. The load of the trains will not result in permanent displacements for the elements. Also, it is not possible to insert height difference in the model to simulate a permanent displacement for example the settlement of the pile foundation. Because, it is not possible in DARTS to enter a height difference, the simulation of the gap between the Rheda slab and SFP and the settlement of the pile foundation have to be modelled with a reduction of the stiffness at those elements to increase the displacements at those locations.

Table 10: Properties of train models.

Train properties		Thalys		Eurostar		Intercity Direct
Train configuration (carriage nr)		1-2-3-3-2-1		1-2-2-2-1		1-2-2-2-2
	Carriage nr.	Properties	Carriage nr.	Properties	Carriage nr.	Properties
Body mass [kg]	1	54000		43400	1	40000
	2	25200			2	34800
	3	25200				
Body length [m]	1	22.15	1	26.035	1	18.9
	2	21.845	2	24.775	2	26.4
	3	18.7				
Bogie mass [kg]		2800		3600	1	16800
					2	2600
Bogie spacing [m]	1	14; 6.275		17.375; 7.4	1	10.44; 7.93
	2	18.7			2	19; 7.4
	3	18.7				
Wheel mass [kg]		1000		1000	1	1500
					2	750
Axle spacing [m]		3		2.5	1	2.6
					2	2.56
Axle loads [kN]		4 x 16.9 + 2 x 13 + 8 x 16 + 2 x 13 + 4 x 16.9		20 x 14.7		4 x 21.4 + 16 x 11.5
Primary suspension stiffness per wheel [kN/m]		1150		400	1	2232
					2	2800
Primary damping per wheel [kNs/m]		15		5	1	45.7
					2	1.25
Secondary suspension stiffness per bogie [kN/m]	1	600		300	1	2400
	2	600; 300			2	1593
	3	300				
Secondary damping per bogie [kNs/m]	1	48		24	1	139
	2	48; 24			2	35
	3	24				
Wheel radius [m]		0.42		0.42	1	0.59
					2	0.46
Total train length [m]		125.39		126.395		124.5

5 Simulations

In this chapter the results from the DARTS simulations will be discussed. First, the model will be validated by comparing the results of the simulations of DARTS with measurements of the HSL-South. The validation of the model will be performed for the wheel loads by comparing the wheel loads of the train models in DARTS with the measured axle loads of the HSL. Also, the displacements will be validated by comparing the displacement of the DARTS model with displacement measured during field measurements. Next, the computational results of the displacements and the internal forces of the track structure will be discussed. Also, the forces that structure will transfer to the pile foundation will be discussed.

In DARTS multiple simulations have been performed. Different versions of the track model have been used to determine the influence of the design of the pile foundation and the stiffness of the pile foundation. Also, the influence of train speed is analysed by performing simulations with different train velocities. The performed simulations in this study are shown in Table 11.

<div align="center">Table 11: Overview of the performed simulations in DARTS.</div>

Model version	Pile stiffness [MN/m]	Train	Velocity [m/s]	Remark
Model A	61.75	Intercity Direct Thalys Eurostar	22; 28; 44 22; 28; 44; 56; 70; 75; 80; 83 22; 28; 44; 56; 70; 75; 80; 83	Model version with short piles and constant pile stiffness
Model B	200	Intercity Direct Thalys Eurostar	44 83 83	Model version with large piles and constant pile stiffness
	Variations within model A			
A.1	Version of model A to simulate changing pile length by altering pile stiffness for a SFP. Pile stiffness used (61.75; 44.46; 52.44 MN/m)			
A.2	Version of model A where settlement of piles is simulated by reducing pile stiffness near joint SFP. Pile stiffness is reduced with 50% for pile next to the joint and for piles further away from the joint the reduction is less.			
A.3	Version of model A with reduced stiffness of the intermediate layer to simulate the gap between Rheda slab and SFP. Stiffness of the intermediate layer is reduced for elements next to the joint.			
	Possible solutions using model A			
A.4	Possible solution using model A by connecting the SFP.			
A.5	Possible solution using model A by placing a Rheda slab over the joint between the SFP			
A.6	Possible solution using model A by increasing the pile stiffness near joint of the SFP			

The results of the simulations performed in DARTS have been analysed near the end of the model. The model starts at element 1 and is 2300 elements long. The results of DARTS have been analysed from element 1725 to 2185. These elements are chosen because there are two joints of the SFP which can be studied. The elements near the end of the model have been selected, so that initial disturbances in the model can damp out before a train passes these selected elements of the model. In Figure 15 also the element numbers of the joints and middle of the SFP are given and the element numbers of the start and the end element.
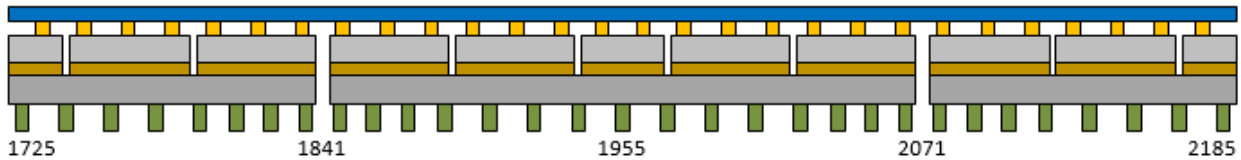

Figure 15: Schematic view of analysed location of DARTS model. Element numbers are given for start, end, middle and location of gaps. The figure is not on scale and not all piles and rail fastening are shown.

5.1 Model validation

The responses of the DARTS model have been compared with field measurements of the HSL to verify the DARTS model. Therefore, the wheel loads of the trains models are compared with the measured wheel loads of the HSL-South, which have been discussed in Chapter 2. Furthermore, the displacements of the DARTS model are compared with displacements that have been measured by Dekra Rail in the field.

5.1.1 Wheel loads

The wheel loads of the trains in DARTS and the average wheel loads measured at the HSL-South, which have been derived from the measured axle loads, can be found in Table 12. In Table 12 also the difference between the measured wheel load and the wheel load used in DARTS is given as a percentage. As can be seen the wheel loads used in DARTS are all lower than the average wheel loads that have been measured at the HSL-South. This difference in wheel loads is the highest for the Jacobs bogies of the Thalys with a maximum difference of 2.24 %.

Table 12: Axle loads in DARTS and measured average wheel load and the difference.

		DARTS [kN]	HSL [kN]	Difference [%]
ICD	Traxx	104.82	106.63	-1.69
	ICR	56.34	57.06	-1.27
Thalys	Motor bogie	83.32	84.66	-1.58
	Trailer bogie	64.70	64.83	-0.20
	Jacob bogie	78.25	80.04	-2.24
Eurostar		71.76	73.26	-2.05

5.1.2 Displacements

Next, the displacements of the HSL-South and the DARTS model have been compared. The displacement of the rail, the Rheda slab and the SFP at the joint between two SFP have been analysed with high-speed cameras at the HSL-South by Dekra Rail [Dekra]. The displacement is measured at one reference location (219.989 km) at Schuilingervliet where no settlements have been measured [15]. Furthermore, Dekra Rail has measured the displacement at one location (219.464 km) before and after pile toe injections have been performed [16, 17]. And at one location (218.333 km) the displacements have been measured two years after pile toe injections [18]. The maximum displacements measured during the field measurements can be found in Appendix C. For the model verification the average of these maximum displacements at the reference location have been compared with the maximum displacements of the DARTS model.

The input parameters of the DARTS model have been discussed in Chapter 2 and 3 and are given in Chapter 4. The simulation has been performed with a vertical stiffness of 60 MN/m for the railway fastening and a pile stiffness of 65 MN/m. The displacement measured at the HSL, the results of DARTS and the difference between them can be found in Table 13.

		Measurements HSL [mm]	Results DARTS [mm]	Difference [%]
Intercity Direct	Rail	1.55	1.28	-17.6
	Rheda slab	0.51	0.61	21.6
	SFP	0.57	0.60	5.6
Thalys	Rail	1.48	1.06	-28.6
	Rheda slab	0.56	0.58	3.4
	SFP	0.56	0.56	0.7
Eurostar	Rail	2.10	0.97	-54.0
	Rheda slab	0.65	0.49	-24.0
	SFP	0.60	0.48	-19.5

Table 13 shows that there is a large difference in rail displacements between DARTS and the field measurements. The modelled displacements of the rails are for all trains lower than measured at the HSL. The displacements of the Rheda slab and the SFP for the Thalys are close to the measured values. The displacement of the SFP for the Intercity Direct is also comparable to the measured displacements. The modelled displacements for the Eurostar are lower than have been measured and the displacement of the Rheda slab for the Intercity Direct is larger than has been measured.

The difference of the Eurostar is much larger than for the other two trains. The field measurements at the reference location were based on only one Eurostar measurement and this measurement could not be accurate. When the field measurements at the other location are compared, they show that the displacements of the Eurostar are comparable with the Thalys and lower than the displacements of the Intercity Direct. Because there is only one measurement for the Eurostar, which is also larger than all other measured displacements, the Eurostar is neglected in the further model verification.
Another possibility for the lower displacements of the Eurostar is that the train model of the Eurostar in DARTS has the average axle load of 14.7 kN, but measurements shows that there are higher axle loads up to 16 kN. These lower axle loads of the model of the Eurostar can result in the lower displacements.

Due to the large difference between the DARTS model and the field measurements, simulations with altered parameters have been performed. In these simulations the stiffness of the rail fastening and the pile stiffness have been changed. The vertical stiffness of the rail fastening ranges between 22 to 60 MN/m. The first simulation was performed with 60 MN/m, but resulted in too small rail displacements. By lowering the stiffness of the rail fastening the displacement of the rail will be increased. Therefore, simulations have been done with a rail fastening stiffness of 30, 35 and 40 MN/m.
The difference in displacement for the Rheda slab and SFP is for the Thalys close to the displacements measured at the HSL. However, by lowering the rail stiffness the displacement of the Rheda slab and SFP decreases and the difference between the results of DARTS and the measurements becomes too large. By lowering the stiffness of the pile foundation, the displacement of the Rheda slab and the SFP can be increased again. The first simulation was performed with an estimate pile stiffness of 65 MN/m. The next simulations have been performed with a pile stiffness of 58.5, 61.75 MN/m.

The results of these simulations have been compared with the field measurements and the difference is shown in Table 14. Differences smaller than 5% have a green background, for displacements between 5 and 10% the background is yellow. For difference between 10 and 20% the background is orange and for differences larger than 20% the background colour is red.

Table 14: Difference between displacements DARTS and field measurements HSL as percentage.

		Rails				Rheda slab				SFP			
Stiffness rail fastening [MN/m]		30	35	40	60	30	35	40	60	30	35	40	60
Pile stiffness [MN/m] 65	Intercity Direct	14.2	5.3	-1.4	-17.6	14.2	15.7	16.8	21.6	-0.4	0.9	1.9	5.6
	Intercity Direct adjusted					1.9	3.2	4.2	8.5				
	Thalys	0.4	-7.1	-12.9	-28.6	-8.8	-6.1	-3.8	3.4	-11.3	-8.7	-6.4	0.7
	Eurostar				-54.0				-23.9				-19.5
Stiffness rail fastening [MN/m]		30	35	40	60	30	35	40	60	30	35	40	60
Pile stiffness [MN/m] 61.75	Intercity Direct			0.0				22.6				7.1	
	Intercity Direct adjusted							9.3					
	Thalys			-11.3				0.0				-2.5	
	Eurostar												
Stiffness rail fastening [MN/m]		30	35	40	60	30	35	40	60	30	35	40	60
Pile stiffness [MN/m] 58.5	Intercity Direct			1.6				28.9				12.7	
	Intercity Direct adjusted							15.0					
	Thalys			-9.5				4.2				1.6	
	Eurostar												

Table 14 shows that decreasing the rail stiffness results in a smaller difference between the measured rail displacement and the DARTS results. Also, the Intercity Direct has smaller differences for the SFP with an higher pile stiffness, but the displacements of the Rheda slab and SFP for the Thalys decreases when the rail stiffness is lowered. By decreasing the pile stiffness the displacement of the Rheda slab and SFP can be increased again to the measured values. The displacement of the Rheda slab for the Intercity Direct is even with a pile stiffness of 65 MN/m too large. A closer look at the field measurements of the Intercity Direct for the Rheda slab shows that the Rheda slabs has an average maximum displacement of 0.51 mm and the SFP has an average maximum displacement of 0.57 mm. This difference in displacement is interesting, because the Rheda slab is constructed on top of the SFP. Thus, a large displacement for the SFP will result in a gap between the Rheda slab and the SFP and the Rheda slab will 'float' above the SFP. If this displacement of the Rheda slab is adjusted to the same displacement of the SFP, the difference for the Rheda slab is much smaller for the Intercity Direct.

Based on the performed simulation and the adjusted measurements, a rail fastening stiffness of 40 MN/m and a pile stiffness of 61.75 MN/m is chosen for the DARTS model. This combination of rail fastening stiffness and pile stiffness results in the smallest total difference. For simulations with these parameters the rail displacement for Intercity Direct is spot on. On the other hand the rail displacement of the Thalys is too small and has a difference of -11.3%. However, for the displacement of the Rheda slab the results of the Thalys are spot on and show the results of the Intercity Direct a difference of 9.3%. But the total difference for these simulations is the lowest with a pile stiffness of 61.75 MN/m and a rail fastening stiffness of 40 MN/m.

5.2 Displacement

First, the displacement of the DARTS model have been analysed. Figure 16 shows the displacement of rails for the Intercity Direct at a speed of 44 m/s (160 km/h) for element 1955 in the middle of a SFP. Clearly visible is that the Traxx locomotive of the Intercity Direct has a larger displacement than the coaches. The firsts displacement at t = 3 s are form the Traxx locomotive with a maximum displacement of 1.75 mm. The displacements due to the Traxx locomotive are almost a factor 2 larger than the displacements of the carriages, which have a maximum displacement of 0.99 mm. This difference in displacement results due to the difference in axle load. The Traxx locomotive has also axle loads that are almost twice as large as that of the carriages.

Figure 17 shows the displacement of the Rheda slab for the Intercity Direct at same location in the middle of the SFP. In Figure 17 can be seen that the displacement of the Rheda slab follows the same pattern as the displacement of the rail. The displacement of the Rheda slab is around half of the displacement of the rail. The maximum displacement is 0.71 mm for the TRAXX locomotive and 0.39 mm for the carriages. Also, here the Traxx locomotive has a displacement that is roughly twice as large as the displacement of the carriages.

Figure 18 shows the displacement of the SFP loaded by the Intercity Direct also in the middle of the SFP. The displacements of the SFP and Rheda slab have the same magnitude. Again the Traxx locomotive has displacements that are double that of the displacement of the carriages. The maximum displacement of the TRAXX locomotive is 0.70 mm and the maximum displacement of the carriages is 0.39 mm.

There is a difference in the magnitude of the displacement between the displacement in the middle of the SFP and at the end of the SFP. Figure 19 shows the displacement of the rail for element 1841 at the joint between two SFP and for element 1955 in the middle of a SFP. The displacement at the end of the SFP is smaller than in the middle of the SFP. In the middle of the SFP the maximum displacement is 1.75 mm and at the end of the SFP the maximum displacement is 1.53 mm. The difference between the maximum displacement at the end and at the middle of the SFP is 13%.

Figure 20 shows the maximum displacement for each element. Around element 1841 and 2071 the maximum displacement is lower than at the other elements. As can be seen in Figure 15 at the location of element 1841 and 2071 the joint between the SFP is located. At the joint between two SFP the piles of the foundation are placed closer together. Due to the smaller centre-to-centre distance for the piles at the end of the SFP, the stiffness of the SFP near the end is increased. The result of this increased stiffness is that the displacement of the construction near the joint between two SFP is lower than in the middle of the SFP.

Figure 21 shows the displacement of the rail for the Thalys and Eurostar with a velocity of 83 m/s (300 km/h) at element 1955 in the middle of the SFP. The displacement of the rail of the Thalys is larger than the displacement of the Eurostar. But the displacement of both trains is lower than the displacements of the Intercity Direct. The maximum displacement of the trains and the difference compared to the maximum displacement of the Intercity Direct is given in Table 15.

Also, the difference in axle loads of the Thalys is visible. The displacement for the wheels of the Thalys is not constant. The wheels at the start and end of the train have higher displacements. The axle loads of the Thalys are at the begin and end of the train also larger because at this position the locomotives of the Thalys are located. The displacement of the Eurostar are constant, but also the axle loads of the Eurostar are more constant than the axle loads of the Thalys.

From the displacements it can be concluded that the rail has larger displacements than the Rheda slab and SFP. Also, the displacements of the Rheda slab and SFP have a similar magnitude. Furthermore, higher axle loads result in larger displacements. The Traxx locomotive has high axle loads and that results in large displacements. The displacements of the Intercity Direct are larger than the displacements of the Thalys or Eurostar. Also, the displacements at the end of the SFP are 13% smaller than in the middle of the SFP. The centre-to-centre distance of the pile foundation is smaller near the end of the SFP, making the structure more stiff. This results in lower displacements at the end of a SFP.

Table 15: Maximum rail displacement and difference.

| Train	Maximum displacement rail [mm]	Difference [-]
Intercity Direct	1.90	1.00
Thalys	1.57	0.83
Eurostar	1.46	0.77
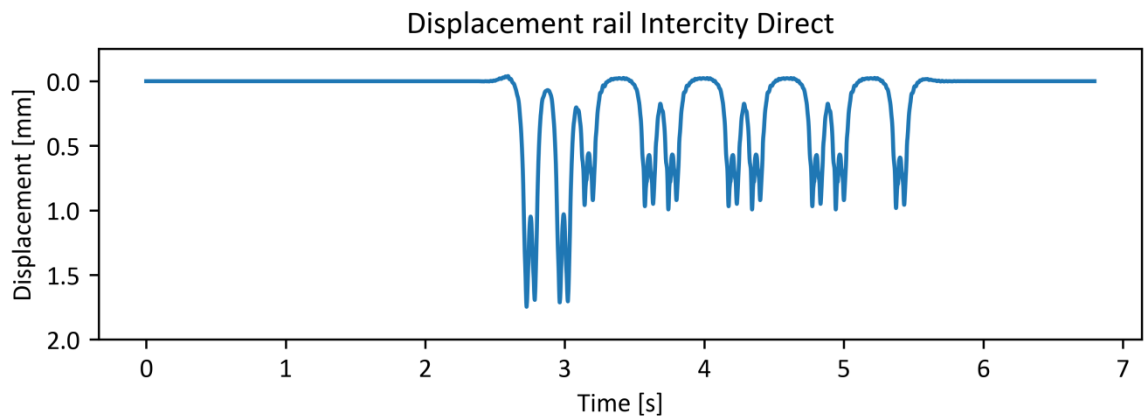
**Figure 16: Rail displacement Intercity Direct at 160 km/h for element 1955.**
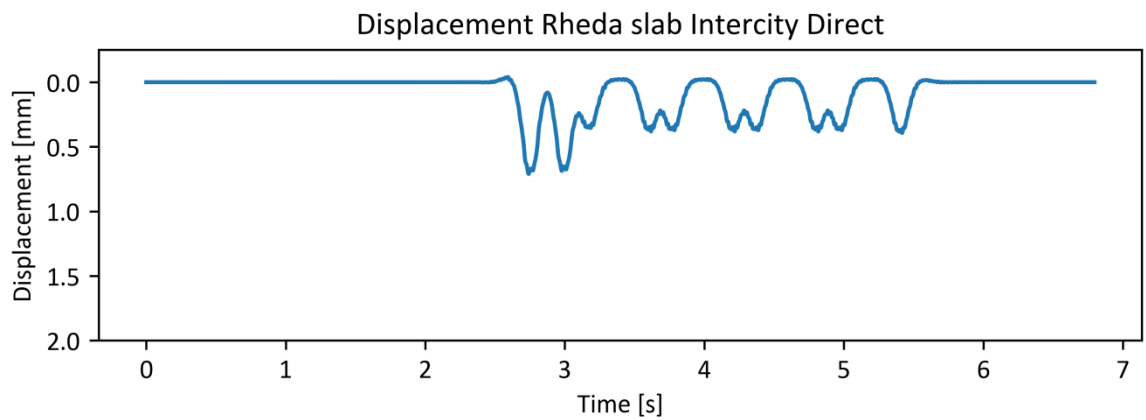
Figure 17: Rheda slab displacement Intercity Direct at 160 km/h for element 1955.
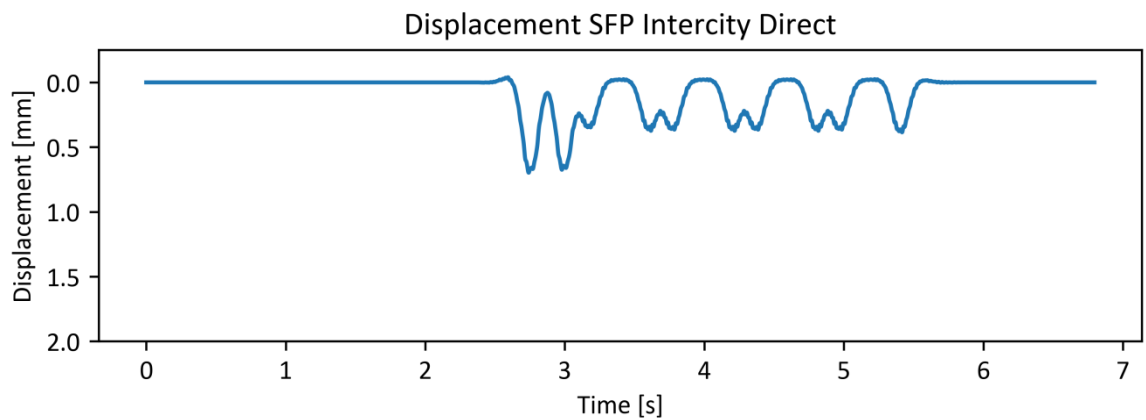

Figure 18: SFP displacement Intercity Direct at 160 km/h for element 1955.
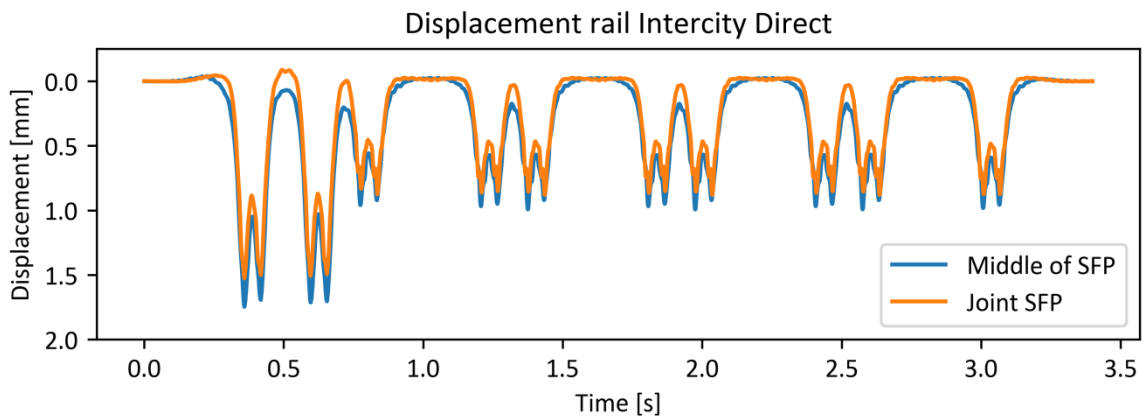
Figure 19: Rail displacement Intercity Direct at 160 km/h for element 1841 and 1955. Both figures are shifted in time to overlap.
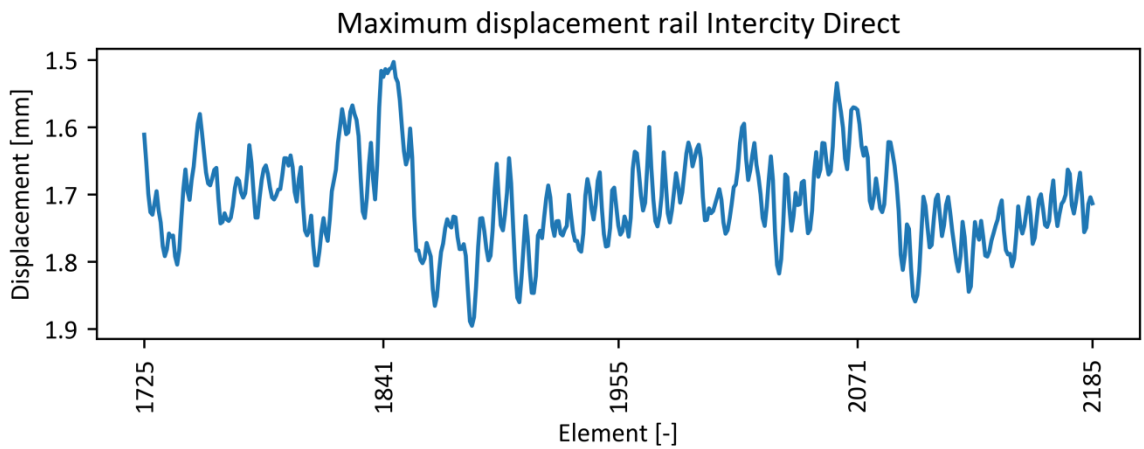

**Figure 20: Maximum rail displacement Intercity Direct at 160 km/h.**
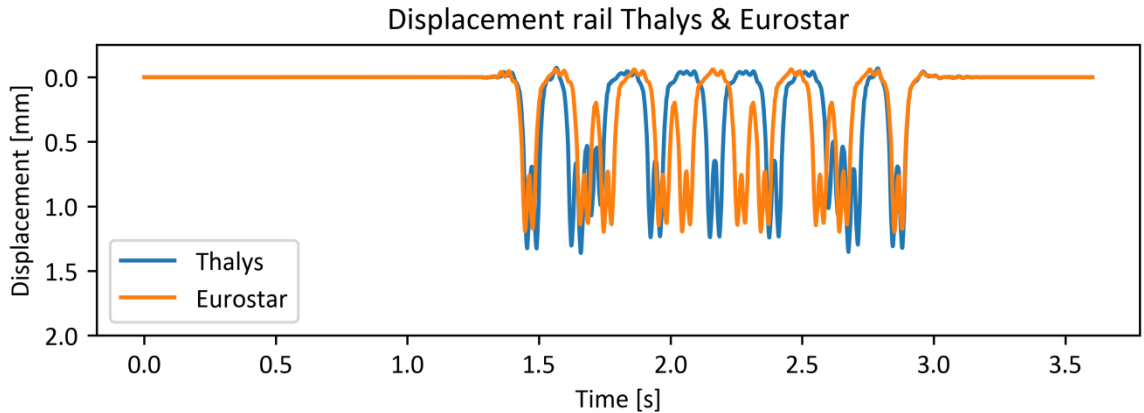
Figure 21: Rail displacement Thalys and Eurostar at 300 km/h for element 1955.

5.3 Support Forces

Next, the support forces of the structure have been analysed. The support forces are the forces that are transferred from the top layer to the layers beneath it. The support forces in DARTS are calculated by multiplying the displacement of an element in the elastic layer with the stiffness of that element. This results in a force for the layer beneath the elastic layer of that element. The loads introduced by the trains are transferred by the structure to the soil. The wheel loads of the trains itself are too large for the soil to resist. Therefore, the loads have to be reduced and spread over a larger area. Figure 22 shows the support forces of the rail for the Intercity Direct at 160 km/h for element 1953 in the middle of a SFP. In Figure 22 can be seen that the support force of the Traxx locomotive is larger than that of the carriages. The support force of the rails is also smaller than the wheel load of the Traxx locomotive. The wheel load of the Traxx locomotive

is 105 kN and the support force of the rail is 42 kN. Therefore, the load has been reduced and transferred over a larger distance to a larger area of the Rheda slab. By spreading the maximum load over a larger area the maximum peak force is reduced by a factor 2.

Figure 23 shows the support force of the Rheda slab that are transferred to the SFP. The support force is further reduced from 42 kN to 9.7 kN. The load of the train is transferred by the Rheda slab over a larger area and thereby reducing the stresses for the SFP. The maximum support forces from the Rheda slab to the SFP occur for the first element of each Rheda slab. The maximum support force for the first element is 42% larger than at locations in the middle of the slab. This is quite strange because the rail is connected to the sleeper at the second element of each Rheda slab. Therefore the first element is not loaded by the train, but it has the highest support force. The second element of the Rheda slab at which the connection to the rail is located has 28% higher support force. The first elements of each Rheda slab have thus higher support forces than the other elements.

The Thalys and Eurostar have a lower wheel load than the Intercity Direct and therefor the support force of the rails is also lower. The support force for the Thalys and Eurostar for 300 km/h in the middle of the SFP for element 1953 can be seen in Figure 24. The support force for the Thalys is a little bit larger than the support force of the Eurostar, which can be explained by higher wheel loads of the Thalys. The support forces of the rail are also a factor 2 smaller than the wheel loads of the Thalys or Eurostar.
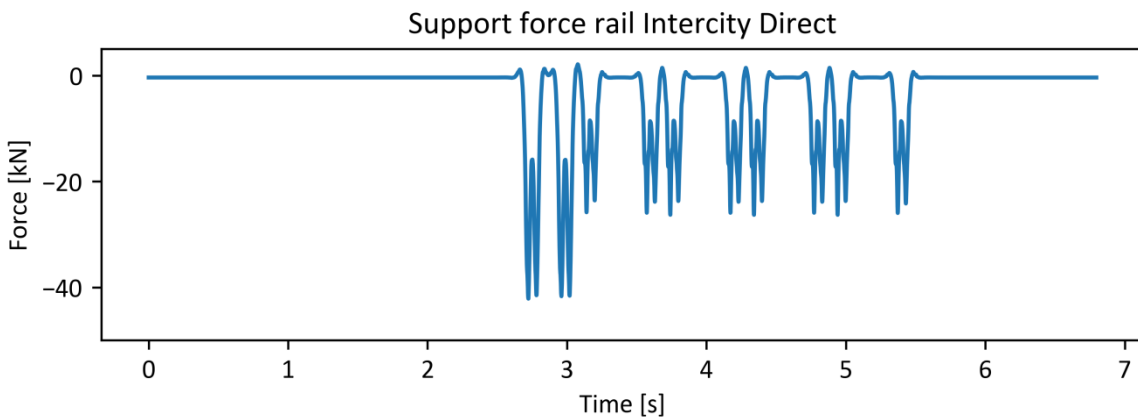
Also, the support force at the end of the SFP and in the middle have been compared. Figure 25 shows that there is no difference in support force between the end of the SFP and the middle of the SFP. Before every wheel load there is however a small increase in the support force.

In Table 16 the maximum support forces in the structure for the trains is given and the factor of which the wheel load is reduced in each layer of the HSL structure. For all trains the wheel load is divided over multiple sleepers and therefore reducing the force in the structure by a factor of 2. The force in the Rheda slab is even smaller as the wheel load is divided over a greater area. The forces of the wheel load is reduced till 18% of its original value.

From the support forces can be concluded that the axle loads of the trains has a large influence. The Intercity Direct with larger axle loads has also larger support forces. Furthermore, the wheel load is distributed over a larger area and thereby reduced in magnitude. The force between the rails and the Rheda slab is 50% of the wheel load. The support force between the SFP and Rheda slab is further reduced to only 18% of the wheel load. Also, there is no difference in support force between the end of the SFP and the middle of the SFP.

Table 16: Maximum forces in HSL structure and as factor of wheel load.

|	Intercity Direct		Thalys		Eurostar	
	Force [kN]	Factor [-]	Force [kN]	Factor [-]	Force [kN]	Factor [-]
Wheel load	104.84	1.00	83.36	1.00	71.92	1.00
Support Force Rail	47.85	0.46	41.43	0.50	37.60	0.52
Support Force Rheda slab	16.84	0.16	14.26	0.17	12.68	0.18

Figure 22: Rail support force Intercity Direct at 160 km/h for element 1953.
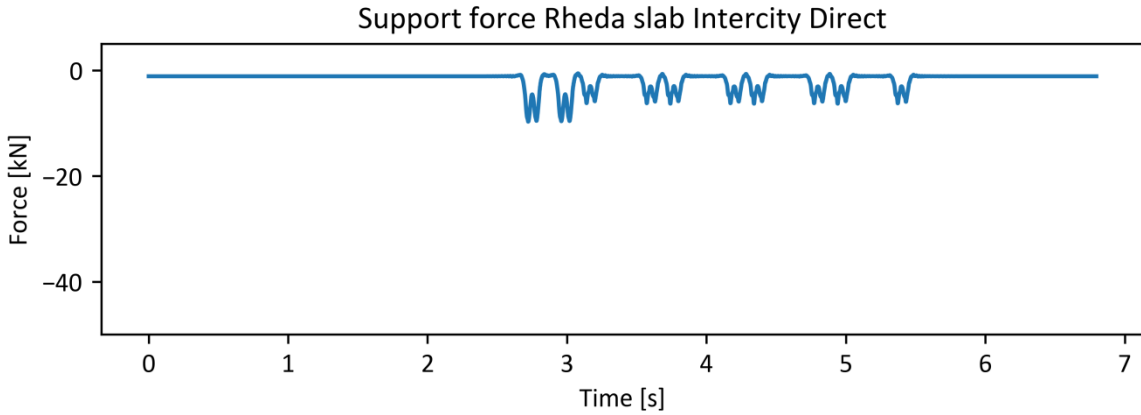
**Figure 23: Rheda slab support force Intercity Direct at 160 km/h for element 1953.**
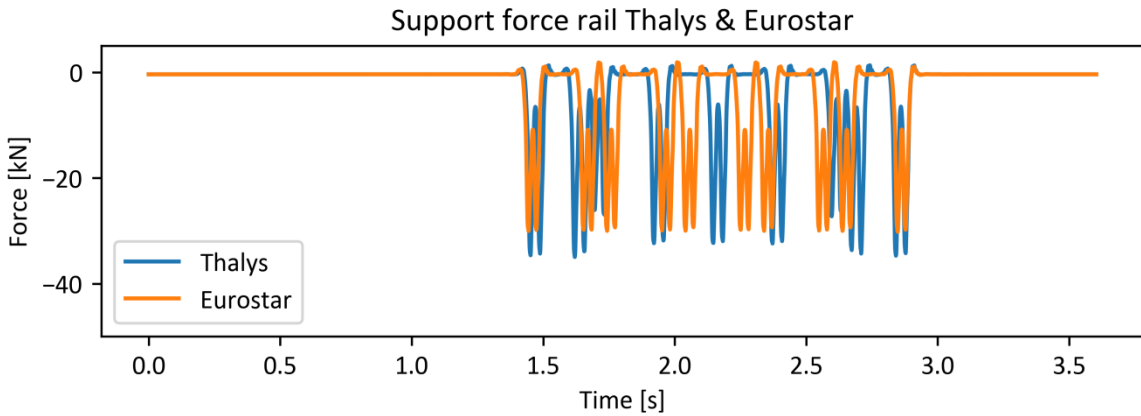
**Figure 24 Rail support force Thalys and Eurostar at 300 km/h for element 1953.**
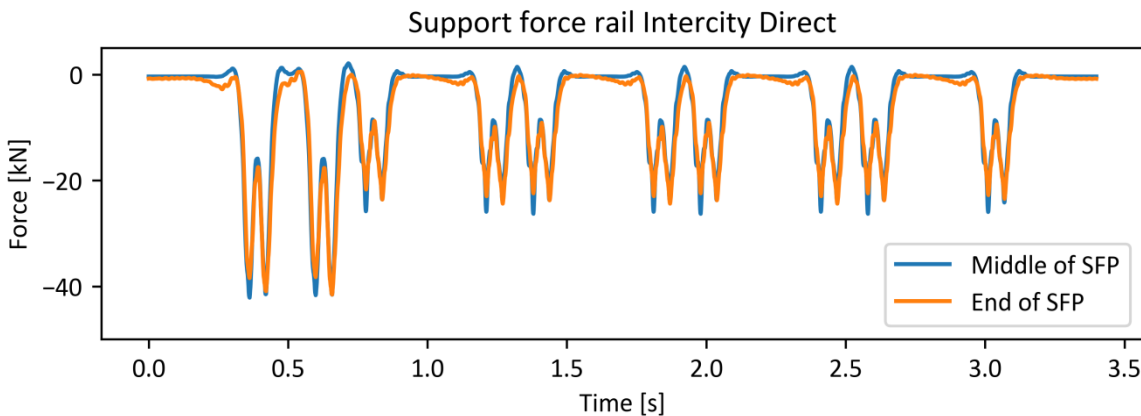
Figure 25: Rail support force Intercity Direct at 160 km/h for element 1953 and 2068. Both figures are shifted in time to overlap.

5.4 Pile forces

Also, the pile forces have been determined with DARTS. The train load is distributed by the SFP to the pile foundation. Therefore, the support forces of the SFP can be used to obtain the pile forces. The foundation piles in the DARTS model consist each of two elements. The pile forces are obtained by summing the support force of both elements for each pile. Figure 26 shows the pile force for a pile in the middle of the SFP. The maximum pile force occurs when the Traxx locomotive of the Intercity Direct drives over the structure. The maximum pile force is 75 kN and when there are no trains driving over the structure the mass of the structure results in a pile force of 31 kN.

The pile force differs largely between the start of the SFP and the middle of the SFP. Figure 27 shows the pile force for a pile in the middle of the SFP and at the begin of the SFP. The difference is caused by the difference in pile distance at the begin of the SFP and in the middle of the SFP. At the start of the SFP the

33

static load is 17 kN and when the pile is loaded by the Intercity Direct the pile force increases to a maximum of 53 kN. The piles at the start of the SFP have therefore a 22% smaller static load and a 30% smaller dynamic load when the Intercity Direct drives by. Figure 28 shows the maximum pile force over the length of the model. Cleary visible is that the pile forces at the ends of the SFP are lower than in the middle of the SFP.

Figure 29 shows the pile forces of the Thalys and Eurostar. Both trains have a lower maximum pile force than the Intercity Direct. The Thalys has a maximum pile force 73 kN, which is 7% lower than the Intercity Direct. The Eurostar has maximum pile force of 69 kN and that is 11% lower than the maximum pile force of the Intercity Direct.

From the pile forces it can be concluded that the pile forces in the middle of the SFP are larger than at the end of the SFP. This difference can be explained by the difference in pile distance. At the end of the SFP the pile distance is smaller and therefore the static load but also the load due to the trains is lower. The higher axle loads of the Traxx locomotive of the Intercity Direct results in higher pile forces.
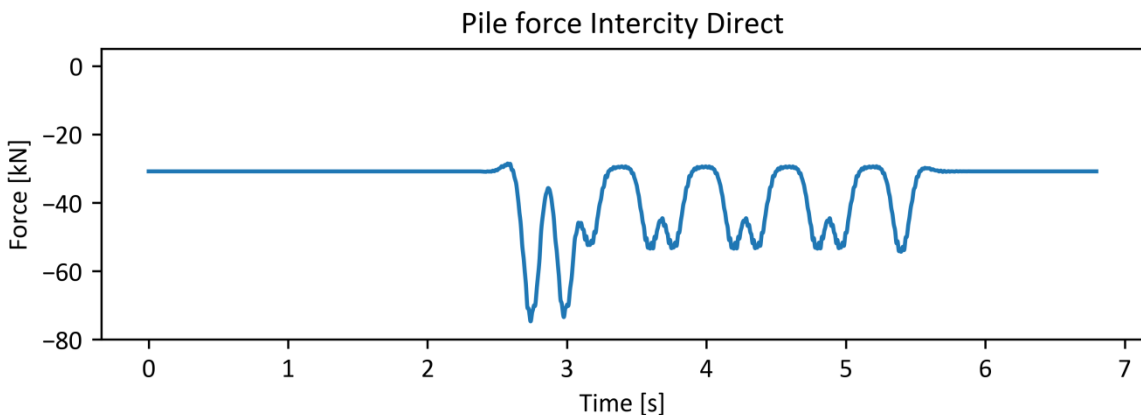

**Figure 26: Pile force Intercity Direct at 160 km/h middle of SFP**
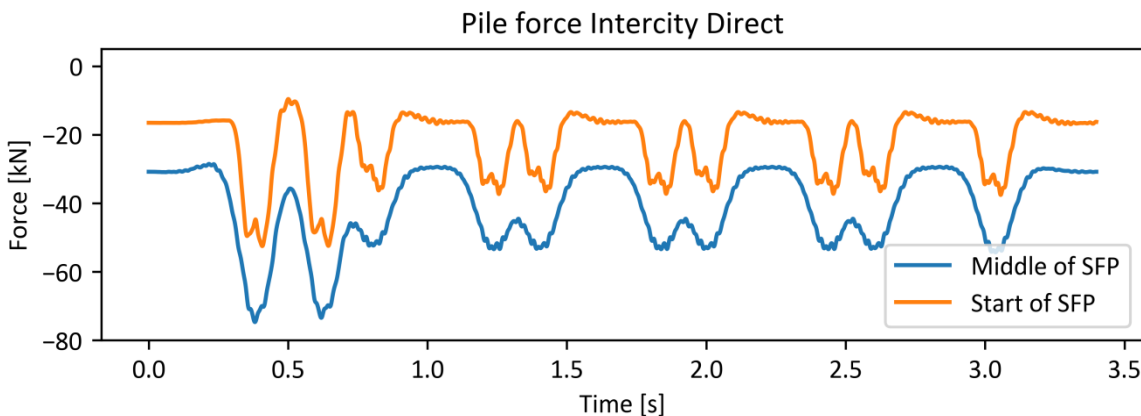
Figure 27: Pile force Intercity Direct at 160 km/h middle and start of SFP. Both figures are shifted in time to overlap.
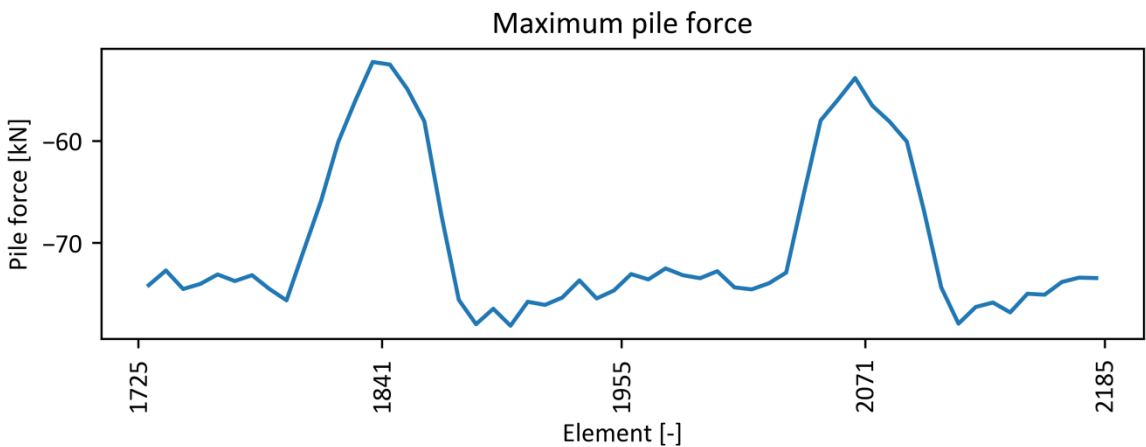
**Figure 28: Maximum pile force Intercity Direct at 160 km/h.**
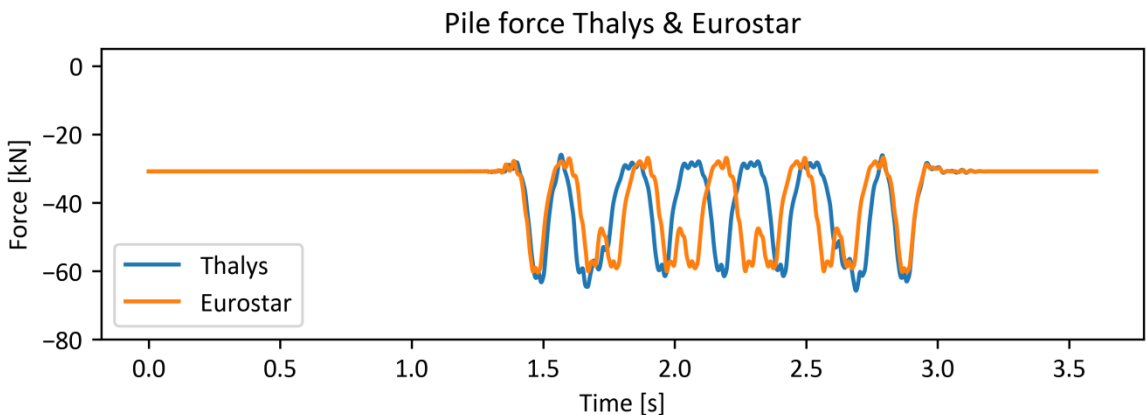
Figure 29: Pile force Thalys and Eurostar at 300 km/h middle of SFP.

5.5 Influence of train speed

Next the influence of the speed of the train on the structure is analysed with DARTS. Therefore simulations have been performed with the three train models at different velocities. The velocities range from 22 m/s (79.2 km/h) to 83 m/s (298.8 km/h) for the Thalys and Eurostar. The velocities for the Intercity Direct range from 22 m/s to 44 m/s (158.4 km/h). Table 17 shows the maximum rail displacements for the different trains at different velocities. The maximum rail displacement for the Intercity Direct increases with 6% when the displacement of 22 m/s and 44 m/s are compared. For the Thalys and Eurostar the maximum rail displacement increase even more. When the displacement at 83 m/s is compared with the displacement at 22 m/s the values increase with 8% and 15% for the Thalys and Eurostar respectively.

The displacement of the Rheda slab and SFP also increases when the speed increases. Table 18 shows the maximum displacement of the SFP. The maximum displacement for the Intercity Direct increases with 4% when the displacement of 22 m/s and 44 m/s are compared. That is of the same order as the rail displacement. The maximum displacement of the Thalys and Eurostar increases much more when the displacement at 83 m/s and 22 m/s are compared. The increase for the Thalys is 21% and for the Eurostar 22%.

The higher displacement result also in higher pile loads, see Table 19. The pile forces increase when the velocity increases. The pile load of the Intercity increases with 3% when the velocity increases from 22 m/s to 44 m/s. The pile force for the Thalys and Eurostar increase respectively with 10% and 11% when the velocity increases from 22 m/s to 83 m/s.

From Table 17, 18 and 19 can be conclude that higher velocities result in larger displacements and higher forces. The displacement of the SFP for the Intercity Direct increases with 4%. However, the Thalys and Eurostar have an increase in maximum displacement of the SFP with more than 20%. The increase for the rail displacement is less with 8% and 15% for the Thalys and Eurostar respectively. The pile force also increase with higher velocities. The pile force for the Intercity Direct increases with 3% and the Thalys and

Eurostar have an increase in pile force of 10% and 11%. With these results only the highest velocity for each train is used in further performed simulations.

Table 17: Maximum rail displacement at different velocities.

Velocity [m/s]	22.0	28	44	56	70	75	80	83
Intercity Direct [mm]	1.79	1.84	1.90					
Thalys [mm]	1.45	1.49	1.50	1.55	1.57	1.57	1.55	1.57
Eurostar [mm]	1.27	1.31	1.33	1.38	1.41	1.44	1.45	1.46

Table 18: Maximum displacement SFP at different velocities.

Velocity [m/s]	22.0	28	44	56	70	75	80	83
Intercity Direct [mm]	0.74	0.74	0.77					
Thalys [mm]	0.56	0.56	0.58	0.62	0.67	0.68	0.68	0.68
Eurostar [mm]	0.51	0.51	0.53	0.55	0.59	0.61	0.62	0.62

Table 19: Minimum pile force for different velocities.

Velocity [m/s]	22.0	28	44	56	70	75	80	83
Intercity Direct [kN]	-75.9	-76.8	-78.1					
Thalys [kN]	-66.0	-66.2	-67.0	-69.2	-72.4	-72.9	-72.9	-72.7
Eurostar [kN]	-62.6	-63.0	-63.7	-64.8	-67.4	-68.4	-69.1	-69.4

5.6 Influence of pile foundation

To determine if the pile foundation has an influence on the structure of the HSL multiple simulations have been performed. First is analysed what effect piles with a larger cross sections have on the results of the DARTS simulations. Therefore, the results of the model version with larger cross sectional piles have been compared with the smaller cross section piles. The model version with the larger piles represents the piles with a cross section of 450x450 mm. For this model version no model verification has been performed due to the absence of data. In this model a pile stiffness of 200 MN/m is used for the larger piles as is given in Chapter 2. For the stiffness of the rail fastening the value of 40 MN/m is used. This value is the same for both model versions and it follows from the model verification in Chapter 5.1.2.

Secondly the difference in pile length of consecutively SFP at the location of Schuilingervliet has been analysed by modifying the stiffness of the foundation layer in DARTS. The stiffness of the pile foundation has been reduced by the ratio in pile length. The stiffness of the SFP with shorter piles is therefore less than the stiffness of the SFP with longer piles.

5.6.1 Small and large piles

The difference in large and small piles for the HSL has been analysed in DARTS. Therefore, the model of the HSL with long piles is also analysed to compare it with the structure with the short foundation piles. Figure 30 shows the displacement of the SFP for the Intercity Direct in the middle of the SFP for element 1955. The model version with the large piles has larger displacements than the model version with the small piles. In Figure 30 the maximum displacement of the SFP for the version with large piles is 0.89 mm and for the version with small piles 0.70 mm. The difference between both version is 28%.

Figure 31 shows the displacement of the SFP for the Intercity Direct at the end of the SFP for element 1841. The maximum displacement of the SFP for the large piles is 0.46 mm. The maximum displacement of the SFP for the small piles is 0.60 mm. The maximum displacement for the version with small piles is therefore 23% larger at the end of the SFP.

The displacements of SFP for simulations with the Thalys and Eurostar show the same results as the simulation of the Intercity Direct. The displacements of the SFP are also smaller at the end of the SFP for the larger piles. And in the middle of the SFP the displacement for the larger piles are larger just like the results of the Intercity Direct.

An explanation for the larger displacements in the middle of the SFP for piles with a cross section of 450x450 mm is that there are less piles and that the distance between these piles is larger (see Table 5). The displacement at the end of the SFP for the larger pile is less than the displacement of the smaller pile with the 220x220 cross section. The larger pile has a stiffness of 200 MN/m and that is higher than the stiffness of the smaller pile of 61.75 MN/m.

On the other hand at the edge of the SFP the smaller pile is placed closer to the edge. Apparently the pile stiffness of 200 MN/m for the larger cross sectional pile is high enough to mitigate the difference in distance to the edge of the SFP and to result in less displacement at the edge of the SFP.

However, due to the larger pile distance between the piles with larger cross section the pile forces are also larger. The small piles have a maximum pile force of 78 kN for the Intercity Direct. The large piles have a maximum pile force of 262 kN for the Intercity Direct. Also the static load is for the large piles higher due to the larger distance between the piles.

To conclude the SFP displacement is thus lower at the end of the SFP for the pile foundation with a cross section of 450x450 mm than for the pile foundation with the 220x220 mm cross section. However, the displacement in the middle of the SFP and the pile forces are larger.
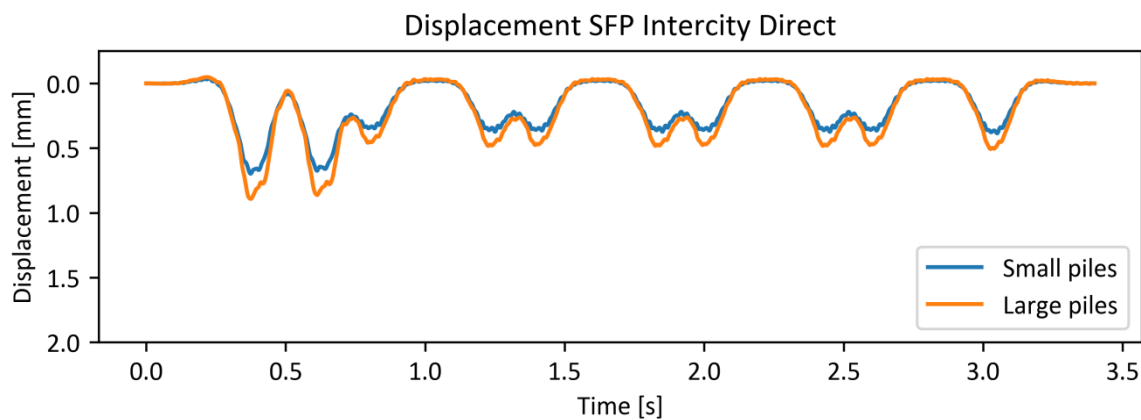

Figure 30: SFP displacement for large and small piles for Intercity Direct at middle of SFP for element 1955.
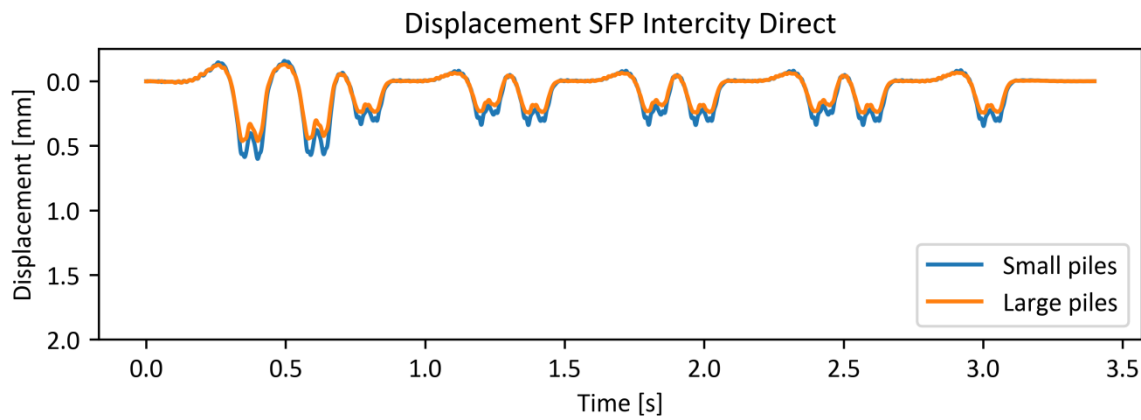

Figure 31: SFP displacement for large and small piles for Intercity Direct at start of SFP for element 1841.

5.6.2 Changing pile lengths

The pile length of the pile foundation at the location of Schuilingervliet is not uniform. The pile length changes for consecutive SFP, because the depth of the sand layer on which the piles are founded varies over the length of the track. The pile foundation in DARTS is modelled as an elastic layer and therefore the pile length cannot be adjusted. The stiffness of the pile foundation is therefore modified to represent the change in pile length. The stiffness of the pile foundation is adjusted with the ratio of the pile lengths. In Table 20 the pile length, ratio, pile stiffness and element numbers at which that stiffness applies can be found.

Pile length [m]	11.605	8.355	9.855
Ratio [-]	1.0	0.72	0.85
Pile stiffness [MN/m]	61.75	44.46	52.44
Element numbers	1725-1840	1841-2070	2071-2185
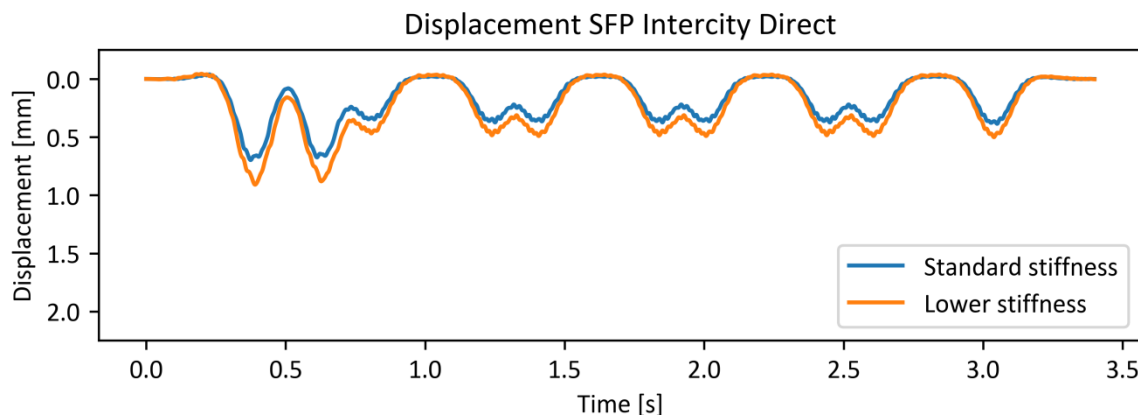
Figure 32 shows the displacement for the Intercity Direct in the middle of the SFP for element 1955. The stiffness of the pile foundation is 72% of the original stiffness. The reduction in pile stiffness results in larger displacements of the SFP. The maximum displacement of the SFP increases from 0.71 mm to 0.92 mm, an increase of 30%. Over the whole length of the SFP the displacements of the SFP are larger due to the reduced stiffness.

Figure 33 shows the displacement of the SFP for element 2185, which is also located in the middle of the SFP, but with a pile stiffness of 85% of the original stiffness. The displacement of the SFP are here also larger when compared with the displacements due the original stiffness. At this location the displacement increases from 0.70 mm to 0.78 mm, an increase of 12%.

Around the joint between the two consecutive SFP the difference with the original situation is much larger. Figure 34 shows the difference for the Thalys between the original situation and when the stiffness is reduced. Before the joint the stiffness is equal to the stiffness in the original situation and after the joint the stiffness is reduced with 28%. The displacement before the joint is reduced with almost 35% and after the joint the displacement is increased with 70% compared with the original situation. This change in stiffness between the two SFP result in a very large deviation in the displacement of the SFP. At the second joint the stiffness before the joint is 72% of the original situation and after the joint the stiffness is 15% of the original situation. This change in stiffness results also at this location in a difference in displacements but the difference at this location is much smaller. This can be understood by the fact that the difference of the pile length ratio at the joint at element 2071 is smaller than at the joint at element 1841.

When the pile forces are analysed there can be found that a reduction in stiffness does not result in change in the pile forces. The maximum pile force in the standard version of the model with small piles is 78 kN and in the stiffness modified model the maximum pile force is 77 kN.

From this can concluded that a decrease in stiffness of the pile foundation results in an increase in displacements. The pile forces do not change significantly when the stiffness is reduced.


Figure 32: SFP displacement for Intercity Direct at middle SFP for element 1955.
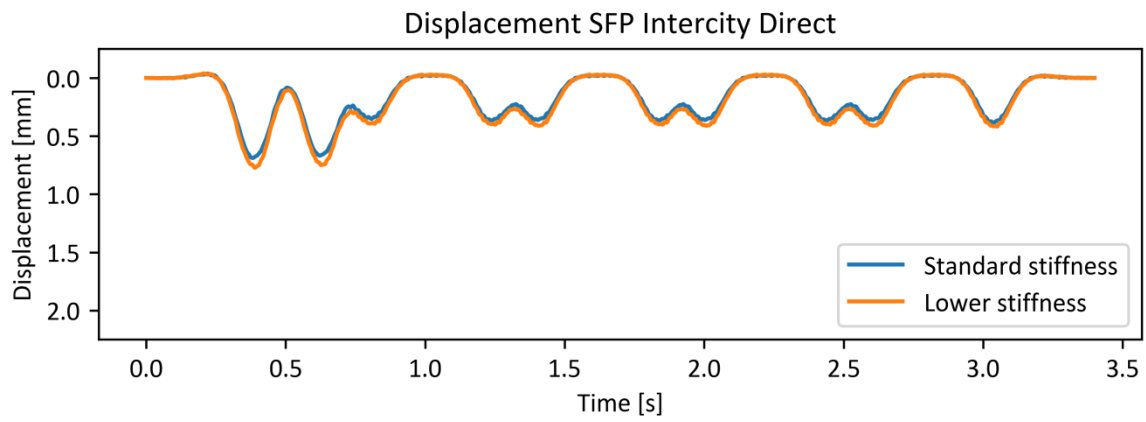
Figure 33: SFP displacement for Intercity Direct at middle SFP for element 2185.
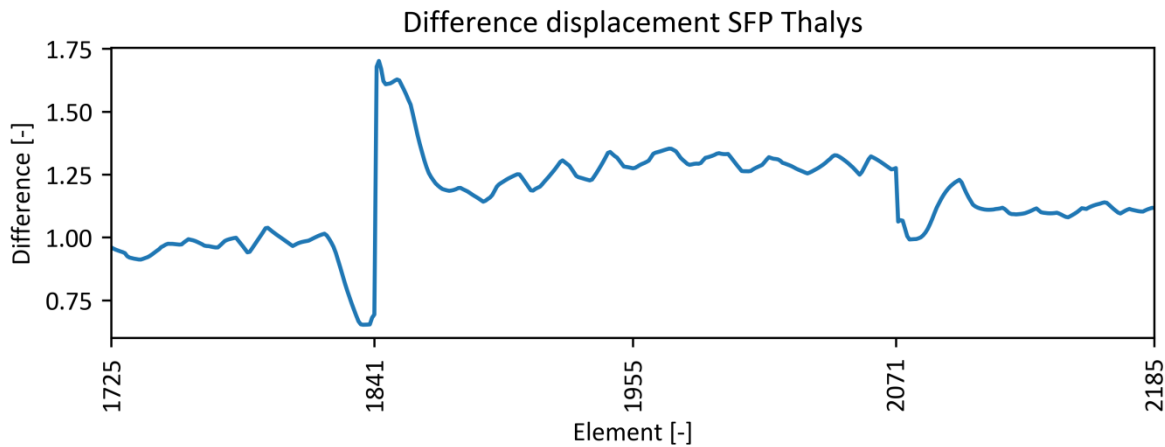
Figure 34: Difference in displacement SFP between different pile stiffness for Thalys. Results reduced pile stiffness are divided by results standard simulation.

5.6.3 Simulating settlements

Next, the settlement of the SFP at the joints between the consecutive SFP is simulated. Therefore, the pile stiffness of the individual piles has been lowered. The piles closer to the joint have a lower stiffness than the piles that are located further away from the joint. The piles stiffness near the edge is reduced to 30.88 MN/m, which is 50% of the original stiffness. The stiffness of the piles increases to original stiffness for piles further away from the edge. The stiffness for the piles is given in Table 21 and shown graphically in Figure 35.

Table 21: Pile stiffness for different distance to edge SFP

Distance to edge [m]	>3.9	2.73	1.69	1.04	0.39
Pile stiffness [MN/m]	61.75	58.66	55.58	46.31	30.88
Factor [-]	1	0.95	0.9	0.75	0.5
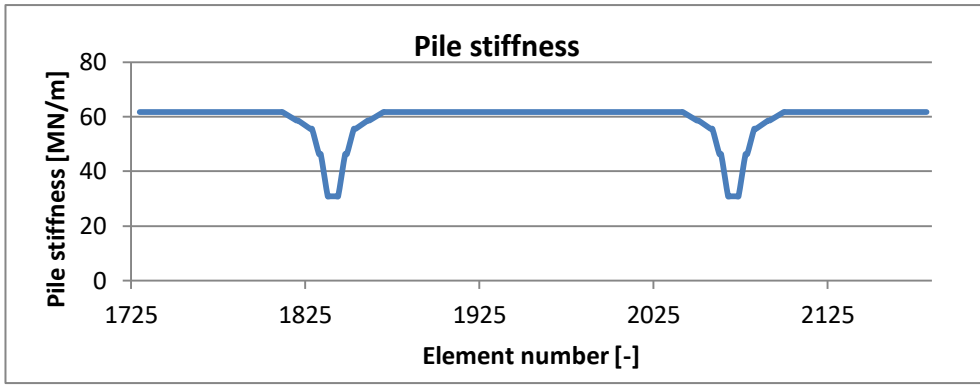
Figure 35: Pile stiffness over length simulation model.

Figure 36 shows the displacement of the rail for the Intercity Direct at the edge of the SFP for element 1841. As can be seen the rail displacement at the edge of the SFP is larger when the pile stiffness is decreased. The rail displacement increases from 1.53 mm to 1.75 mm. The reduction in pile stiffness results in a 15% increase in rail displacement. For the Thalys an increase of 18% in rail displacement is found and for the Eurostar also an increase of 15% in rail displacement is found.

The displacements of the Rheda slab and SFP are larger than the standard stiffness. Figure 37 shows the displacements of the SFP. The displacement of the SFP increases from 0.60 to 0.92 mm. The reduction of the pile stiffness results in an increase in displacements of the SFP with 53%. The same result can be found for the displacement of the Rheda slab. The displacements of the Thalys for the Rheda slab and SFP increase with 45% in the simulations with reduced pile stiffness and the displacements of the Eurostar increase with 53%.

Figure 38 shows the pile force at the location of the joint. The reduced pile stiffness results in lower pile forces. The maximum pile force decreases from 53 kN to 40 kN. This is a reduction of 24%. Also, for the Thalys and Eurostar the lower pile stiffness results in lower pile force with 24%.

From the results it can be concluded that a reduction in pile stiffness with 50% at the joint results in an increase in displacements. The displacements of the Rheda slab and SFP increase with 50% and the rail displacement increases with 15%. The reduction in pile stiffness results also in lower pile forces. The pile force are reduced with 25% due to the lower pile stiffness.
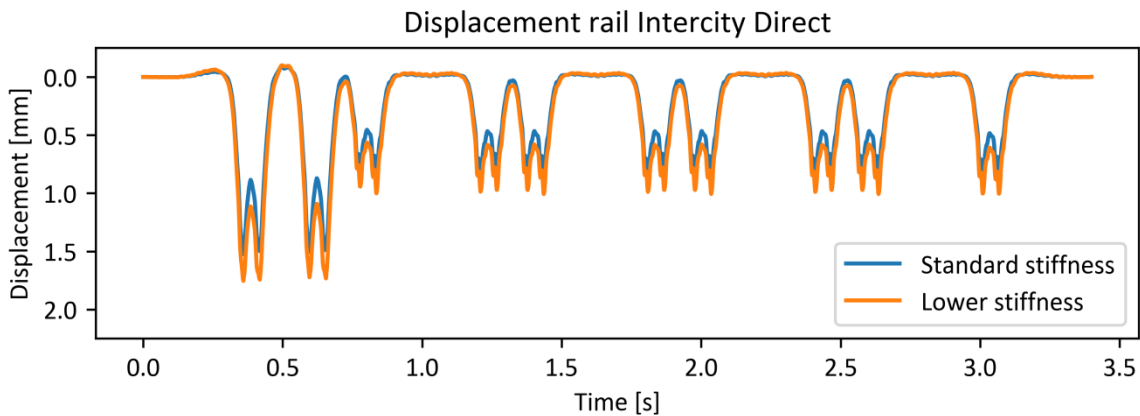
Figure 36: Rail displacement for Intercity Direct at 160 km/h at element 1841.
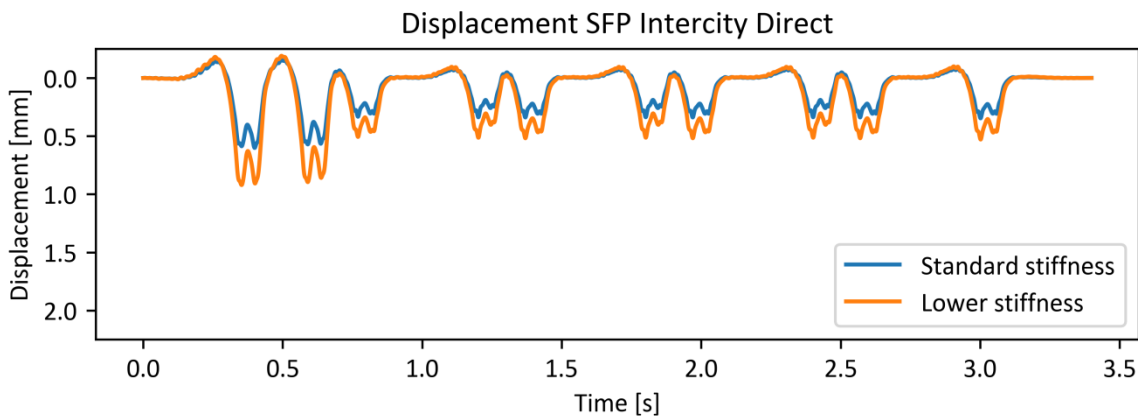
**Figure 37: Displacement SFP for Intercity Direct at 160 km/h at element 1841.**
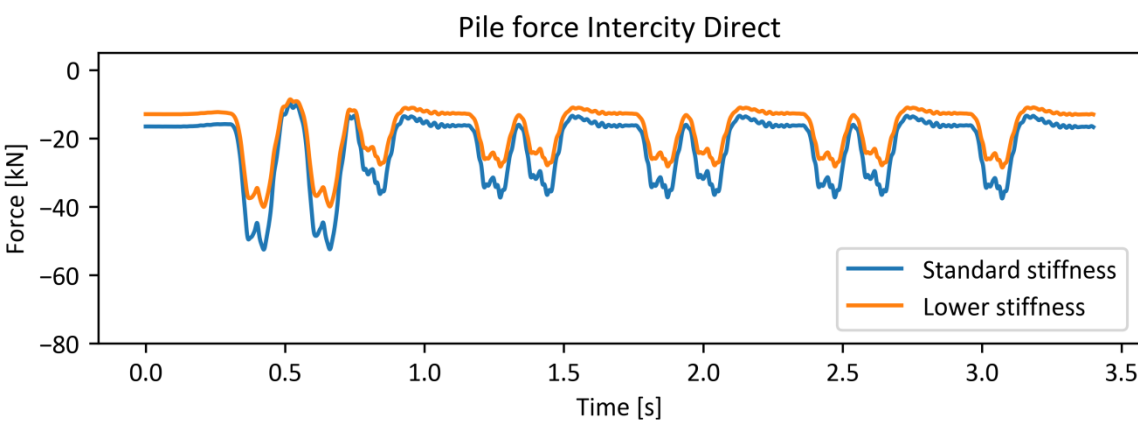
Figure 38:Pile force Intercity Direct at 160 km/h at joint.

5.7 Influence of gap between Rheda slab and SFP

The gap between the Rheda slab and the SFP is formed due to settlements of the SFP. The settlement of the SFP causes a gap because the Rheda slab starts to hang on the rails. The gap itself cannot be modelled in DARTS because it is impossible in DARTS to model a gap between two layers. Therefore the gap between the Rheda slab and SFP is modelled by reducing the stiffness of the intermediate layer for 10 elements on each side of the joint between two consecutive SFP. The stiffness has been reduced to 6% of the original stiffness and the damping is reduced to the 24% of the original damping. The reduction of the damping is lower because the damping is reduced by the square root of the stiffness. This reduction results in displacement close to 1 mm for the Rheda slab, which corresponds to the measured displacement.

Figure 39 shows the displacement of the rail for the Intercity Direct at edge of the SFP for element 1841. Due to the reduced stiffness of the intermediate layer the displacement of the rail has increased. The rail displacement is increased from 1.53 mm to 1.78 mm, an increase of 17%. For the Thalys and Eurostar the same increase in rail displacement can be found.
In Figure 40 the displacement of the Rheda slab is shown at location of element 1843. The first sleeper after the joint between two SFP is located at the place of element 1843. At this location the displacement of the Rheda slab is increased with 56%, from 0.61 mm to 0.96 mm. The increase in displacement of the Rheda slab for the Thalys is much larger with an increase of 70%. The Eurostar has the same order of increase as the Intercity Direct with 58%.
The SFP has around the joint between the SFP small deviations in the displacement due to reduced stiffness of the intermediate layer. Before the joint the displacement of the SFP has an small decrease in displacement up to 5%. And after the joint the displacement of the SFP has an small increase in displacement up to 8% for the Thalys and the Eurostar.

The pile force has a small decrease with 3% for the Intercity Direct when the stiffness of the intermediate layer is reduced. The simulations of the Thalys and Eurostar show a small increase of 3% for the pile force when the stiffness of the intermediate layer is reduced. Because it is not possible in DARTS to model a gap, also the closing of the gap cannot be simulated properly. Therefore DARTS cannot be used to determine if closing the gap between the Rheda slab and the SFP result in an extra force on the pile foundation.

To conclude by lowering the stiffness of the intermediate layer with 94%, the displacement of the Rheda slab is increased with 56% to 1 mm. The displacement of the rail increases with 17%. A reduction in stiffness of the intermediate layer has an small influence on the displacement of the SFP or on the pile forces.
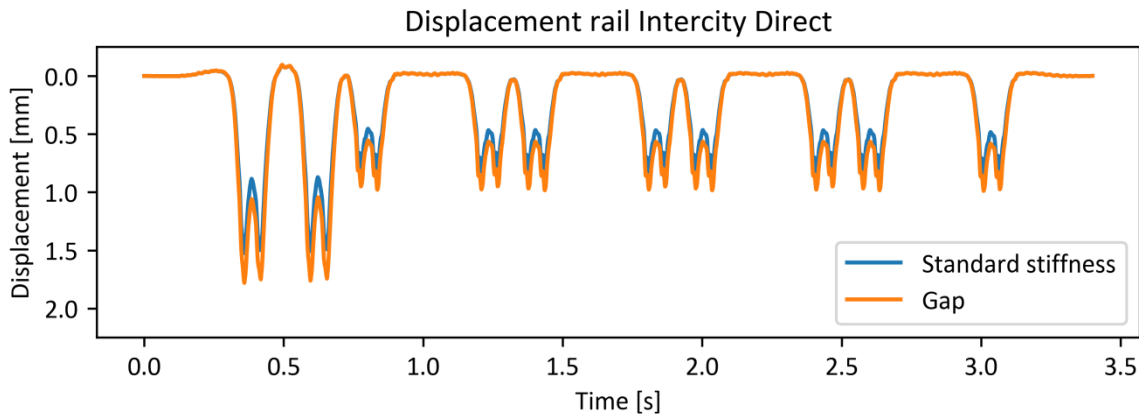
Figure 39: Rail displacement for Intercity Direct at 160 km/h at element 1841.
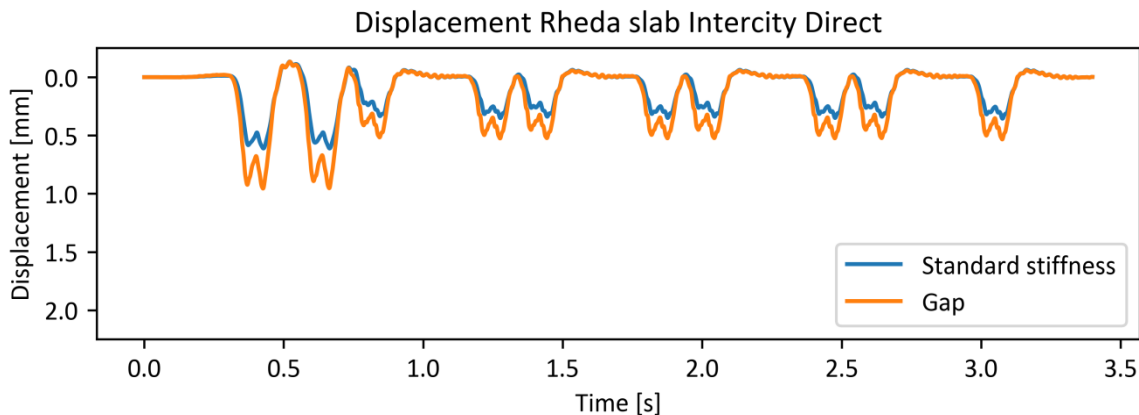
Figure 40: Rheda slab displacement for Intercity Direct at 160 km/h at element 1843.

5.8 Influence of vertical rail geometry

The vertical rail geometry is the vertical position of the rail along the track. The vertical rail geometry is not constant but deviates over the length of the track of the HSL. In DARTS the dynamic train load is determined by the vertical rail geometry. Deviations in the vertical rail geometry result in dynamic forces from the train on to the track. To determine the influence of the vertical rail geometry two other sections of the vertical rail geometry of the HSL have been compared with the standard section that is used in the simulations.

- For the standard section the vertical rail geometry at 218.348 km has been used. This is the location of Schuilingervliet with large settlements and where the first pile toe injections have been performed.
- Another location at Schuilingervliet around 221.543 km is also simulated. This location has also large settlements and the deviation in vertical rail geometry is larger compared to the standard section.
- The last vertical rail geometry that has been used for simulations is at a location 219.943 km at Schuilingervliet. At this location no settlements have occurred and there is a smaller deviation in vertical rail geometry when compared with the standard section.

The vertical rail geometry of the three locations is aligned with the model such that the locations of the joints of the SFP in the vertical rail geometry are at the location of the joint of the SFP in the model. Figure 41 shows the vertical rail geometry of the three sections at the two analysed joints of the model. The joint between the SFP is located at 15 meter and 45 meter. As shown in Figure 41 the section with larger deviation has at the location of the joints larger drops than the other two sections. Figure 41 also shows that the section with smaller deviation is more constant than the standard section.

The results of the simulations with different vertical rail geometry show differences between the simulations. Figure 42 shows the difference in displacement for the Intercity Direct when the different vertical rail geometry are compared. In the middle of the SFP the difference between the simulations are small and within 5% for the Intercity Direct. Around the joints of the SFP the difference between the simulations is larger and a maximum difference of 12% is observed at the second joint at element 2071. At this location the displacement of the SFP is 12% smaller for the vertical rail geometry with large deviation compared with the standard vertical rail geometry.
Figure 43 shows the difference in pile force for the Intercity Direct. Also, the difference for the pile forces is small and mostly within 5% of the standard vertical rail geometry. Around the joints in the SFP the difference becomes larger and has a maximum difference of 8%. At the second joint at element 2071 the pile force is 8% smaller for the vertical rail geometry with large deviation when it is compared with the standard vertical rail geometry.

The Thalys and Eurostar show larger differences than the Intercity Direct. The results of the Eurostar are smaller but similar as the results of the Thalys. Figure 44 shows the difference in displacement for the Thalys when the different vertical rail geometry are compared. In the middle of the SFP the difference between the vertical rail geometry is smaller than near the joints of the SFP. In the middle of the SFP the difference is mostly within 5% of the standard vertical rail geometry. Before the first joint at element 1841 the difference between the displacement of the SFP is 23% for the Thalys. The displacement of the SFP for the vertical rail geometry with small deviation is 23% smaller than for the displacement due to the standard vertical rail geometry. The difference in displacement of the SFP for the vertical rail geometry with large deviation is 20% smaller than the standard vertical rail geometry. After the first joint the difference in displacement of the SFP is 15% larger for the simulation with small deviation in the vertical rail geometry. The difference for the simulation with large deviation in vertical rail geometry is 11% larger. At the second joint the difference between the SFP displacement is smaller with a maximum of 10% for the simulation with the large deviation in the vertical rail geometry. After the second joint there is a peak of 25% difference for the simulation with large deviation in the vertical rail geometry. After the joint the simulation with large deviation in the vertical rail geometry is 25% than the simulation in which the standard vertical rail geometry is used. The difference is probably caused by the sharper drop in the vertical rail geometry at this location.

Figure 45 shows the pile force of the Thalys. The difference in the pile force for the simulations with different rail geometry is mostly within 5% of the simulation in which the standard vertical rail geometry was used. At the location of the joints between the SFP the difference in the pile force are larger. At the location of the first joint at element 1841 the pile force is 16% smaller for the vertical rail geometry with small deviation. The pile force for the simulation with large deviation in vertical rail geometry is 13% smaller compared with the pile force in the simulation with the standard vertical rail geometry. After the joint the pile force is 7% larger for the simulation with the small deviation and 6% larger for the simulation with large deviation when these simulations are compared with the standard vertical rail geometry. At the location of the second joint at element 2071 the difference between the pile forces is smaller with a difference of 7%. Before the second joint the pile force is 7% smaller and after the joint the pile force is 7% larger for the simulation with large deviation in vertical rail geometry. The vertical rail geometry with large deviation has higher pile forces for the first piles after the second joint at element 2071. The pile force is 14% larger than the pile force in the simulation with the standard vertical rail geometry. The difference is probably caused due the sharper drop in the vertical rail geometry with larger deviation at the location of the second joint which is located 1.5 meters after the second joint. Also, the vertical rail geometry of the standard deviation is at this location more constant, which increases the difference.

From the simulations with different vertical rail geometry it can be concluded that the Intercity Direct is less sensitive for deviations in the vertical rail geometry. The results of the Intercity Direct are mostly within 5% of each other for the displacements of the SFP and for the pile forces. At the locations where the joints in the SFP are located the differences are larger and 8%. The Thalys and Eurostar are more sensitive for deviations in the vertical rail geometry and at the locations near the joints in the SFP the difference are larger. The difference in displacement of the SFP has a maximum difference of 23% before the first joint. At this location the pile forces have a difference of 13%. The results show that the largest difference between the simulations are around the joints between the SFP. At the locations of the joints the difference in the vertical rail geometry is also the largest. At these locations the vertical rail geometry shows the largest deviations with drops in the vertical rail level.
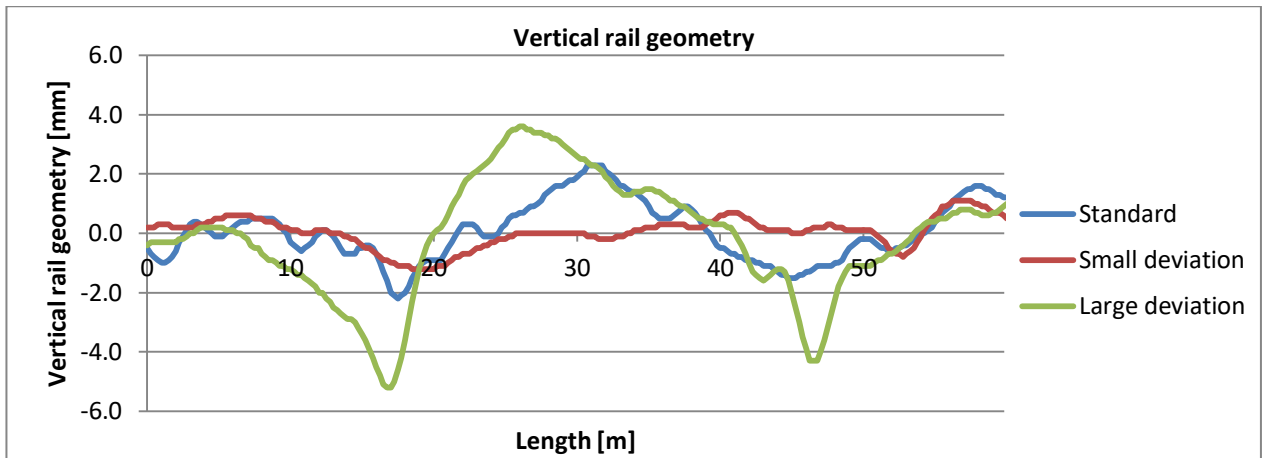
Figure 41: Vertical rail geometry for different sections at Schuilingervliet.
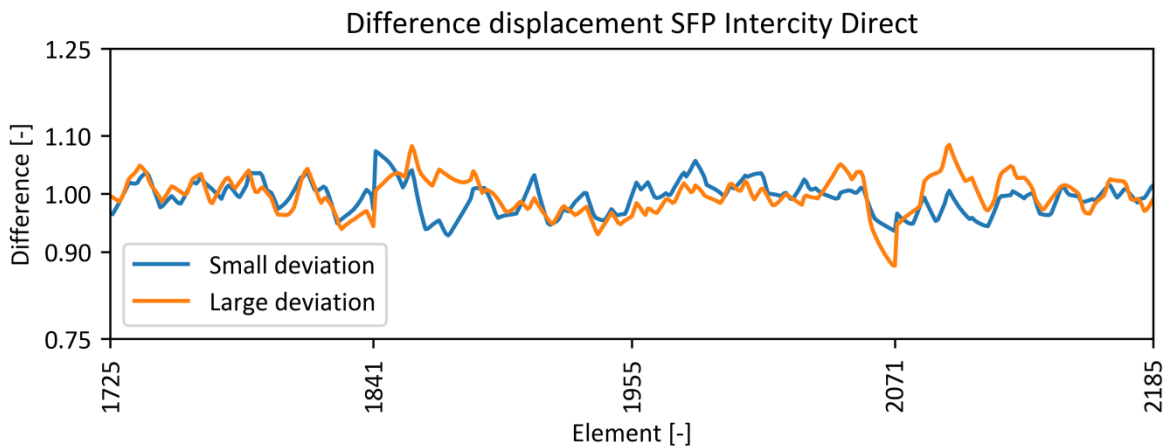
Figure 42: Difference in displacement SFP between vertical rail geometry for Intercity Direct. Results small and large deviation are divided by results standard simulation
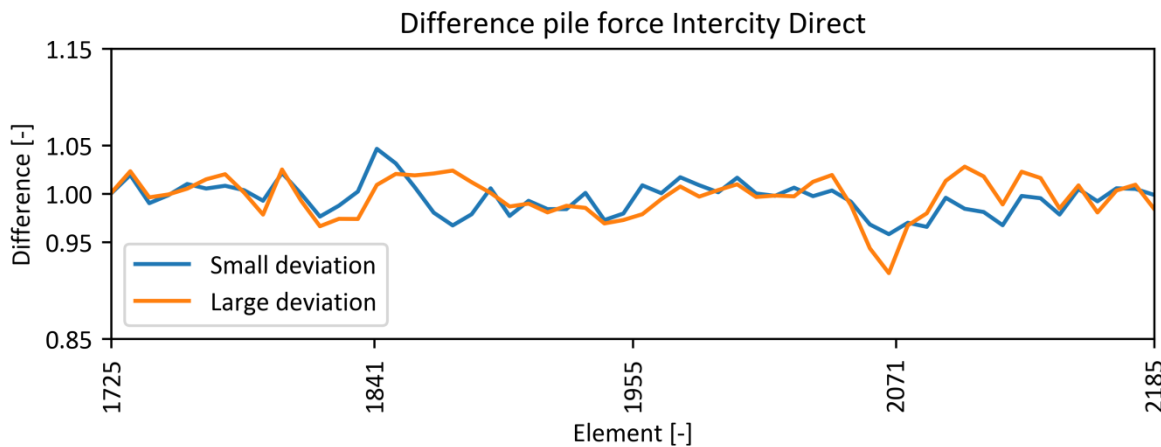
Figure 43: Difference in pile force between vertical rail geometry for Intercity Direct. Results small and large deviation are divided by results standard simulation
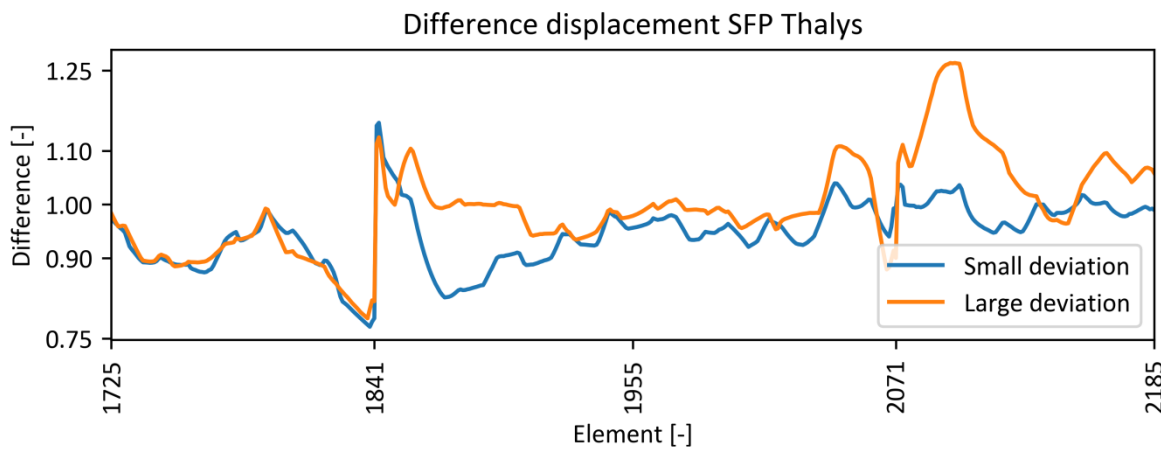

Figure 44: Difference in displacement SFP between vertical rail geometry for Thalys. Results small and large deviation are divided by results standard simulation
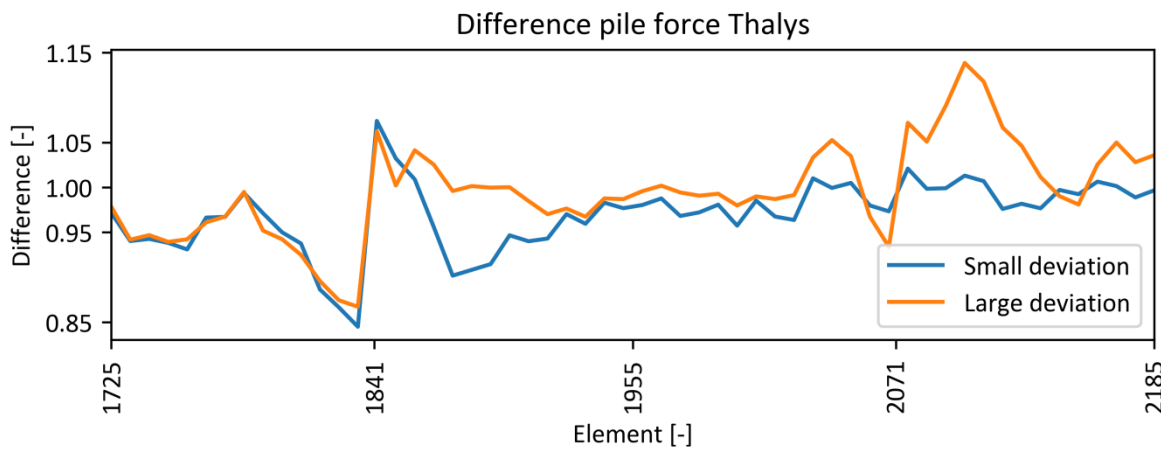

Figure 45: Difference in pile force between vertical rail geometry for Thalys. Results small and large deviation are divided by results standard simulation

6 Simulating possible solutions

To mitigate the problems of the settlements of the HSL-South three different solutions have been simulated. The solutions that have been simulated are: connecting the SFP, placing a Rheda slab over the joint of the SFP and increasing the pile stiffness of the pile foundation near the joint. The results of these simulations are analysed to determine which of these solutions might reduce the problems at the HSL.

6.1 Connecting the SFP

The first solution that is analysed is connecting the SFP. Therefore, in the model of DARTS an element is placed at the joint between the SFP. This element has the same properties as the SFP to make a connection between the SFP. As a result the SFP is now continuous and there is no joint anymore between the two consecutive SFP.

Figure 46 shows the rail displacement for the Intercity Direct when the SFP are connected. It shows the rail displacement in the original situation. The difference between the simulations is small. In the original situation the rail displacement is 1.53 mm and when the SFP are connected the rail displacement is 1.49 mm. The difference between the two simulations is 2.5%. For the Thalys and Eurostar also only a small difference is observed. For the Thalys the difference is 5% and for the Eurostar the difference is 9%.
Figure 47 shows the displacement of the Rheda slab for the Intercity Direct. The difference in displacement of the Rheda slab is much larger. In the original situation the displacement of the Rheda slab is 0.61 mm and when the SFP are connected the displacement is 0.49 mm. The difference between the displacements is 21%. By connecting the SFP the displacement of the Rheda slab can be reduced. For the Thalys and the Eurostar the displacement is also reduced when the SFP are connected. The displacement for the Thalys is reduced with 27% and for the Eurostar with 30%.
Figure 48 shows the displacement of the SFP in the original situation and when the SFP are connected for the Intercity Direct. The displacement of the SFP is reduced from 0.60 mm to 0.47 mm, a reduction of 22%. For the Thalys and Eurostar also a reduction of the displacement of the SFP is observed with respectively 26% and 31%.

Figure 49 shows the pile forces for the Intercity Direct for the first pile after the first analysed joint at element 1841. As can be seen in Figure 49 the pile force is different when the SFP are connected than in the original situation. Due to the connection the static load on the pile has increased with 3.2 kN. Furthermore, due to the connection the maximum pile force is also reduced with 7%. The maximum pile force is reduced from 53 kN to 49 kN. For the first pile at the location of the second analysed joint at element 2071 also a reduction in pile force is observed. At this location the maximum pile force is reduced from 57 kN to 48 kN a reduction of 15%.
Figure 50 shows the pile force for the Thalys at location of the first joint at element 1841. At this location the maximum pile force increases from 42 kN to 46 kN, an increase of 10%. This increase in maximum force can be caused by an increase in the wheel forces of the Thalys. Figure 51 shows the wheel force of the second wheel of the Thalys when it drives over the first analysed joint. As can be seen in Figure 51 is the wheel force in the simulation where the SFP are connected higher than in the original simulation. The maximum difference between the peaks of both simulations in Figure 51 is approximately 10%. On the other hand the last pile before the connection has a decrease in the pile force from 51 kN to 47 kN. This is a decrease of 8% in the pile force.
Figure 52 shows the pile force for the Thalys at the location of the second joint at element 2071. At the location of the second joint the pile force is reduced from 47 kN to 43 kN, a decrease of 8%. Also at this location the wheel forces have been analysed. Figure 53 shows the wheel force of the second wheel at the location of the second joint. The maximum wheel force at this location is lower than in the original simulation. The difference between the peaks in Figure 53 is around 8%.

The results of the Eurostar show the same trend as the results of the Thalys. However, at the location of the first joint the pile forces of the Eurostar are roughly the same in both simulations. The difference between both simulations is 1%. On the other hand, the wheel forces of the Eurostar have a difference of 8% between the peaks in both simulations. At the second joint the pile force of the Eurostar is reduced by 12%. The difference in the peaks of the wheel force of the Eurostar is around 6%. So the reduction in pile force is larger than the change in the wheel force. Therefore, connecting the SFP could have a positive effect at the pile forces of the SFP.

From the results can be concluded that connecting the SFP results in smaller displacements for the Rheda slab and SFP with a decrease in displacement of more than 20%. Also, the pile forces can be reduced with 7 to 15%. However, at the first analysed joint the Thalys has an increase in the pile force of 10%, which could be caused by an increase in the wheel force. The wheel force at the location of the connection is also 10% higher. However, at this location also the results of the Eurostar were analysed and the Eurostar did not show an increase in pile force. The Eurostar had at this location change in the wheel force of 8%, but this change in wheel force did not result in a change in the pile force. Therefore, the connection of the SFP can have a positive effect on the pile forces and result in a decrease in the pile forces at the edge of the SFP. However, the increase in the pile force of the Thalys should be further analysed.
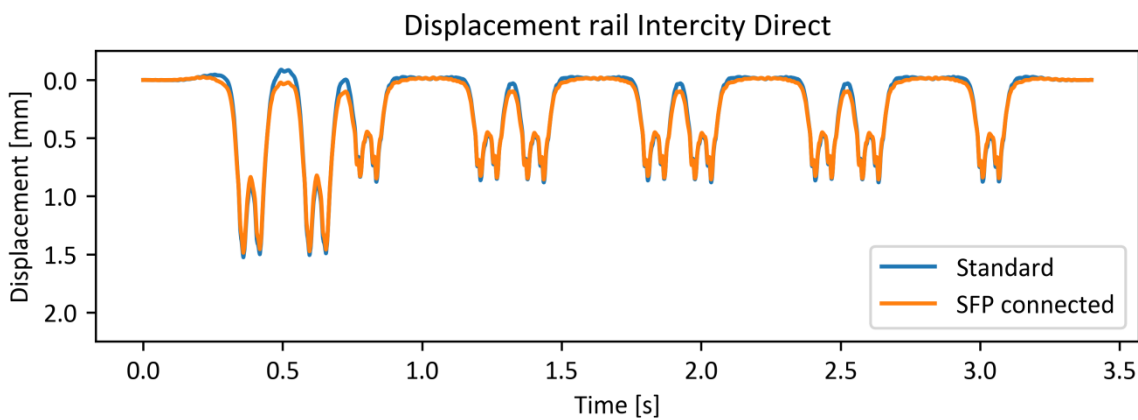
Figure 46: Rail displacement Intercity Direct 160 km/h at element 1841.
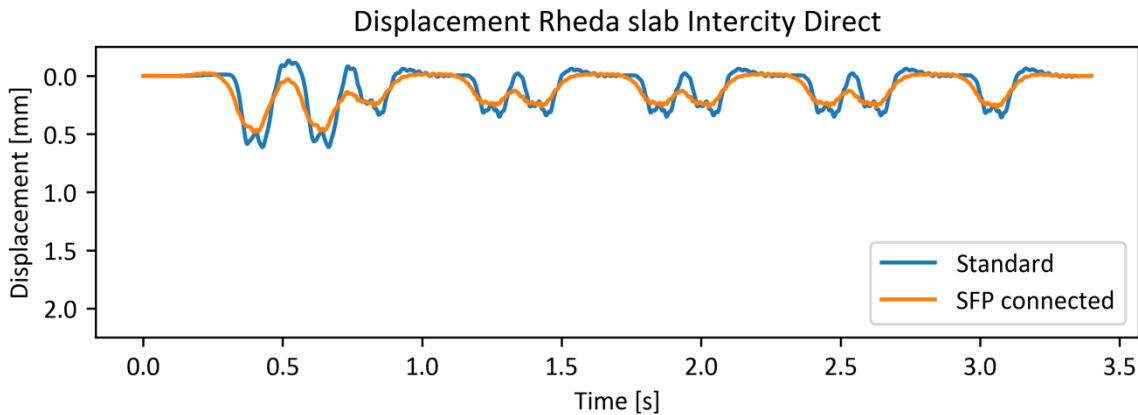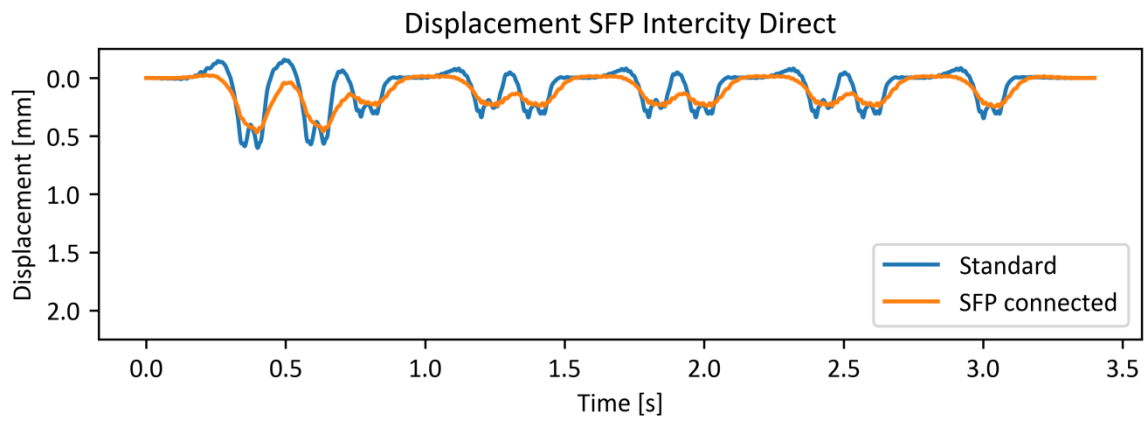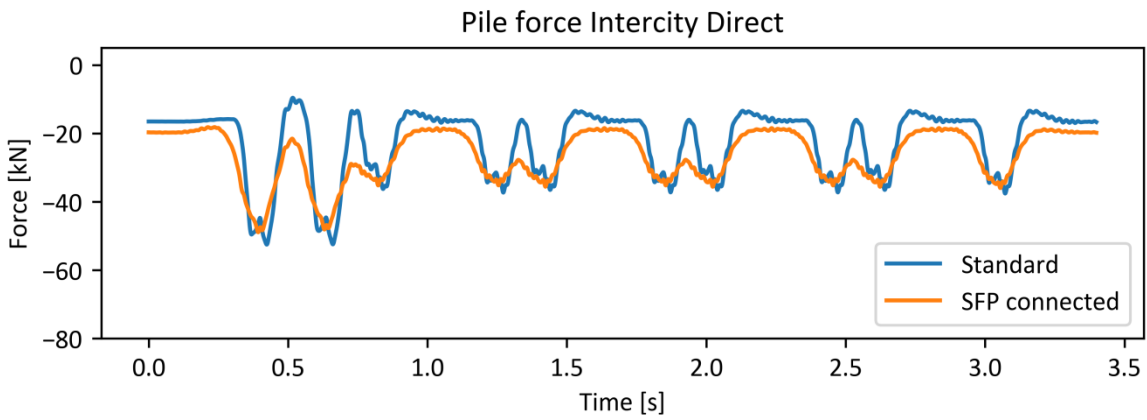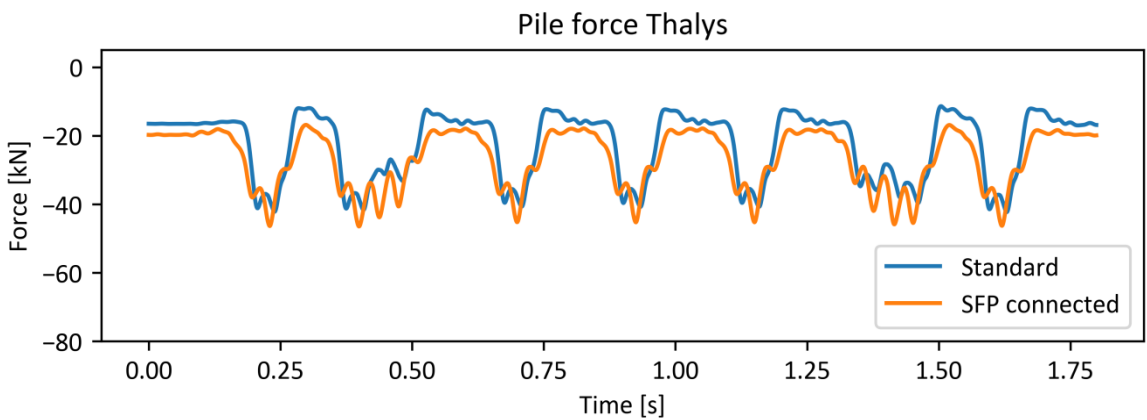
Figure 47: Rheda slab displacement Intercity Direct 160 km/h at element 1843.

Displacement SFP Intercity Direct

Figure 48: SFP displacement Intercity Direct 160 km/h at element 1841.

Pile force Intercity Direct

Figure 49: Pile force Intercity Direct 160 km/h at joint (element 1843-1844).

Pile force Thalys

Figure 50: Pile force Thalys 300 km/h at first joint (element 1843-1844).
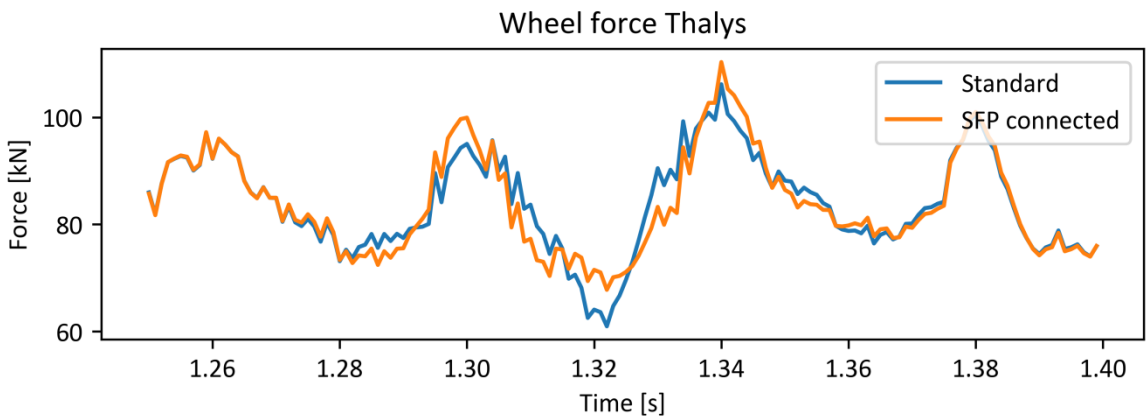
Figure 51: Wheel force second wheel Thalys at first joint (element 1841).
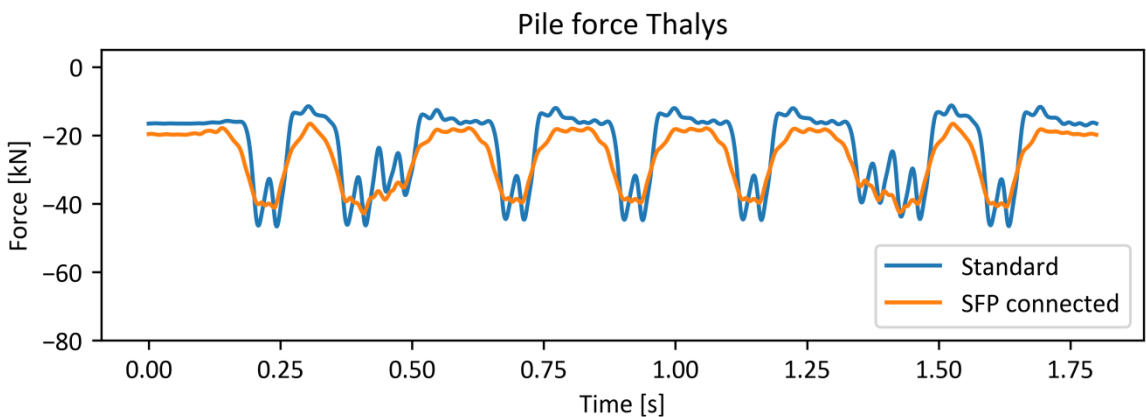
Figure 52: Pile force Thalys 300 km/h at second joint (element 2073-2074).
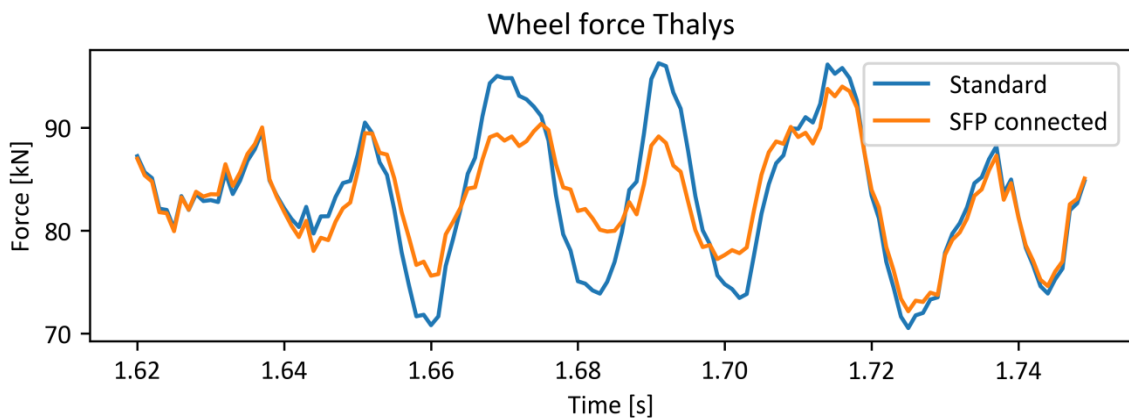
Figure 53: Wheel force second wheel Thalys at second joint (element 2071).

6.2 Rheda slab over joint SFP

The next solution that is analysed to reduce the problem is placing a Rheda slab over the joint of the SFP. Therefore, the Rheda slabs at the edge of the SFP on both sides of the joint are reduced in length with 10 elements. This free space is then used for a new Rheda slab that is placed over the joint between two SFP.

Figure 54 shows the displacement of the SFP for the Intercity Direct in the standard situation and when the Rheda slab is placed over the joint. Figure 54 shows that the results of the simulation with a Rheda slab placed over the joint can reduce the displacements of the SFP. The maximum displacement at the location of the first joint between the SFP is in the original analysis 0.60 mm. In the simulation with a Rheda slab placed over the joint the displacement is 0.55 mm, an reduction of displacement of 9%.

The Thalys and Eurostar show also a reduction in displacement for the SFP. The reduction for the Thalys and Eurostar is larger with a reduction of 20% in displacement of the SFP.

Figure 55 shows the pile force of the Intercity Direct for the first pile after the joint at the location of the first analysed joint. The pile force is reduced with 7%, from 53 kN to 49 kN in the analysis with a Rheda slab placed over the joint. The simulations of the Thalys also shows a reduction of 7% for the pile force at this location. For the Eurostar no difference in the results for the pile force is found at this location.

From these simulations it can be concluded that placing a Rheda slab over the joint can reduce the displacement of the SFP of the HSL with 9% to 20%. Also, placing a Rheda slab over the joint between can reduce the pile force at the location of the joint with a reduction in pile force of 7%.
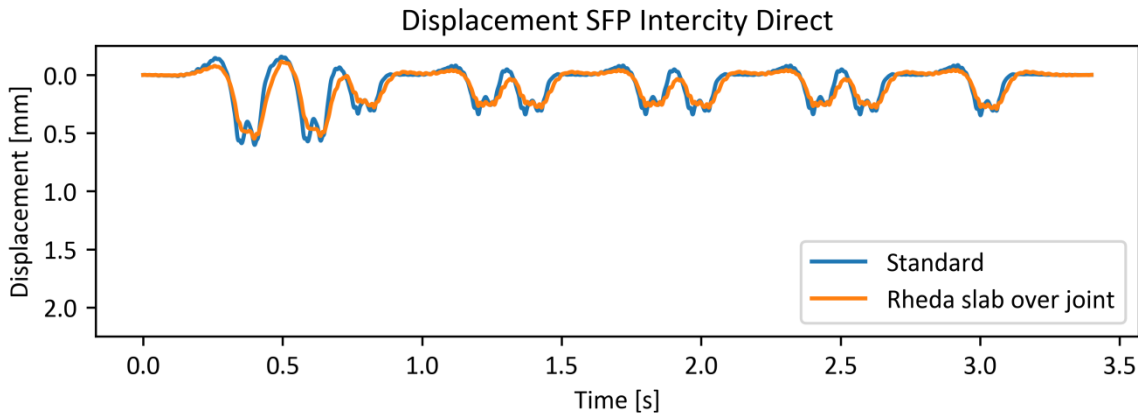
**Figure 54: SFP displacement Intercity Direct 160 km/h at element 1841.**
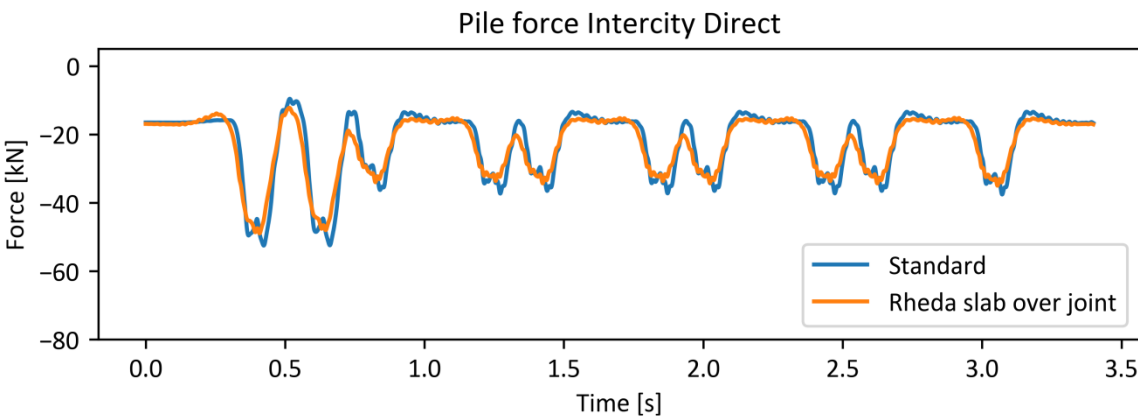
**Figure 55: Pile force Intercity Direct 160 km/h at joint.**

6.3 Increased pile stiffness

The last solution that has been modelled is an increase in the pile stiffness of the pile foundation. The pile foundation can be improved by pile toe injections or compact grouting to increase the strength and stiffness of the pile foundation. The injections can also reduce or stop the settlement of the pile foundation. However, in the simulations of DARTS it is not possible to model or analyse permanent displacements. Therefore, this solution focuses only on the elastic displacements. In this simulation the pile stiffness for the four piles the closest to the joint of the SFP at both sides of the joint has been increased. It is possible to increase the pile stiffness with pile toe injections with a factor of 2.3 as is given in Chapter 3. Therefore, the pile force has been increased from 61.75 MN/m to 140 MN/m. However, due to the settlements that still happened despite the pile toe injection and due to the slightly overestimated pile stiffness, also a simulation has been performed with a smaller increased pile stiffness. In this simulation the pile stiffness has been increased with 30% from 61.75 MN/m to 80 MN/m.

Figure 56 shows the displacement of the SFP for the Intercity Direct in the original situation and for the situation with a pile stiffness of 140 MN/m. The displacement of the SFP is decreased with 55% from 0.60 mm to 0.27 mm. The displacement of the Rheda slab decreases with 53%. The Thalys and Eurostar show the same decrease in displacement of the SFP and Rheda slab.

Figure 57 shows the pile force for the first pile after the joint between the consecutive SFP for the Intercity Direct in the standard situation and for the situation with a pile stiffness of 140 MN/m. The pile force decreases with 8% from 53 kN to 48 kN. However, the piles with the largest distance to the joint with higher pile stiffness show an increase in pile force of around 45%. This pile has a higher pile stiffness than the pile next to it, which has the original stiffness, and is likely to attract more load, which increases the pile forces. The Thalys and Eurostar also show a small decrease in pile force up to 12% and an increase in pile force for the piles with higher stiffness that are located the furthest from the joint between the SFP.

Figure 58 shows the displacement of the SFP for the Intercity Direct in the original situation and when the pile stiffness is increased to 80 MN/m. The displacement of the SFP is reduced with 22% from 0.60 mm to 0.47 mm. The same reduction in displacement is found for the displacement of the Rheda slab. The rail displacement is reduced with 6% from 1.53 mm to 1.43 mm. The simulations of the Thalys and Eurostar show also a reduction in displacement of the SFP. The Thalys has a reduction of 20% in displacement of the SFP and the Eurostar has a reduction of 25% in displacement of the SFP.
Figure 59 shows the pile force for the first pile after the joint of the SFP for the Intercity Direct in the standard situation and in the situation when the pile stiffness is increased. The pile forces are almost the same in both simulations. The pile force for the simulation with increased pile stiffness is reduced with 3%, from 53 kN to 51 kN. The same results can be found for the simulations with the Thalys and Eurostar.

The increase in pile force results thus in a decrease of the displacements of the SFP and Rheda slab. The simulation with a pile stiffness of 140 MN/m shows a decrease of 55% and the simulation of 80 MN/m shows a decrease of 22%. The pile forces near the joint of the SFP are also slightly decreased with 3% due to the increased pile stiffness to 80 MN/m. For the simulation with 140 MN/m the pile force decreases with around 8%, but the piles with an increased stiffness the furthest of the joint have an increase in the pile force of around 45%.
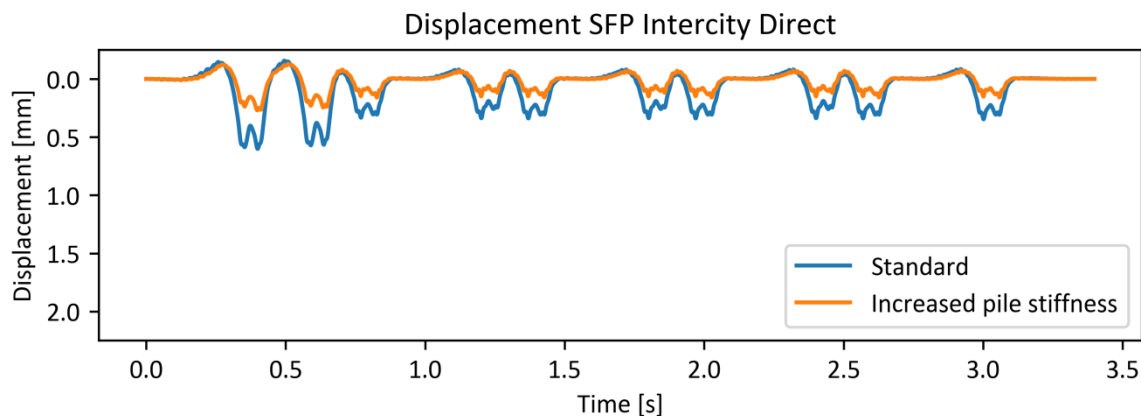
Figure 56: SFP displacement Intercity Direct 160 km/h at element 1841 with 140 MN/m pile stiffness.
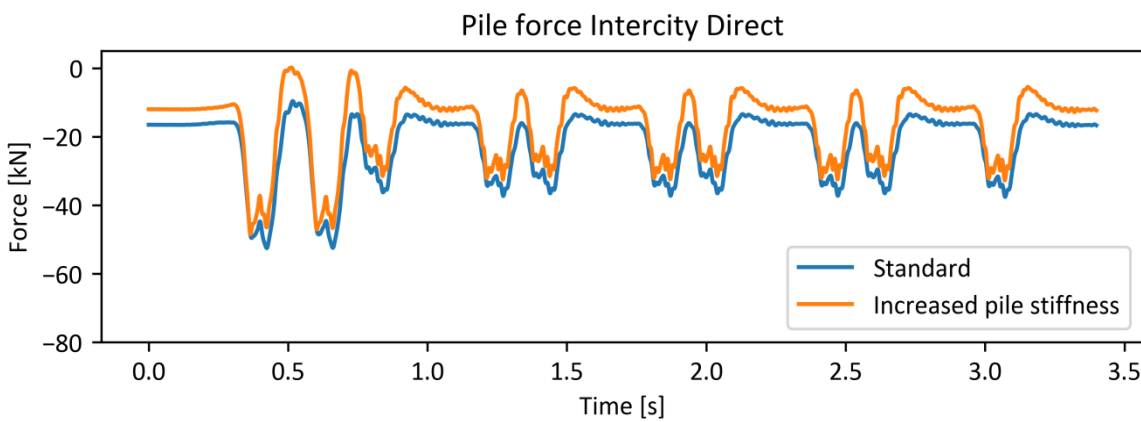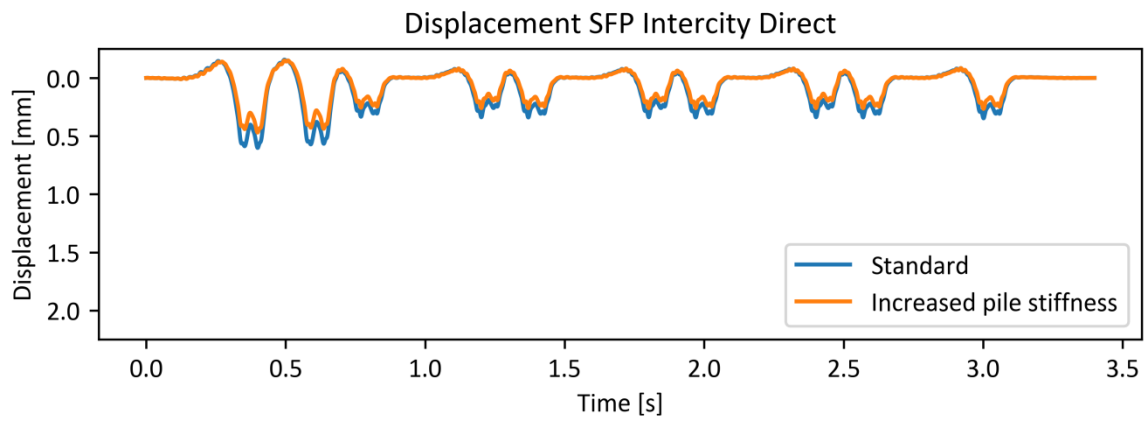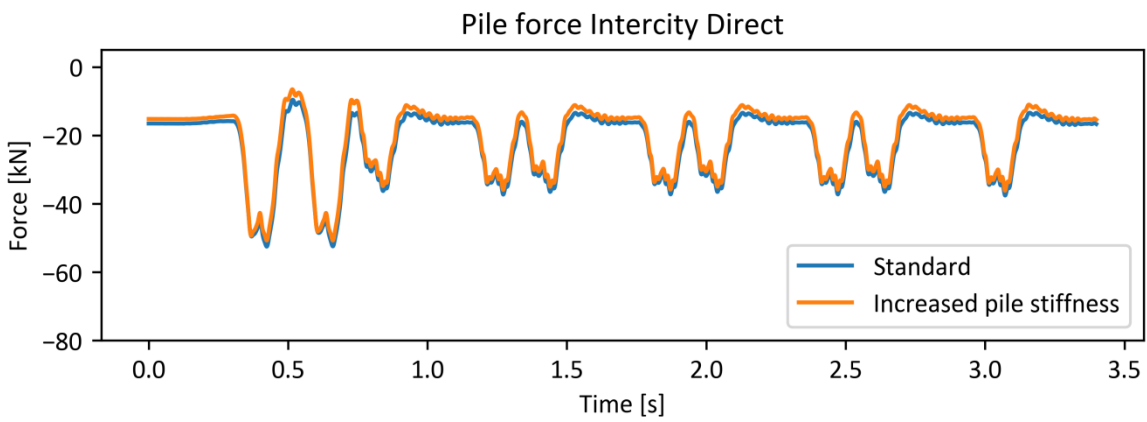
Figure 57: Pile force Intercity Direct 160 km/h at joint with 140 MN/m pile stiffness.

Figure 58: SFP displacement Intercity Direct 160 km/h at element 1841 with 80 MN/m pile stiffness.


Figure 59: Pile force Intercity Direct 160 km/h at joint with 80 MN/m pile stiffness.

7 Discussion

In DARTS a model of the structure of the HSL has been made to analyse the problem with settlements of the pile foundation. This model has been used to determine the effects of different factors and to model different solutions to find mitigations for the problem. In this chapter the results of the simulations will be discussed.

First, the results of the model have been compared with displacement measurements of the HSL. The displacement of the HSL is measured for the SFP, Rheda slab and the rails at the location of the joint between the consecutive SFP. The simulations of DARTS give also the results of the displacement for the SFP, Rheda slab and rail. When the results of the simulations were compared with the measurements it was found that the rail displacements of the model in DARTS were too low. Therefore, the stiffness of the pile foundation and the rail fastening were reduced. This increased the displacements and eventually an optimum is found with a pile stiffness of 40 MN/m and a rail fastening stiffness of 61.75 MN/m. The results of the simulations with these parameters are not a perfect fit but they approach the measured data quite good. However, there are two problems with the measured data that is used for the model validation:

- In the middle of the SFP no displacement measurements have been performed. The only measurement data are the displacement measurements at the edge of the SFP. Therefore, the displacement results of the DARTS simulations in the middle of the SFP cannot be compared with any measurements. The simulations results show on the other hand that in the middle of the SFP the displacements are larger than at the edge of the SFP. Also, the pile forces of the piles in the middle of the SFP are larger than the pile forces at the edge.
- The number of data points of the displacement measurements is scarce. The displacement measurements of the Eurostar consists of only one measurement. The displacement of this measurement is also much larger than the measured displacements of the other trains. Therefore, the Eurostar is not used in the model validation. For the Thalys the measured displacement of 5 trains is used and for the Intercity Direct measured data consists of 9 trains.

Despite these points, the results of DARTS and the measured data show that the displacements are comparable and within 10% of each other. Therefore, the model in DARTS can be used to analyse and to compare different situations to see which factors might reduce or contribute to the problem of the HSL.

Next, multiple simulations have been performed to determine which factors have an influence on the problem of the HSL. The following factors have been altered to determine their influence:

- Different trains: simulations were performed with the different trains that use the HSL. From the Intercity Direct, Thalys and Eurostar the displacement and pile force due to the Intercity Direct are the largest. The displacements due to the Intercity Direct are 17 % larger and the maximum pile force is 7% larger for the Intercity Direct compared with the Thalys. Also, the displacements in the middle of the SFP are 13% larger than at the edge of the SFP, due to a smaller distance between foundation piles at the edge of the SFP.
- Train velocity: the velocity of trains has been altered to analyse the influence of the velocity on the results. The results show that trains driving on their maximum speed have the largest displacements. The displacement of the SFP for the Intercity Direct increases with 4% when the velocity increases from 80 km/h to 160 km/h. The displacements of the SFP for the Thalys increase with 21% when the velocity increases from 80 km/h to 300 km/h.
- Cross section pile foundation: at Schuilingervliet for the pile foundation a smaller cross section is used. A model with a pile foundation with a larger cross section was made and the results of both models were compared. The model with the larger cross sectional piles has in the middle of the SFP 28% larger displacements. Also, the pile forces are larger. Both are caused by the larger distance between the piles. At the edge of the SFP the displacements of the SFP are 23% smaller than the displacements of the model with small cross sectional piles. The increased stiffness of the larger cross sectional pile, although placed further away from the edge, results in smaller displacements.
- Pile stiffness: the pile stiffness of the model is altered. Over the length of the HSL the length of the pile foundation is not constant. Also, settlements of the pile foundation have occurred at the joint between the SFP. In DARTS the pile foundation is modelled by an elastic element with a stiffness. It is not possible to model a permanent displacement due to a settlement or to model a change in the length of the pile

foundation. Therefore, the pile stiffness is reduced to model the different pile lengths and the settlement of the pile foundation. The results show that decreasing the pile stiffness results in larger displacement of the SFP. A reduction in pile stiffness of 50% result in an increase of displacements of the SFP with 50%.

- Gap between Rheda slab and SFP. In DARTS it is not possible to make a gap between two element layers or to add a permanent displacement to elements. Therefore, the gap between Rheda slab and the SFP has been modelled by decreasing the stiffness of the intermediate layer until a displacement of 1 mm for the Rheda slab was obtained. The stiffness of the intermediate layer was reduced to 6% of the original stiffness of the intermediate layer. Except for an increased displacement of the Rheda slab, the reduced stiffness of the Intermediate layer resulted in small differences for the displacement of the SFP and pile forces.
- Vertical rail geometry: for the simulations the vertical rail geometry is used by DARTS to determine the wheel loads. To determine what effect the vertical rail geometry has on the simulations, two simulations have been performed with different vertical rail geometry. From the simulations becomes clear that around the joints between the SFP the largest difference between the simulations occurs. The difference between the simulations for the Intercity Direct is 12% and for the Thalys 25%.

From the performed simulations it becomes clear that the pile stiffness has a large influence on the results of DARTS. Due to the simplicity of how the pile foundation with an elastic spring is modelled in DARTS, modifications to the pile stiffness result in inverse proportional changes to the displacement of the SFP. A decrease in the pile stiffness with 50% results in an increase in the displacement of the SFP with 50%. Therefore, to optimize the model results an accurate estimate of the pile stiffness is required. With an accurate estimate of the pile foundation the influence of the pile foundation on the superstructure can be better modelled and analysed.

Finally, three possible solutions to the settlement problem of the HSL have been modelled and analysed. The three solutions are:

- Coupling of the SFP at the joint: the consecutive SFP are coupled which removes the joint between the SFP. By coupling the SFP the displacement of the SFP can be reduced with 20%. Also, the pile forces can be reduced with 8% up to 15%. Coupling the SFP results in an small increase in the static load of the pile near the joint with 3.2 kN.
- Placing a Rheda slab over the joint: the Rheda slab at the edges of the SFP are shortened and a new Rheda slab is placed over the joint. This solution results in a reduction of displacement for the SFP with 9% up to 20%. Also, the pile forces can be reduced with 7%.
- Increasing pile stiffness: by injecting micro-cement at the level of the pile toes a higher pile stiffness can be obtained. In this simulation the pile stiffness was increased with 30% to 80 MN/m. This results in a decrease of the displacement of the SFP with 20%. The pile forces are slightly reduced with 3%.
  Also, a simulation with an increased pile stiffness of 140 MN/m have been performed. This simulation results in a decrease of the displacement of the SFP with 55%. However, it is unknown if the values can be obtained, because earlier pile toe injections started to show settlements two years after injection.

The three solutions show that they can reduce the elastic displacements of the SFP. It is not possible to determine if the three solutions can stop or reduce the settlements of the pile foundation, because it is not possible in DARTS to model permanent displacements. However, from these three solutions only the solution where the pile stiffness is increased by pile toe injections could have the possibility to solve the problem of the settlement of the pile foundation. If the pile toe injections are successful the settlement of the pile foundation could be stopped. However, at one test location where pile toe injections have been performed with micro-cement new settlements have occurred two years after the pile toe injection.

The other two solutions will probably not solve the cause of the problem of the settlement of the pile foundation. The solution with coupling the SFP will reduce the displacement of the SFP. By coupling the SFP also the difference in settlement between two consecutive SFP will be reduced. This can mitigate the problem where the maximum adjustability of the rail fastening system is reached, due to the reduced displacement and difference in settlement.

The solution with placing a Rheda slab over the joint between the SFP can also mitigate the problem with reaching the maximum adjustability of the fastening system by reducing the displacements of the SFP. However, this solution will not prevent that there will be a difference in settlement between two consecutive SFP.

The results of the simulations in DARTS show that the model is sensitive to changes in the pile stiffness. The measurements of the settlements of the HSL also show that the structure of the HSL is sensitive for settlements of the pile foundation. Therefore, the stability of the foundation is important for slab track structures. If the substructure of the slab track undergoes a settlement the limited adjustability of the slab track can quickly be reached. Therefore, it is crucial to prevent large settlements of the slab track, so that the limited adjustability will not be reached. To prevent settlements of the slab track it is important to do a geotechnical research into the soil properties. These soil properties are used during the design of the pile foundation. However, during the design of the substructure also attention should be paid to where settlements can occur and what the effect of settlements on these locations will be on the substructure and superstructure and if these settlements will lead to adjustments of the slab track. During the design of the foundation also attention should be paid to locations where a settlement of one element can result in a difference in settlement between two elements. And what this difference in settlement will result to for the adjustability of the slab track. Therefore, it is crucial that during the design of the foundation of the slab track critical locations where settlements can occur are found and that the effects of the settlement on the slab track structure are analysed. This can prevent that the limited adjustability of the slab track structure will be reached during its lifetime.

8 Conclusions

In this research project the behaviour of slab track on a pile foundation has been studied. Thereby especially the case-study of high speed line at the location of Schuilingervliet was analysed. At the location of Schuilingervliet settlements of the pile foundation of the HSL were observed. The goal of this research is to analyse the structure of the HSL and to find solutions to reduce the problem due to settlement of the pile foundation. In the software program DARTS a numerical model of the HSL has been developed. With this model multiple simulations have been performed to determine the response of the structure and to analyse the influence of various parameters. From these simulations performed in DARTS the following conclusions can be formulated for the research questions.

The HSL is used by three different type of trains. The Thalys and Eurostar are high speed trains which drive 300 km/h and the Intercity Direct, a conventional train that consists of two Traxx locomotives and carriages, which drives with 160 km/h. The Intercity Direct has the highest axle loads of these trains and this results also in the largest displacements of the SFP and the largest pile forces. The displacements of the SFP are 17% larger for the Intercity Direct and the pile forces are 7% larger when compared with the Thalys.

The structure of the HSL transfers the loads of the trains to the soil. To reduce the stresses the structure divides the forces to a larger area. The wheel load of the trains is transferred by the rails and fastening system into the Rheda slab. The rails spread the maximum wheel load over a larger area and only 50% of the maximum wheel load is directly transferred to the Rheda slab. The Rheda slab distributes the load even further and only 16% of the original maximum wheel load is transferred directly onto the SFP. The SFP transfers the forces to the pile foundation. The distance between the piles is at the edge of the SFP smaller than in the middle of the SFP and this results in a 30% lower pile force in the piles at the edge of the SFP.

The influence of the velocity of the trains, the uncertainties in the pile foundation and the deviation in the vertical rail geometry have also been analysed. From these simulations can be concluded that the model in DARTS is sensitive to changes to the stiffness of the pile foundation. In DARTS the pile foundation is modelled as an elastic layer with an estimated pile stiffness. Therefore differences in the pile foundation are modelled with a different pile stiffness. A reduction of 50% of the pile stiffness results in an increase of 50% in displacement of the SFP. A change in the pile stiffness has a minimal effect on the pile forces.
The other uncertainties show that the maximum velocity of the trains results in the largest displacements and the highest pile forces. The deviation of the rail geometry results mostly around the joints between the SFP for differences in the results.

In DARTS it is not possible to add a permanent displacement to an element or to insert a gap between two element layers. The settlement of the pile foundation is therefore modelled with a reduction in stiffness of the pile foundation. This results in increased displacements but has no influence on the pile forces.
The gap between the Rheda slab and SFP is modelled with a reduction of the stiffness of the intermediate layer. The results show that a reduction of the stiffness of the intermediate layer has, except for larger displacement of the Rheda slab, a small influence on the displacement of the SFP or pile forces.
From these simulations it can be concluded that DARTS is not the most preferable software package to determine the influence of a settlement of a pile foundation or to determine the influence of the gap between the Rheda slab and SFP.

Three possible solutions have been modelled to determine if they could reduce the settlement problem of the HSL. The three solutions that have been analysed are, coupling the SFP, placing a Rheda slab over the joint and increasing the pile stiffness by pile toe injections.
From these three solutions it can be concluded that all three solutions can reduce the displacement of the SFP with 20%. From these three solutions only the injection of the pile toes could have the possibility to solve the cause of the settlement problem. The other two solutions can reduce the effects of the settlement of the pile foundation and reduce the pile forces with 7%. By coupling the SFP and with that removing the joint between the SFP reduces the difference in settlement between two consecutive SFP. However, with this solution settlements of the pile foundation can still occur.

From the simulations in DARTS and the measurements of the HSL at Schuilingervliet can be concluded that the slab track structure of the HSL is sensitive for changes in the pile stiffness and settlements of the pile foundation. Due to the limited adjustability of slab track during its lifetime it is crucial to prevent that large settlements occur. Therefore, it is important that during the design of slab track settlements of the pile foundation and the effect of settlements of the pile foundation on the slab track structure are analysed. This can prevent that the limited adjustability of slab track will be reached.

9 Recommendations

After analysing the results of the model in DARTS, a couple of recommendations for future research can be made. These recommendations focus on obtaining better data to increase the accuracy of the DARTS model, but can also be useful for further investigations into the settlement of the pile foundation at Schuilingervliet.

The first recommendation is to perform more displacement measurements at Schuilingervliet. These extra measurements should measure the displacement of the SFP, Rheda slab and rail. These measurement are ideally performed at least at two locations. One location at Schuilingervliet where settlement of the pile foundation has occurred and at a second location where no settlements of the pile foundation has occurred. It is preferable to perform these measurements at the edge of SFP and in the middle of the SFP. The reason for these measurements at the edge and in the middle of the SFP is that the results of the DARTS model show that in the middle of the SFP the displacements are larger than at the edge of the SFP. Also, the measurements of the settlement of the SFP have shown that at some locations the SFP also underwent a settlements in the middle of the SFP. The displacement measurements preferable obtain enough data of the different trains that use the HSL. The current data contains only one measurement of the Eurostar. These extra measurements can be used for a better validation of the DARTS model and to get a better insight into the settlement of the HSL at the edge and in the middle of the SFP.

The second recommendation is to investigate the soil properties at Schuilingervliet. The simulations in DARTS are performed with an estimated pile stiffness. From the results of the simulations it becomes clear that the model is sensitive for changes to the pile stiffness, also due to the manner how the soil and pile foundation are simulated in DARTS. To improve the simulation results, a proper estimate for the pile stiffness is required. At the location of Schuilingervliet the depth of the pile foundation is for every SFP different. Also, the soil layers deviate over the length of the track and accordingly the strength and stiffness of these layers. Therefore, it is advised to perform investigations into the soil properties at these critical locations. With these investigations into the soil properties an estimated pile stiffness can be derived in which the properties of the soil layers and the length of the pile foundation are taken into account. The investigations into the soil properties can also be used to determine why the pile foundation at the location of Schuilingervliet undergoes a settlement, which at this moment is still unknown.

The last recommendation is to perform further research into the gap between the Rheda slab and the SFP. In DARTS it is not possible to model a gap between two element layers. The simulations in DARTS were therefore performed with a lowered stiffness of the intermediate layer to obtain the same displacement. The results show that this has no influence on the displacement of the SFP or the pile forces. However, to see if closing the gap between the Rheda slab and SFP by a train has really no influence further research has to be performed. Therefore, other software packages have to be used in which a gap due to a permanent displacement can be properly modelled.

Bibliography

[1]   Esveld, C. (2001). *Modern Railway Track* (2nd ed.). MRT-Productions.
[2]   Infraspeed. (2005). *Rheda slab typical cross sections* (IDE(TRK=TDEBA&CLW#000031)*.
[3]   Infraspeed. (2015). *Sub-subsystem specifications Rheda track Cat. A, B, C and switches* (IDE(TRK=TDEB&CEC#000018)*.
[4]   BAM HSL Infraprovider vof. (2004). *Slab Cat. A on SFP, SACE of Dimensions* (IDE(TRK=TDEBA&CBB#000001)*.
[5]   BAM HSL Infraprovider vof (2004). *Connection sub-superstructure Cat. A on SFP* (IDE(TRA=TDEBA&CBB#000007)*.
[6]   Bouwcombinatie HSL Drechtse Steden v.o.f. (2001). *Ontwerpbasis Baan* (HSL4-22208-C-R-55000)*.
[7]   Dammers, R. (2018). *PuttershoekThalys TGV-PBA-4532 trein 9358 naar Paris Nord.* https://www.flickr.com/photos/robdammers/41907553872/in/album-72157647502613824/
[8]   Dammers, R. (2019). *Puttershoek HSL Eurostar 4029-4030 London-Amsterdam.* https://www.flickr.com/photos/robdammers/46967387494/in/album-72157647502613824/
[9]   Dammers, R. (2016). *Benthuizen NS 186 004 – AmRo – 186 148 als trein 1044 Rotterdam.* https://www.flickr.com/photos/robdammers/28619913802/
[10]   Padmoes, T. (2016). *HSL-Zuid ZVP Schuilingervliet.*
[11]   Infraspeed. (2018). *Prioritering Schuilingervliet.*
[12]   Iv-Infra b.v. (2018). *Monitoring HSL-Zuid, Schuilingervliet.*
[13]   Infraspeed. (2015). *Schuilingervliet rondom KM 218.300, Metingen met behulp van de Windhoff* (IAV(IMC=TRK$TA&MEC#000007)*.
[14]   Bouwcombinatie Drechtse Steden. (2000). *HSL-Zuid Geotechnisch lengteprofiel kilometrering 17,800-18,600* (HSL4-00001-G-T-11007)*.
[15]   Dekra Rail. (2019). *Meetrapport verplaatsingen onderbouwplaten HSL-Zuid, referentielocatie km 219,989* (180443.008).
[16]   Dekra Rail. (2019). *Meetrapport verplaatsingen onderbouwplaten HSL-Zuid, voor grouten locatie km 219,464* (180443.009)*.
[17]   Dekra Rail. (2019). *Meetrapport verplaatsingen onderbouwplaten HSL-Zuid, na grouten locatie km 219,464* (180443.006).
[18]   Dekra Rail. (2019). *Meetrapport verplaatsingen onderbouwplaten HSL-Zuid, groutlocatie 218,333* (180443.007).
[19]   Crux. (2017). *Zettingsvrije plaat HSL Zuid, Injectieproef: geschiktheid typen injectie en opzet* (RA16390a7).
[20]   Volker Staal en Funderingen bv. (2017). *Bodeminjectie Microcement Voeg moot 14-03 / 14-04* (W16-041-85-001_as-built)*.
[21]   Kok, A.W.M. (2000). *RAIL: Theoretical Manual, Moving loads and vehicles on a rail track structure.*
[22]   Kok, A.W.M. (2002). *RAIL: The Dynamic Analysis of Rail Track Structures.*
[23]   Bouwcombinatie HSL Drechtse Steden v.o.f. (2002). *Dynamische berekeningen Zettingsvrije Plaat* (HSL4-22208-S-B-55090).
[24]   Infraspeed. (2003). *Dynamic Train Figures, Train Properties* (IDE(IFS)HSL&ABCLT#001088).
[25]   Iv-Infra b.v. (2018). *Monitoring HSL-Zuid, Lindeweg.*
[26]   Bouwcombinatie Drechtse Steden. (2000). *HSL-Zuid Geotechnisch lengteprofiel kilometrering 13,300-14,100* (HSL4-00001-G-T-11002)*.
[27]   Bouwcombinatie Drechtse Steden. (2000). *HSL-Zuid Geotechnisch lengteprofiel kilometrering 14,100-15,000* (HSL4-00001-G-T-11003)*.
[28]   Bouwcombinatie Drechtse Steden. (2000). *HSL-Zuid Geotechnisch lengteprofiel kilometrering 18,600-19,400* (HSL4-00001-G-T-11008)*.
[29]   Bouwcombinatie Drechtse Steden. (2000). *HSL-Zuid Geotechnisch lengteprofiel kilometrering 19,400-20,200* (HSL4-00001-G-T-11009)*.
[30]   Bouwcombinatie Drechtse Steden. (2000). *HSL-Zuid Geotechnisch lengteprofiel kilometrering 20,200-21,000* (HSL4-00001-G-T-11010)*.
[31]   Bouwcombinatie Drechtse Steden. (2000). *HSL-Zuid Geotechnisch lengteprofiel kilometrering 21,000-21,800* (HSL4-00001-G-T-11011)*.
[32]   Bouwcombinatie Drechtse Steden. (2000). *HSL-Zuid Geotechnisch lengteprofiel kilometrering 21,800-22,600* (HSL4-00001-G-T-11012)*.
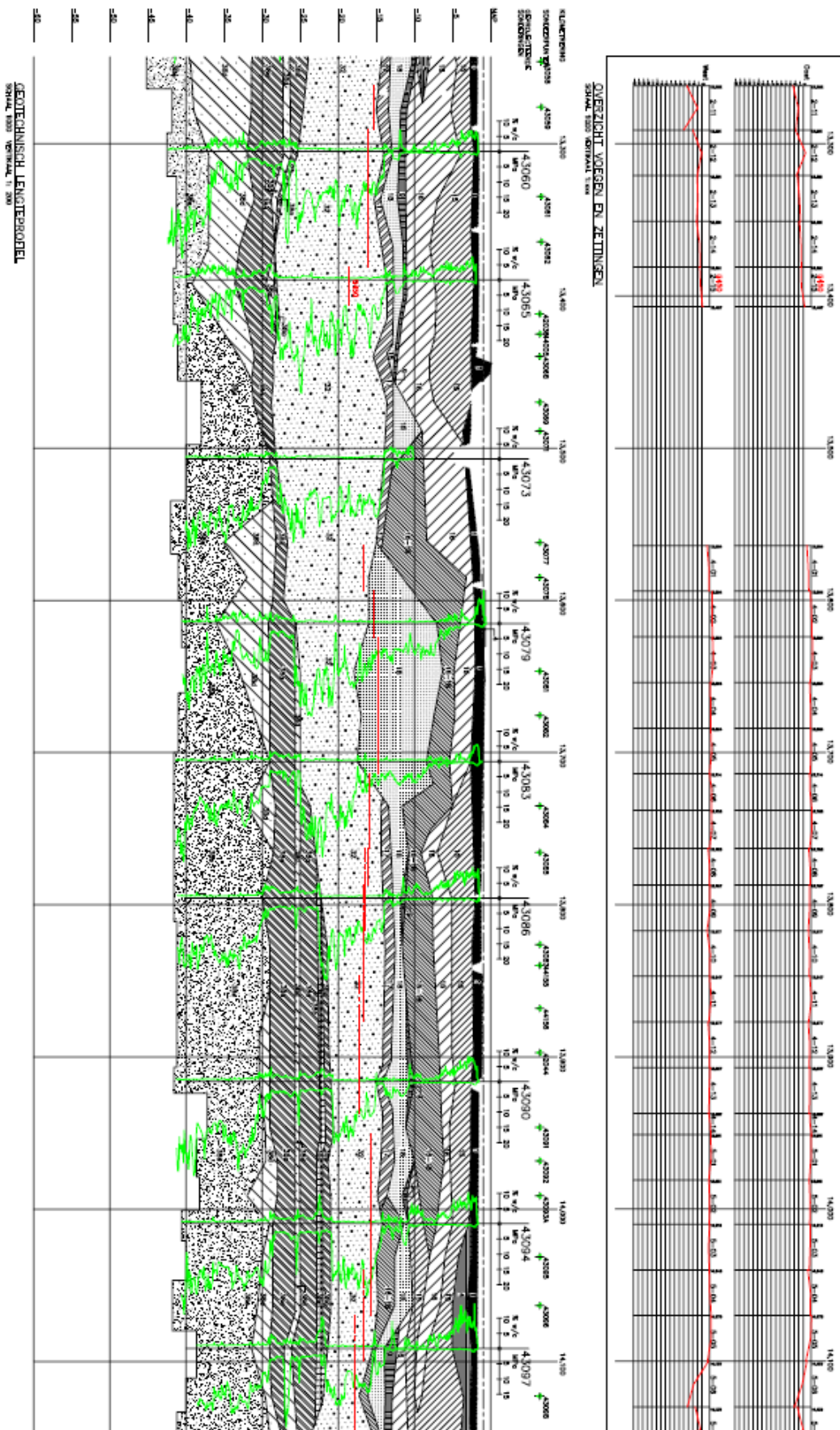
Appendix A: Foundation

At Schuilingervliet the settlement of the SFP along the track was measured by Iv-Infra [12] [25]. Three measurement points per SFP were taken, at both ends and at the middle of the SFP.

The figures below show the settlement measurements. These settlement measurements were plotted above a figure of the geotechnical profile of the soil along the track [14] [26] [27] [28] [29] [30] [31] [32]. In the figures of the geotechnical profile the cone penetration test is shown with a green line. The red horizontal lines show the pile depth of each individual SFP.

When the figures are observed no connection can be found between the settlements and the pile depth nor the travel direction of the trains. The settlement of the SFP occurs often on the same spot for both tracks. Between both tracks there is a difference in the amount of settlement, but this difference cannot be linked to the travel direction. Also, the settlement of the SFP cannot be linked to the difference in pile length for consecutive SFP, because at some locations settlement occur but at other locations no settlement can be observed.

Figure 60: Settlement of SFP in mm and pile depth in meter for km 13.3-14.1. [25][26]
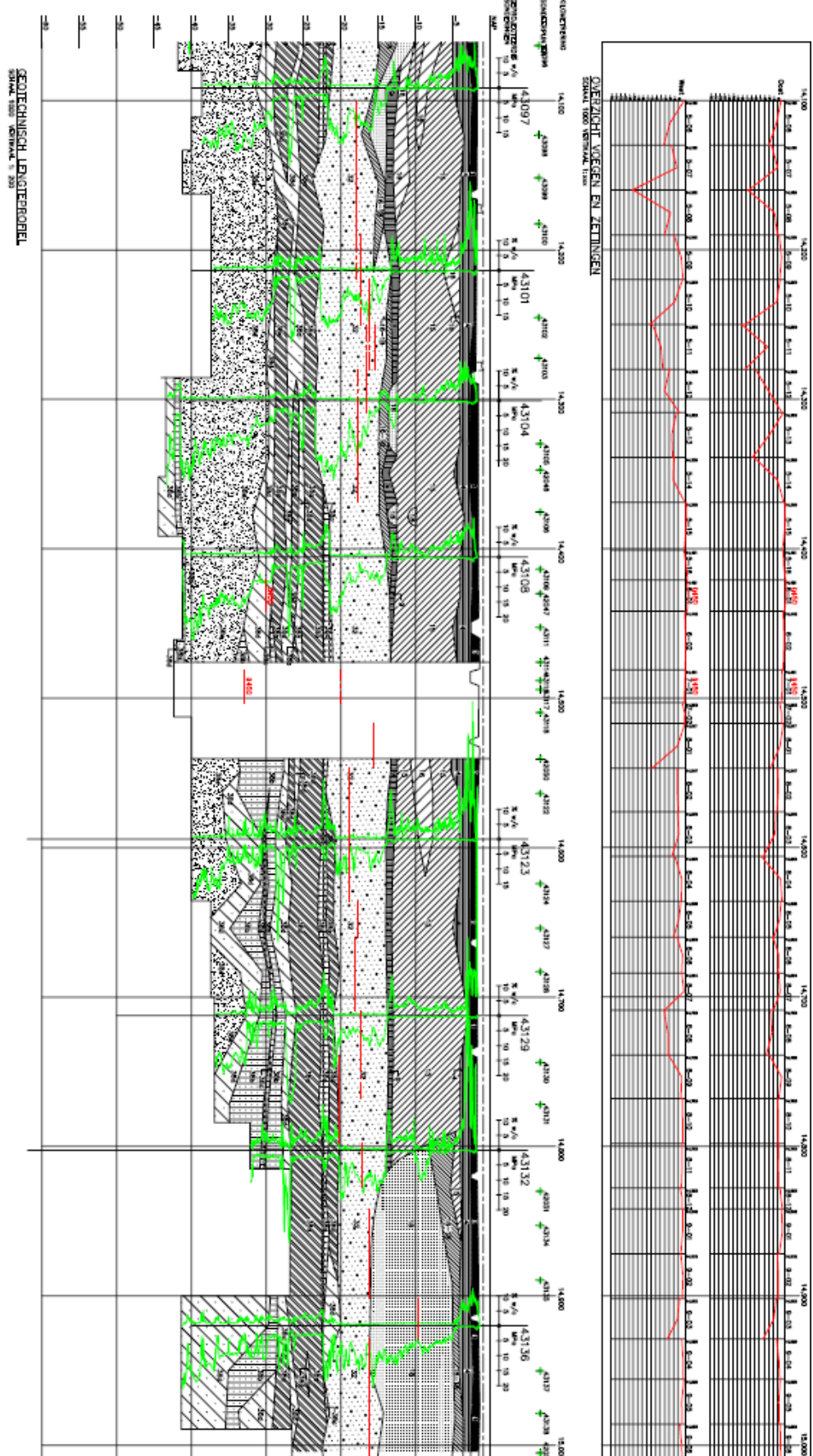
Figure 61: Settlement of SFP in mm and pile depth in meter for km 14.1-15.0. [25][27]
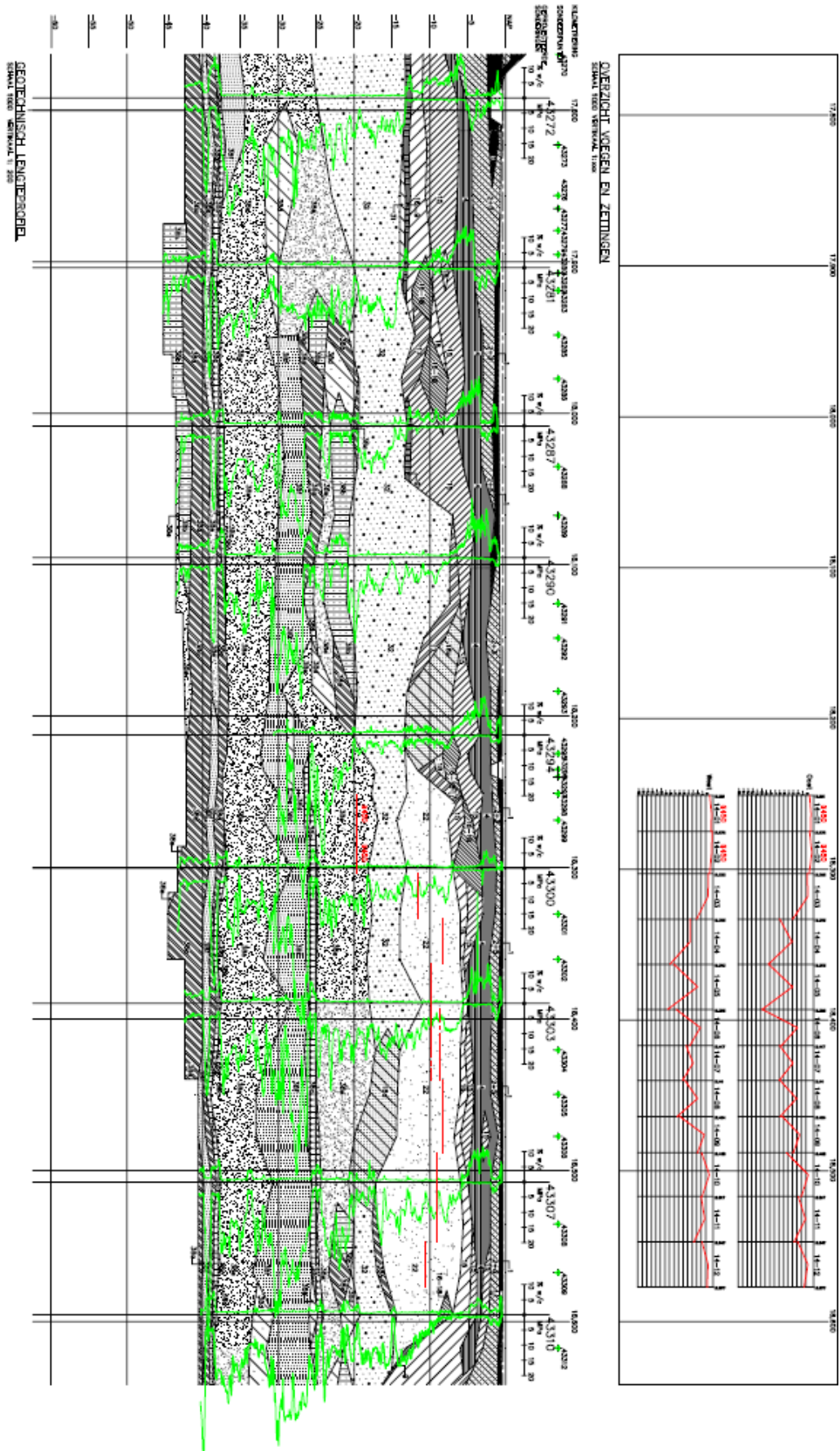
Figure 62: Settlement of SFP in mm and pile depth in meter for km 17.8-18.6. [12][14]
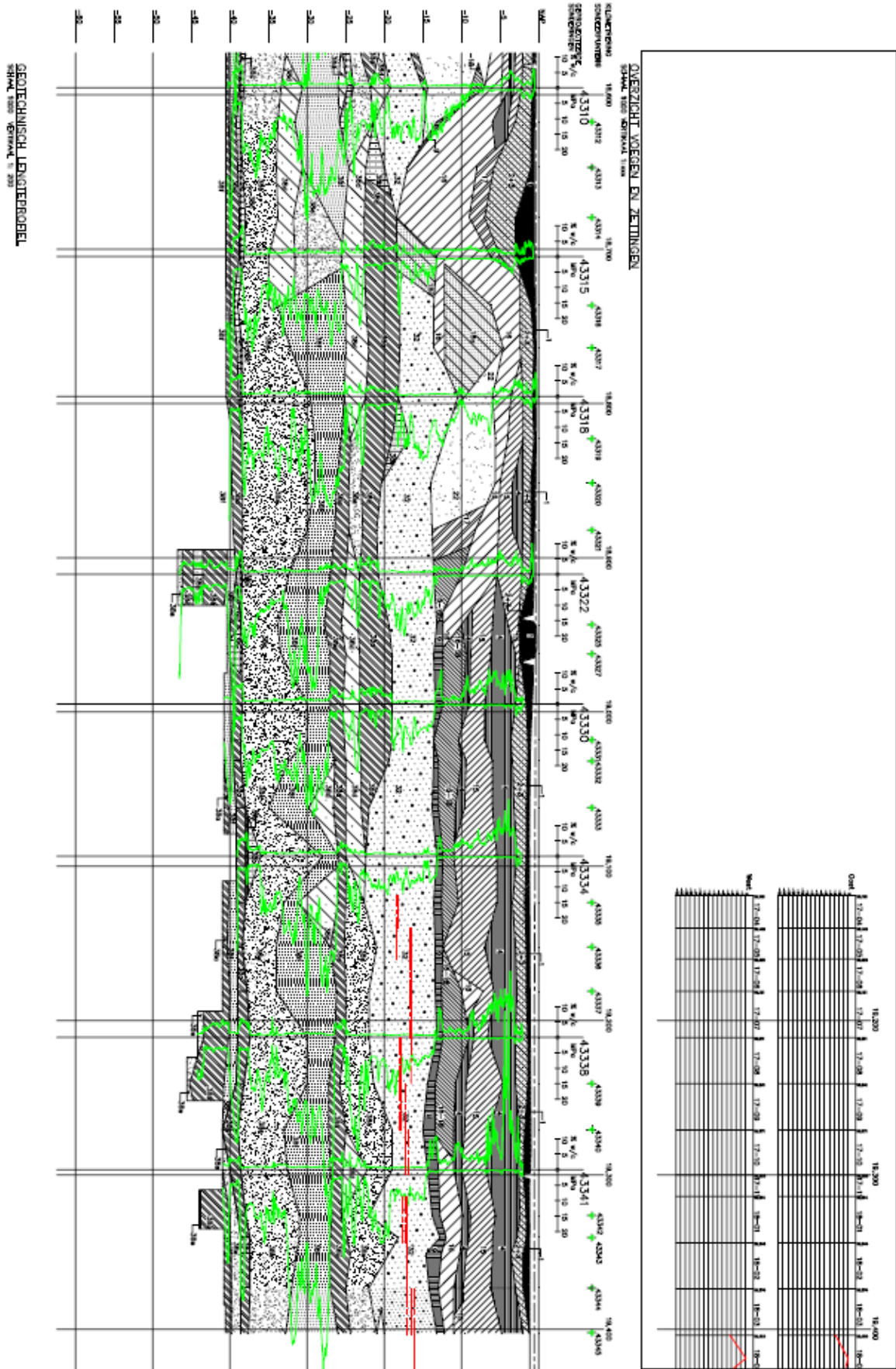
Figure 63: Settlement of SFP in mm and pile depth in meter for km 18.6-19.4. [12][28]
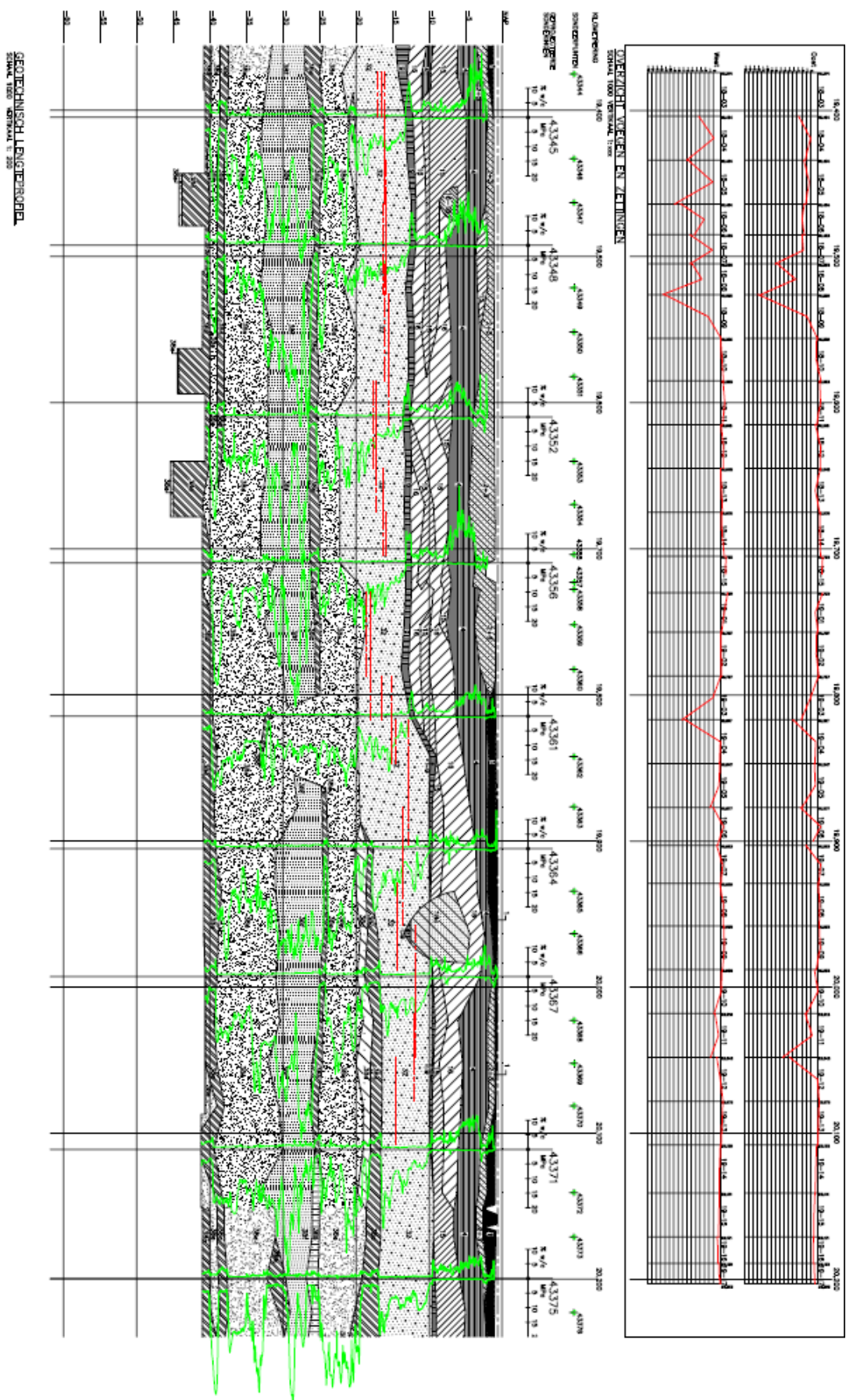
Figure 64: Settlement of SFP in mm and pile depth in meter for km 19.4-20.2. [12][29]
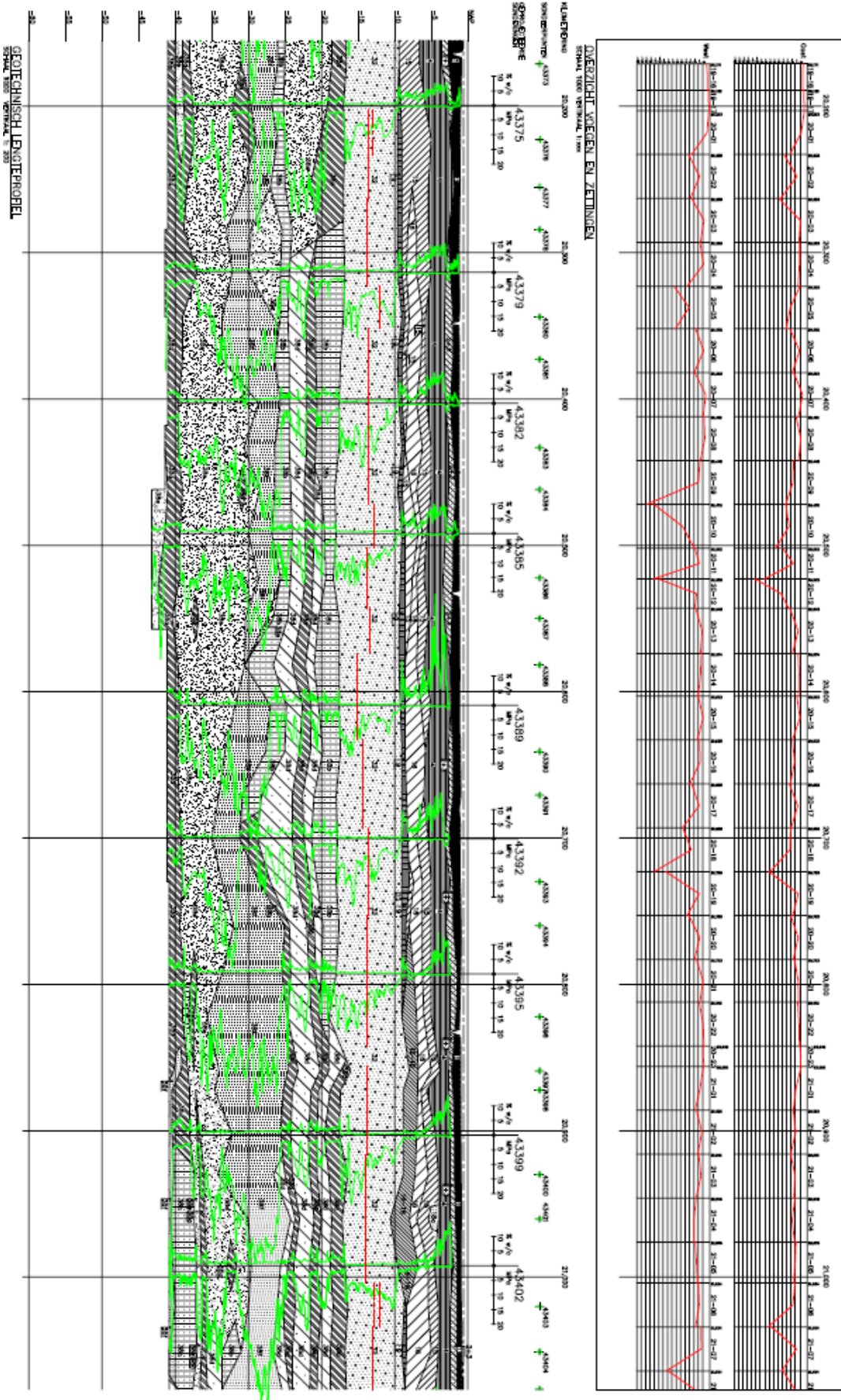
Figure 65: Settlement of SFP in mm and pile depth in meter for km 20.2-21.0. [12][30]
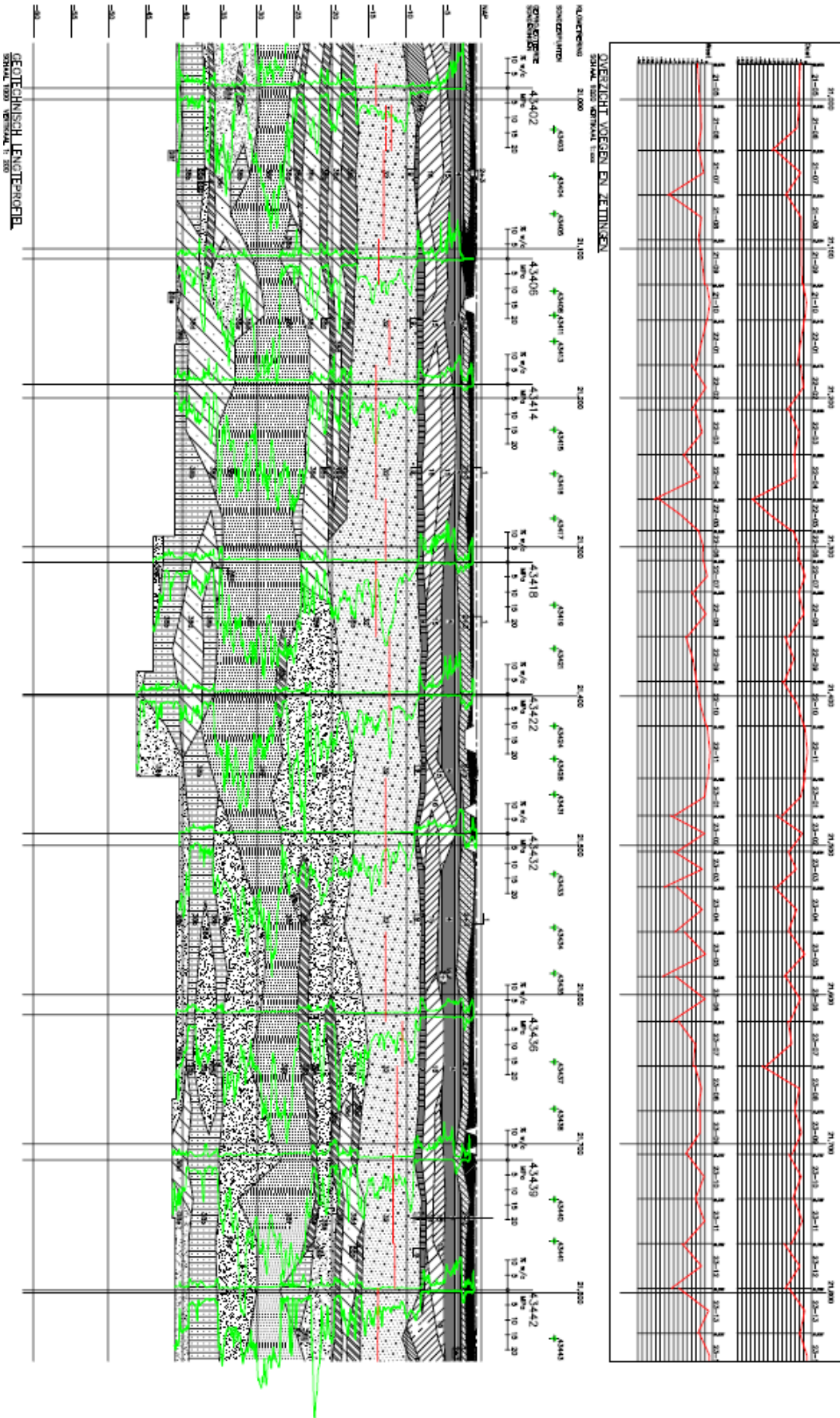
Figure 66: Settlement of SFP in mm and pile depth in meter for km 21.0-21.8. [12][31]
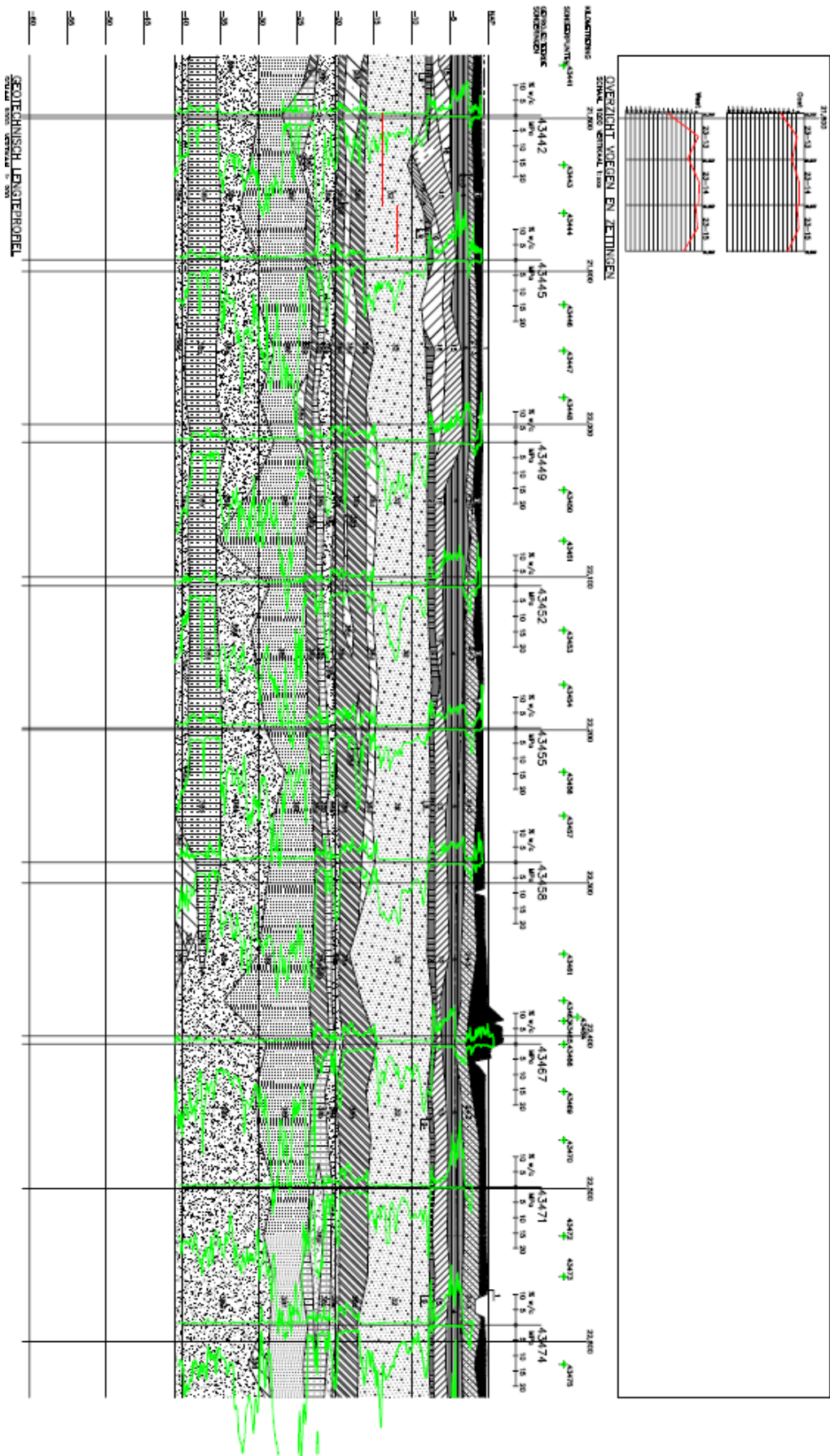
Figure 67: Settlement of SFP in mm and pile depth in meter for km 21.8-22.6. [12][32]

Appendix B: DARTS model

Table 22 shows the train characteristic on which the train models in DARTS are based [24]. These characteristics have been used in earlier simulations. The weight, bogie and body length have been altered compared with the earlier models used. The altered characteristics used in the simulations can be found in Tabel 10 in Chapter 4.

Table 22: Properties of train models [24].

Train configuration (carriage nr.)		1-2-3-2-1		1-1-1-1-1		1-2-2-2-2
	Carriage nr.	Properties	Carriage nr.	Properties	Carriage nr.	Properties
Body mass [kg]	1	54310	1	48642	1	44278
	2	40733			2	43300
	3	27073				
Body length [m]	1	22.15	1	24.775	1	17.9
	2	21.85			2	27.05
	3	18.7				
Bogie mass [kg]		2791	1	3625	1	16796
					2	2600
Bogie spacing [m]	1	14; 6.3	1	17.375; 7.4	1	9.7; 8.1
	2	18.7			2	19; 8.1
	3	18.7				
Wheel mass [kg]		1013.5	1	1013.5	1	1516.25
					2	437.5
Axle spacing [m]		3	1	2.5	1	2.8
					2	2.5
Axle loads [kN]		16 x 170	1	20 x 160		4 x 225 + 16 x 130
Primary suspension stiffness per wheel [kN/m]		1150	1	400	1	2232
					2	2800
Primary damping per wheel [kNs/m]		15	1	5	1	45.7
					2	1.25
Secondary suspension stiffness per bogie [kN/m]	1	600	1	300	1	2400
	2	600; 300			2	1539
	3	300				
Secondary damping per bogie [kNs/m]	1	48	1	24	1	139
	2	48; 24			2	35.8
	3	24				
Wheel radius [m]		0.42	1	0.42	1	0.5
					2	0.46
Total train length [m]		106.7		123.875		126.1

To determine the axle loads for the train models in DARTS, the measured axle load data of the month July 2019 were used. The data consists the axle loads of 7075 trains. The axle load has been measured for 5182 Intercity Direct, 1566 Thalys and 327 Eurostar. The average axle load of each axle for each train is shown in the following table.

Table 23: Axle loads Intercity Direct, Thalys and Eurostar per axle.

Intercity Direct							
Axle number	Axle load [Ton]	Axle number	Axle load [Ton]	Axle number	Axle load [Ton]	Axle number	Axle load [Ton]
1	21.08	10	11.12	19	11.51	28	11.09
2	21.52	11	11.19	20	11.43	29	11.54
3	21.42	12	11.12	21	11.47	30	11.54
4	21.33	13	11.48	22	11.48	31	11.36
5	11.37	14	11.47	23	11.62	32	11.33
6	11.32	15	11.53	24	11.54	33	20.93
7	11.51	16	11.45	25	11.12	34	21.49
8	11.43	17	11.45	26	11.13	35	21.33
9	11.13	18	11.45	27	11.17	36	21.29
Thalys							
Axle number	Axle load [Ton]	Axle number	Axle load [Ton]	Axle number	Axle load [Ton]	Axle number	Axle load [Ton]
1	16.78	8	16.42	15	15.72	22	13.12
2	17.51	9	16.01	16	15.76	23	16.71
3	16.46	10	16.09	17	16.04	24	17.36
4	17.51	11	15.72	18	16.08	25	16.16
5	13.11	12	15.78	19	16.31	26	17.12
6	12.97	13	15.68	20	16.36		
7	16.30	14	15.72	21	12.92		
Eurostar							
Axle number	Axle load [Ton]	Axle number	Axle load [Ton]	Axle number	Axle load [Ton]	Axle number	Axle load [Ton]
1	15.14	17	14.44	33	13.87	49	13.03
2	15.23	18	14.43	34	14.36	50	13.02
3	13.66	19	13.58	35	15.09	51	14.13
4	14.26	20	13.59	36	15.67	52	14.10
5	15.69	21	15.45	37	14.69	53	14.49
6	15.63	22	15.83	38	14.66	54	14.90
7	15.51	23	15.04	39	14.92	55	14.99
8	15.53	24	15.66	40	14.88	56	15.58
9	15.09	25	14.93	41	14.64	57	15.07
10	15.50	26	14.94	42	15.02	58	15.07
11	14.82	27	14.81	43	15.05	59	15.54
12	15.41	28	14.82	44	15.65	60	15.58
13	14.25	29	15.07	45	13.05	61	13.90
14	14.26	30	15.51	46	13.05	62	14.32
15	13.28	31	13.97	47	14.12	63	14.59
16	13.33	32	14.48	48	14.13	64	15.44

From these axle loads the average axle load of the Traxx locomotive and the carriages of the Intercity Direct is determined. Also, the average axle load for the motor carriages, the first axle of the trailer carriage and for the Jacob bogies of the Thalys are determined. As well as the average axle load for the Eurostar.

Table 24: Average axle load for different axles of each train.

Average axle load [Ton]		
Intercity Direct	Traxx locomotive	21.30
	Carriage	11.37
Thalys	Motor carriage	16.95
	Trailer carriage	13.03
	Jacobs bogie	16.00
Eurostar		14.68

Input file for the basic model of the HSL in DARTS. The other simulations are based on this file.

```
RAIL 'Model HSL with small piles'
UNIT Mete Newt
BOTT LAYE FORM
GENE RAIL N=2300 dx=0.13
BOUN cond   on
surface file 'HSL_SW_2' x=623.75 scale=-1.0

DELE
FILL ELEMENTS 1 TO 2
*
DELE
FILL ELEMENTS 4 TO 7
REPEAT 458 TIMES SPACING 5
*
DELE
FILL ELEMENTS 2299 TO 2300
*

DELE
SLAB ELEMENTS 1 TO 1
REPEAT 9 TIMES SPACING 230
*
DELE
SLAB ELEMENTS 51 TO 51
REPEAT 9 TIMES SPACING 230
*
DELE
SLAB ELEMENTS 101 TO 101
REPEAT 9 TIMES SPACING 230
*
DELE
SLAB ELEMENTS 131 TO 131
REPEAT 9 TIMES SPACING 230
*
DELE
SLAB ELEMENTS 181 TO 181
REPEAT 9 TIMES SPACING 230
*

DELE
BED ELEMENTS 1 TO 1
REPEAT 9 TIMES SPACING 230
*
DELE
BED ELEMENTS 51 TO 51
REPEAT 9 TIMES SPACING 230
*
DELE
BED ELEMENTS 101 TO 101
REPEAT 9 TIMES SPACING 230
*
DELE
BED ELEMENTS 131 TO 131
REPEAT 9 TIMES SPACING 230
*
DELE
BED ELEMENTS 181 TO 181
REPEAT 9 TIMES SPACING 230
*

DELE
FOUN ELEMENTS 1 TO 1
REPEAT 9 TIMES SPACING 230
*

DELE
FORM ELEMENTS 1 TO 2
REPEAT 9 TIMES SPACING 230
*
DELE
FORM ELEMENTS 5 TO 7
REPEAT 9 TIMES SPACING 230
*
DELE
FORM ELEMENTS 10 TO 12
REPEAT 9 TIMES SPACING 230
*
DELE
FORM ELEMENTS 15 TO 20
REPEAT 9 TIMES SPACING 230
*
DELE
FORM ELEMENTS 23 TO 29
REPEAT 9 TIMES SPACING 230
*
DELE
```

```
FORM ELEMENTS 32 TO 38
REPEAT 9 TIMES SPACING 230
*
DELE
FORM ELEMENTS 41 TO 47
REPEAT 9 TIMES SPACING 230
*
DELE
FORM ELEMENTS 50 TO 56
REPEAT 9 TIMES SPACING 230
*
DELE
FORM ELEMENTS 59 TO 65
REPEAT 9 TIMES SPACING 230
*
DELE
FORM ELEMENTS 68 TO 74
REPEAT 9 TIMES SPACING 230
*
DELE
FORM ELEMENTS 77 TO 83
REPEAT 9 TIMES SPACING 230
*
DELE
FORM ELEMENTS 86 TO 92
REPEAT 9 TIMES SPACING 230
*
DELE
FORM ELEMENTS 95 TO 101
REPEAT 9 TIMES SPACING 230
*
DELE
FORM ELEMENTS 104 TO 110
REPEAT 9 TIMES SPACING 230
*
DELE
FORM ELEMENTS 113 TO 119
REPEAT 9 TIMES SPACING 230
*
DELE
FORM ELEMENTS 122 TO 128
REPEAT 9 TIMES SPACING 230
*
DELE
FORM ELEMENTS 131 TO 137
REPEAT 9 TIMES SPACING 230
*
DELE
FORM ELEMENTS 140 TO 146
REPEAT 9 TIMES SPACING 230
*
DELE
FORM ELEMENTS 149 TO 155
REPEAT 9 TIMES SPACING 230
*
DELE
FORM ELEMENTS 158 TO 164
REPEAT 9 TIMES SPACING 230
*
DELE
FORM ELEMENTS 167 TO 173
REPEAT 9 TIMES SPACING 230
*
DELE
FORM ELEMENTS 176 TO 182
REPEAT 9 TIMES SPACING 230
*
DELE
FORM ELEMENTS 185 TO 191
REPEAT 9 TIMES SPACING 230
*
DELE
FORM ELEMENTS 194 TO 200
REPEAT 9 TIMES SPACING 230
*
DELE
FORM ELEMENTS 203 TO 209
REPEAT 9 TIMES SPACING 230
*
DELE
FORM ELEMENTS 212 TO 217
REPEAT 9 TIMES SPACING 230
*
DELE
FORM ELEMENTS 220 TO 222
REPEAT 9 TIMES SPACING 230
*
DELE
FORM ELEMENTS 225 TO 227
```

```
REPEAT 9 TIMES SPACING 230
*
DELE
FORM ELEMENTS 230 TO 230
REPEAT 9 TIMES SPACING 230
*

RAIL PROP AX= 7.687E-03 AY= 3.45915E-03 IYY= 3.055E-05 R= 0.3
FILL MATE KF= 3.07692E+08 CF= 6.15385E+04 W= 0.
SLAB PROP W= 1.3 H= 0.24 EY= 8.57E+09 POI= 0.16 RHO= 2500 GSH= 0.3694E+10
ELAS BED  KF= 2.2308E+09 CF= 2.3077E+04 W= 1.3
FOUN PROP W= 1.5 H= 0.5 EY= 2.0E+10 POI= 0.16 RHO= 2500 GSH = 0.86207E+10
FORM KF= 9.1346E+08 CF= 2.5982E+06 W= 0.26

arti damp rail=1.          slab=1.          her =0.5

movi trai 'RICD' velocity= 44.        offset=  15.000
int  u  =6.796        by  =.001

SAVE RESULTS
ELEMENTS 1725 TO 2185
*

dynamic analysis
*

FINISH
```

Train models used for the simulations in DARTS.

Intercity Direct

```
units m kn
body   spacing 18.9 26.4*4
bogie spacing 10.44 7.93 19. 7.4 19. 7.4 19. 7.4 19. offset 4.23

body properties
type=1 k1=2400.  c1=139.  m=40  front=0.3  back=0.3
type=2 k1=1593.  c1=35.   m=34.8
*
bogie properties
type=1 k=2232. c=45.7 mb=16.8 mw=1.5 r=0.59 dw=2.60
type=2 k=2800. c=1.25 mb=2.6  mw=0.75 r=0.46 dw=2.560
*
define train
body  1 type=1 inc 1
body  2 type=2 inc 3
body  3 type=2 inc 5
body  4 type=2 inc 7
body  5 type=2 inc 9
bogie 1 type 1
bogie 2 type 1
bogie 3 type 2
bogie 4 type 2
bogie 5 type 2
bogie 6 type 2
bogie 7 type 2
bogie 8 type 2
bogie 9 type 2
bogie 10 type 2
*
```

Thalys

```
units m kn
body   spacing 22.15 21.845 18.7*2 21.845 22.15
bogie spacing 14. 6.275 18.7*4 6.275 14. offset 5.02

lumped masses
body 1 m=6500.0   dx=-7.945
body 2 m=2000.0   dx=7.775
body 5 m=2000.0   dx=-7.775
body 6 m=6500.0   dx=7.945
*
body properties
type=1 k1=600.  c1=48.0                     m=48.0  front=2.
type=2 k1=600.  c1=48.0 k2=300. c2=24.0  m=30.2
type=3 k1=300.  c1=24.0                     m=25.2
type=4 k1=300.  c1=24.0 k2=600. c2=48.0  m=30.2
type=5 k1=600.  c1=48.0                     m=48.0  back=2.
*
bogie properties
type=1 k=1150. c=15 mb=2.8 mw=1.0 r=0.42 dw=3.
*
define train
body  1 type=1 inc 1
body  2 type=2 inc 3
body  3 type=3 inc 4
body  4 type=3 inc 5
body  5 type=4 inc 6
body  6 type=5 inc 8
*
```

Eurostar

```
units m kn
body  spacing 26.035 24.775*3 26.035
bogie spacing 17.375 7.4 17.375 7.4 17.375 7.4 17.375 7.4 17.375 offset 4.96

lumped masses
body 1 m=2900.0   dx=-9.3175
body 5 m=2900.0   dx=9.3175
*
body properties
type=1 k1=300.  c1=24.            m=40.6  front=2.
type=2 k1=300.  c1=24.            m=43.4
type=3 k1=300.  c1=24.            m=40.6  back=2.
*
bogie properties
type=1 k=400. c=5. mb=3.6 mw=1.0 r=0.42 dw=2.50
*
define train
body  1 type=1 inc 1
body  2 type=2 inc 3
body  3 type=2 inc 5
body  4 type=2 inc 7
body  5 type=3 inc 9
*
```

Appendix C: Field measurements

Field measurement data of the displacement measurements at Schuilingervliet measured at reference joint at km 219.989 by Dekra Rail [15].

Table 25: Maximum displacement for Eurostar [15].

Maximum displacement				Left side of the joint [mm]			Right side of the joint [mm]		
Date	Time	Train	V [km/h]	Rail	Rheda slab	SFP	Rail	Rheda slab	SFP
13/11/2018	12:25	Eurostar	283.6	2	0.7	0.6	2.2	0.6	0.6

Table 26: Maximum displacement for Intercity Direct [15].

Maximum displacement				Left side of the joint [mm]			Right side of the joint [mm]		
Date	Time	Train	V [km/h]	Rail	Rheda slab	SFP	Rail	Rheda slab	SFP
13/11/2018	09:57	Intercity Direct	160.5	1.6	0.5	0.6	1.5	0.6	0.6
13/11/2018	10:07	Intercity Direct	159.1	1.6	0.4	0.6	1.6	0.5	0.5
13/11/2018	10:27	Intercity Direct	160.5	1.8	0.5	0.8	1.7	0.5	0.6
13/11/2018	10:37	Intercity Direct	160.2	1.6	0.3	0.6	1.6	0.5	0.5
13/11/2018	10:58	Intercity Direct	159.7	1.4	0.6	0.6	1.7	0.6	0.5
13/11/2018	11:04	Intercity Direct	160.3	1.5	0.5	0.5	1.7	0.6	0.6
13/11/2018	11:27	Intercity Direct	160.5	1.5	0.4	0.5	1.5	0.6	0.5
13/11/2018	11:40	Intercity Direct	160.2	1.3	0.4	0.6	1.2	0.4	0.4
13/11/2018	12:39	Intercity Direct	159.3	1.6	0.6	0.6	1.5	0.6	0.6
		Average:	160.1	1.5	0.5	0.6	1.5	0.5	0.5
		Standard deviation:	0.5	0.2	0.1	0.1	0.1	0.1	0.1

Table 27: Maximum displacement for Thalys [15].

Maximum displacement				Left side of the joint [mm]			Right side of the joint [mm]		
Date	Time	Train	V [km/h]	Rail	Rheda slab	SFP	Rail	Rheda slab	SFP
13/11/2018	10:01	Thalys	264	1.4	0.5	0.7	1.4	0.6	0.6
13/11/2018	10:51	Thalys	259.3	1.4	0.6	0.5	1.5	0.4	0.6
13/11/2018	12:50	Thalys	193.2	1.5	0.6	0.6	1.4	0.6	0.6
13/11/2018	13:51	Thalys	187.7	1.5	0.3	0.4	1.4	0.5	0.4
13/11/2018	14:51	Thalys	294.2	1.5	0.7	0.6	1.8	0.8	0.6
		Average:	239.7	1.5	0.5	0.5	1.5	0.6	0.5
		Standard deviation:	46.9	0.1	0.1	0.1	0.2	0.2	0.1